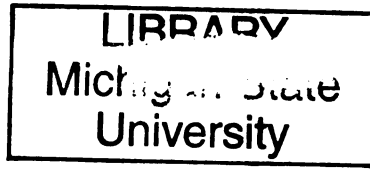


THESIS
2003
54754360



This is to certify that the
dissertation entitled

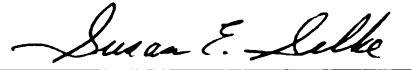
MICROCELLULAR FOAM OF POLYMER BLENDS OF HDPE/PP
AND THEIR COMPOSITES WITH WOOD FIBER

presented by

Pornchai Rachtanapun

has been accepted towards fulfillment
of the requirements for

Ph.D. degree in Packaging


Major professor

Date June 30, 2003

**PLACE IN RETURN BOX to remove this checkout from your record.
TO AVOID FINES return on or before date due.
MAY BE RECALLED with earlier due date if requested.**

| DATE DUE | DATE DUE | DATE DUE |
|------------------------|----------|----------|
| OCT 16 2006 0515 06 | | |
| APR 23 2007 1508 1 | | |
| | | |
| | | |
| | | |
| | | |
| | | |
| | | |
| | | |
| | | |
| | | |

**MICROCELLULAR FOAM OF POLYMER BLENDS OF HDPE/PP
AND THEIR COMPOSITES WITH WOOD FIBER**

By

Pornchai Rachtanapun

A DISSERTATION

**Submitted to
Michigan State University
in partial fulfillment of the requirements
for the degree of**

DOCTOR OF PHILOSOPHY

School of Packaging

2003

MICROCELLULAR FOAM OF POLYMER BLENDS OF HDPE/PP AND THEIR COMPOSITES WITH WOOD FIBER

PORNCHAI RACHTANAPUN

Ph.D. Dissertation
School of Packaging, Michigan State University

ABSTRACT

Microcellular foams of HDPE/PP blends and their composites with wood fiber were investigated to determine the effects of batch processing conditions (foaming time and temperature), blend composition, and wood fiber content on the crystallinity, sorption behavior of CO₂, void fraction, and cellular morphology (cell size and cell density) of the blends and composites. Differential scanning calorimetry (DSC) was used to investigate the heat of fusion, the melting temperature and crystallinity of the samples. Optical microscopy was employed to investigate the miscibility and crystalline morphology of the HDPE/PP blends. Environmental scanning electron microscopy (ESEM) was used to investigate the phase separation, interphase adhesion and cellular morphology of the samples. The microcellular structure of foamed HDPE/PP blends and their composites is strongly dependent on the foaming temperature, foaming time and blend composition as well as wood fiber content. Blending decreased the crystallinity of HDPE and PP and facilitated the formation of microcellular structures in polyolefins due to the poorly bonded interfaces of immiscible HDPE/PP blends, which favored cell nucleation. Well-developed microcellular structures were produced in HDPE/PP blends with ratios such as 50:50 and 30:70 at a foaming temperature of 175°C for 30 sec, but when wood fiber was introduced, a uniform and well-developed microcellular structure was not produced. The cell morphology had a strong relationship with the impact strength of foamed

samples. Improvement in impact strength was associated with well-developed microcellular morphology. The effects of HDPE/PP blending on crystallinity as a function of HDPE melt index were also studied. The melting temperature and total amount of crystallinity in HDPE/PP blends were lower than those of pure polymers regardless of blend composition and melt index. The void fraction of the foamed 30:70 HDPE/PP blend was always higher than that of the foamed 50:50 HDPE/PP blend, regardless of HDPE melt flow index. The microcellular structure can be greatly enhanced by using a suitable ratio of HDPE/PP in the blend and foaming above the melting temperature for sufficient time; however, using high melt index HDPE in the blend has a deleterious effect on both the void fraction and cell morphology of the blend, probably related to cell coalescence in the highly softened matrix.

Copyright by
PORNCHAI RACHTANAPUN
2003

ACKNOWLEDGEMENTS

I would like to express my sincere gratitude to my research guidance committee: Dr. Susan Selke, my major advisor, for her help, encouragement, patience and invaluable guidance during the past four years. Moreover, I realized what the word “advisor” means from her. She is a model for me how to be a good advisor and teacher. I believe what I experienced and learned from her will benefit my entire professional career. I would like to thank Dr. Laurent Matuana, my co-advisor, for his valuable help and advice. He always teaches me “how to work smart more than work hard and how to work like a Ph.D student”. I would like to thank Dr. Gary Burgess and Dr. Bruce Harte for their guidance, encouragement, and constant greeting which make me comfortable like I stay at home. I would like to thank Dr. Indrek S. Wichman for his valuable help and advice. I would also like to thank Dr. Ruben Hernandez, my former committee member. He always had good suggestions and wonderful ideas. I believe he is in heaven. I thank Dr. Richard L. Schalek and Dr. Per Askeland for helping me with ESEM. I thank Mr. Micheal Rich for teaching me to use the extruder. I thank Dr. John Williams for allowing me to use the notch machine when I worked in Michigan Technological University. I thank Fernando Cardoso for helping me with statistics. I thank and appreciate Dr. Qingxiu Li, Krittika Tanprasert, Palarp Sailabada, Bob Hurwitz, Uruchaya Sonchaeng, Hsin-Yen Chung (Julia), High Hong for their assistance and friendship. I would like to thank the faculty, staff and friends in the School of Packaging and Department of Forestry for their encouragement and friendship.

I would like to thank Abitibi Corporation, Dupont and Dow Plastic Company for supplying materials for this study.

I would like to acknowledge the Royal Thai Government for the scholarship and support throughout my study at Michigan State University.

I would like to specially thank, my girl friend, Chitsiri Thongson for her support, understanding and friendship.

I would like to thank Dr. Siri Karinchai and resource persons from the Young Buddhist Association of Thailand for teaching me how to practice Dhama of Buddha and apply for living.

Finally, I wish to heartily thank my mom, dad and family for their support, care and unconditional love.

Dedication to my mom and dad
POUNGPHET AND TAO RACHTANAPUN

TABLE OF CONTENTS

| | |
|--|-------------|
| Acknowledgements | v |
| List of Tables | xi |
| List of Figures | xii |
| List of Abbreviation | xv |
| List of Symbols | xvii |
| | |
| Chapter 1: Introduction | 1 |
| Objectives..... | 4 |
| References..... | 5 |
| | |
| Chapter 2: Literature Review | 9 |
| Polyolefins and Their Composites..... | 9 |
| Microcellular Foam..... | 15 |
| Critical Process Parameters in Microcellular Foaming..... | 20 |
| Effect of Crystallinity on Microcellular Foam..... | 25 |
| Microcellular Foams of Polymer Blends..... | 28 |
| References..... | 31 |
| | |
| Chapter 3: Microcellular Foam of Polymer Blends of HDPE/PP and Their Composites with Wood Fiber | 39 |
| Abstract..... | 40 |
| Introduction..... | 41 |
| Methodology..... | 43 |
| Sample Preparation..... | 43 |
| Sorption Experiments..... | 44 |
| Microcellular Experiments..... | 44 |
| Characterization of Foams..... | 44 |
| Differential Scanning Calorimetry (DSC)..... | 45 |
| Results and Discussion..... | 46 |
| Effects of HDPE/PP Blending on Crystallinity..... | 46 |
| Effects of Polymer Blend Composition and Wood Fiber Content on Solubility and Diffusivity of Carbon Dioxide..... | 48 |
| Effects of Foaming Conditions, Blend Composition, and Wood Fiber Content on Void Fraction of Foamed Samples..... | 52 |
| Cell Morphology of Foamed HDPE/PP Blends..... | 56 |
| Conclusions..... | 66 |
| References..... | 68 |

| | | |
|-------------------|---|------------|
| Chapter 4: | Cell Morphology and Impact Strength of Microcellular Foamed HDPE/PP Blends..... | 71 |
| | Abstract..... | 72 |
| | Introduction..... | 73 |
| | Methodology..... | 75 |
| | Materials..... | 75 |
| | Blend and Sample Preparation..... | 75 |
| | Optical Microscope (OM)..... | 75 |
| | Microcellular Foaming Experiments and Property Characterization..... | 76 |
| | Statistical Analysis..... | 76 |
| | Results and Discussion..... | 77 |
| | Optical Microscopy Observations..... | 77 |
| | Effects of Foaming Conditions and Blend Composition on Morphological Transformation of Foamed HDPE/PP Blends..... | 79 |
| | Impact Strength of Foamed Samples..... | 87 |
| | Conclusions..... | 91 |
| | References..... | 93 |
| | | |
| Chapter 5: | Characterization of Microcellular Foam Polyolefin Blend Composites with Wood Fiber..... | 96 |
| | Abstract..... | 97 |
| | Introduction..... | 98 |
| | Materials..... | 100 |
| | Methodology..... | 100 |
| | Sample Preparation..... | 100 |
| | Sorption Experiments..... | 101 |
| | Microcellular Foaming Experiments and Foam Characterization..... | 103 |
| | Statistical Analysis..... | 104 |
| | Results and Discussion..... | 105 |
| | Effects of Wood Fiber Content on Sorption Behaviors of CO ₂ | 105 |
| | Effect of Wood Fiber Content on Void Fraction and Cell Morphology of Foamed HDPE/PP Blend Composites... | 109 |
| | Effect of Wood Fiber Content on Impact Strength of Samples..... | 114 |
| | Conclusions..... | 117 |
| | References..... | 118 |
| | | |
| Chapter 6: | Effect of Melt Index of HDPE on Microcellular Foaming HDPE/PP Blends..... | 121 |
| | Abstract..... | 122 |
| | Introduction..... | 123 |

| | |
|--|------------|
| Methodology..... | 126 |
| Sample preparation..... | 126 |
| Differential Scanning Calorimetry (DSC)..... | 128 |
| Microcellular Foam Experiments and Characterization of Foams..... | 129 |
| Results and Discussion..... | 131 |
| Effect of Blending on Crystallinity as a Function of Melt Index..... | 131 |
| Effect of Melt Index, Polymer Blending, Foaming Time and Foaming Temperature on Void Fraction and Sample Morphology..... | 137 |
| Conclusions..... | 142 |
| References..... | 143 |
| Chapter 7: Summary of Findings..... | 148 |
| Recommendations and Future Work..... | 153 |
| Appendix..... | 154 |

List of Tables

| Tables | | page |
|------------------|---|-------------|
| Chapter 3 | Table 1: Melting temperature (T_m) and percent crystallinity (χ) of HDPE/PP blend samples..... | 47 |
| Chapter 4 | Table 1: Effect of blend composition on average cell size and cell-population density of samples foamed at 175°C for 30 sec... | 83 |
| Chapter 5 | Table 1: The solubility and diffusivity of CO ₂ in HDPE/PP 30:70 blends and their composites with wood fiber, and percent void fraction in foamed samples as a function of wood fiber content..... | 106 |
| Chapter 6 | Table 1: Typical properties of HDPE and PP, as supplied by manufacturer..... | 127 |
| | Table 2: Compounding conditions..... | 127 |
| | Table 3: Effects of blend composition on melting temperature (T_m) and percent crystallinity reduction of blend samples as a function of melt index..... | 136 |

List of Figures

| Figures | page |
|------------------|---|
| Chapter 2 | Figure 1: Energy dissipation around the bubbles (microvoids)..... 16 |
| Chapter 3 | Figure 1: Measured solubility of CO ₂ in the polyolefin blends as a function of blend composition..... 49 |
| | Figure 2: Desorption curves of polymer blends and composites with wood fiber (a) polymer blends, (b) composites with wood fiber..... 51 |
| | Figure 3: Effects of foaming time and blend composition on the void fraction of unfilled HDPE/PP blends foamed at (a) 135°C, (b) 160°C, (c) 175°C..... 53 |
| | Figure 4: Effects of foaming time and blend composition on the void fraction of HDPE/PP blend filled with 30 phr wood fibers foamed at (a) 135°C, (b) 160°C, (c) 175°C..... 54 |
| | Figure 5: ESEM micrographs of unfoamed polymers and their blends: (a) HDPE, (b) PP, (c) HDPE/PP 70:30, (d) HDPE/PP 50:50, and (e) HDPE/PP 30:70 (all scale bars 45 microns)..... 57 |
| | Figure 6: ESEM micrographs of foamed polymer blends at 175°C for 30 sec (a) HDPE (surface) (scale bars 450 μm), (b) HDPE (center) (scale bars 45 μm), (c) PP (surface) (scale bars 450 microns); (d) PP (center), (e) HDPE/PP 70:30, (f) HDPE/PP 50:50, and (g) HDPE/PP 30:70 (all scale bars 45 μm)..... 59 |
| | Figure 7: ESEM micrographs of foamed HDPE/PP 30:70 samples at (a) 135°C for 10 sec, (b) 160°C for 30 sec, (c) 175°C for 30 sec (scale bar 45 μm)..... 61 |
| | Figure 8: ESEM micrographs of foamed HDPE/PP 30:70 samples at 175°C for (a) 5 sec, (b) 10 sec, (c) 20 sec, (d) 30 sec (all scale bars 45 μm)..... 63 |
| | Figure 9: ESEM micrographs of foamed composite with wood fiber at 175°C for 30 sec (a) HDPE (b) HDPE /PP 70:30 (c) PP (all scale bars 450 μm)..... 65 |

| | |
|------------------|--|
| Chapter 4 | <p>Figure 1: Optical micrographs of HDPE/PP blends (Left column is light and right column is polarized light) a) Pure HDPE, b) Pure PP, c) HDPE/PP 70:30, d) HDPE/PP 50:50, and e) HDPE/PP 30:70 (all scale bars 25 μm)..... 78</p> <p>Figure 2: ESEM micrographs of foamed polymer blends for 30 sec (at 135°C, left column), (at 160°C, middle column) and (at 175°C, right column) a) Pure HDPE, b) Pure PP, c) HDPE/PP 70:30, d) HDPE/PP 50:50, and e) HDPE/PP 30:70 (all scale bars 100 μm)..... 80</p> <p>Figure 3: ESEM micrographs of foamed polymer blends at 175°C (Pure HDPE, left column), (Pure PP, middle column) and (HDPE/PP 70:30, right column) a) 5 sec, b) 10 sec, c) 20 sec, and d) 30 sec (all scale bars 100μm)..... 85</p> <p>Figure 4: ESEM micrographs of foamed polymer blends at 175°C (HDPE/PP 50:50, left column) and (HDPE/PP 30: 70, right column) a) 5 sec, b) 10 sec, c) 20 sec and d) 30 sec (all scale bars 100μm)..... 86</p> <p>Figure 5: Effects of foaming temperature and blend composition on notched Izod impact strength of HDPE/PP blend samples foamed for 30 sec. The notched impact strength of unfoamed HDPE is 176.9\pm47.2 J/m..... 89</p> |
| Chapter 5 | <p>Figure 1: Effect of wood fiber content on desorption curves of 30:70 HDPE/PP blend with wood fiber..... 107</p> <p>Figure 2: ESEM micrograph of foamed pure 30:70 HDPE/PP blend observed at different magnifications: (a) 250X, (b) 500X, (c) 1000X, and (d) 2000X..... 111</p> <p>Figure 3: ESEM micrographs of foamed HDPE/PP 30:70 blend composite samples with 5 phr wood fiber observed at different magnifications: (a) 250X, (b) 500X, (c) 1000X, and (d) 2000X..... 112</p> <p>Figure 4: ESEM micrographs of foamed HDPE/PP 30:70 blend composite samples with 10 phr wood fiber observed at different magnifications: (a) 250X, (b) 500X, (c) 1000X, and (d) 2000X..... 113</p> <p>Figure 5: Effect of wood content on impact strength of</p> |

| | | |
|------------------|--|-----|
| | microcellular foamed HDPE/PP 30:70 blend composites with wood fiber..... | 115 |
| Chapter 6 | Figure 1: DSC thermograms of HDPE1/PP blends..... | 133 |
| | Figure 2: Effect of blending on the crystalline fraction of HDPE and PP in HDPE/PP blends as a function of melt index..... | 135 |
| | Figure 3: Effect of blending on the total amount of crystallinity in HDPE/PP blends as a function of melt index..... | 135 |
| | Figure 4: Effect of melt flow index, blending and foaming time on void fraction at 160°C..... | 139 |
| | Figure 5: Effect of melt flow index, blending and foaming time on void fraction at 175°C..... | 139 |
| | Figure 6: ESEM micrographs of foamed polymer blends for 30 sec at 175°C observed at 500X a) HDPE1/PP 30:70, b) HDPE1/PP 50:50, c) HDPE2/PP 30:70, d) HDPE2/PP 50:50 e) HDPE3/PP 30:70, and f) HDPE3/PP 50:50..... | 141 |

LIST OF ABBREVIATIONS

| | | |
|-----------------|---|---|
| ABS | = | Acrylonitrile-butadiene-styrene |
| ANOVA | = | Analysis of variance |
| CO ₂ | = | Carbon dioxide |
| CPET | = | Poly(ethylene terephthalate) containing a polyolefin nucleating agent |
| DOP | = | Diethyl phthalate |
| DSC | = | Differential scanning calorimetry |
| EPA | = | Environmental Protection Agency |
| ESEM | = | Environmental scanning electron microscopy |
| HDPE | = | High density polyethylene |
| HIPS | = | High impact polystyrene |
| HSD | = | Tukey's studentized range |
| ICI | = | Imperial Chemical Industries |
| IPE | = | Ionomer modified polyethylene |
| iPP | = | Isotactic polypropylene |
| LDPE | = | Low density polyethylene |
| LLDPE | = | Linear low density polyethylene |
| MAPP | = | Maleic anhydride modified polypropylene |
| MDSC | = | Modulated differential scanning calorimetry |
| MSW | = | Municipal solid waste |
| M _w | = | Molecular weight |

| | | |
|-----------|---|------------------------------------|
| M_w/M_n | = | Polydispersity or Dispersion Index |
| N_2 | = | Nitrogen |
| OM | = | Optical microscopy |
| PB | = | Polybutylene |
| PC | = | Polycarbonate |
| PET | = | Poly(ethylene terephthalate) |
| phr | = | Parts per hundred parts resin |
| PMMA | = | Poly(methyl methacrylate) |
| PP | = | Polypropylene |
| PS | = | Polystyrene |
| PVC | = | Polyvinyl chloride |
| PVDF | = | Poly(vinylidene fluoride) |
| SAN | = | Styrene-co-acrylonitrile |
| T_g | = | Glass transition temperature |
| T_m | = | Melting temperature |
| VLDPE | = | Very-low-density polyethylene |
| WVT | = | Water vapor transmission |

LIST OF SYMBOLS

| | | |
|----------------|---|---|
| ρ | = | Density of unfoamed sample, g/cm ³ |
| ρ_f | = | Density of foamed sample, g/cm ³ |
| M_a | = | Weights of unfoamed and foamed samples were measured in air, g |
| M_w | = | Weights of unfoamed and foamed samples were measured in distilled water, g |
| VF | = | Void fraction, % |
| N_o | = | Cell-population density per unit volume of the original unfoamed polymer, cells/cm ³ |
| d | = | Average cell size, μm |
| n | = | Number of cells (bubbles) in the ESEM micrograph |
| A | = | Area of the micrograph, cm ² |
| M | = | Magnification factor of the micrograph |
| χ_{HDPE} | = | Percent crystallinity of HDPE, % |
| χ_{PP} | = | Percent crystallinity of PP, % |
| S_c | = | Solubility of CO ₂ in the composite, % |
| $S_{am, HDPE}$ | = | Solubility of CO ₂ in the amorphous regions of HDPE, % |
| $S_{am, PP}$ | = | Solubility of CO ₂ in the amorphous regions of PP, % |
| $S_{cr, HDPE}$ | = | Solubility of CO ₂ in the amorphous regions of HDPE, % |
| $S_{cr, PP}$ | = | Solubility of CO ₂ in the crystalline regions of HDPE, % |
| S_{wood} | = | Solubility of CO ₂ in wood fiber, % |

- x_{HDPE} = Weight fractions of HDPE in the HDPE/PP blends
- x_{PP} = Weight fractions of PP in the HDPE/PP blends
- $S_{measured\ HDPE}$ = Measured solubility of CO₂ in pure HDPE from the sorption experiments, %
- $S_{measured\ PP}$ = Measured solubility of CO₂ in pure PP from the sorption experiments, %
- $\Delta H_{m,HDPE}^{\circ}$ = Heats of fusion for HDPE (J/g)
- $\Delta H_{m,PP}^{\circ}$ = Heats of fusion for PP (J/g)

Chapter 1

INTRODUCTION

Packaging is the largest user of plastics in the U. S., accounting for approximately 33 % in 1998 [1]. Among those plastic packaging materials, polyolefins are the most used plastics, approximately 47 % in 1995, including very-low-density polyethylene (VLDPE), linear low density polyethylene (LLDPE), low density polyethylene (LDPE), high density polyethylene (HDPE) and polypropylene (PP) [2]. They are widely used because of their versatile properties, light weight, resistance to breakage, low cost, ease of manufacture, fabrication and shaping, etc. These plastic materials can be used as rigid containers, flexible film, trays, drums, caps, plastic cans, cushions, etc. Moreover, they can be used by combining with other materials or laminating or blending with other polymers to gain the benefit of their various attributes [1-3]. However, since the 1980s and early 1990s the environmental concern about municipal solid waste has increased because of the expansion of the quantity of municipal solid waste, the cost, and the lack of landfill space [1]. Municipal solid waste (MSW) is commonly known as garbage such as packaging, containers, bottles, newspapers, batteries, etc. In 1999, over 230 million tons of MSW was produced in the United States [4]. The U.S. Environmental Protection Agency (EPA) [4] reported that the amount of waste each person produces has almost doubled from 2.7 pounds per day in 1960 to 4.6 pounds per day in 1999. EPA's goals for the nation are to recycle 35 percent of MSW generated by 2005; to reduce waste generation to 4.3 pounds per person per day; to empower state, local, and tribal governments to better manage solid waste; to provide leadership in source reduction and

recycling; to build stronger public and private partnerships; and to ensure the environmental soundness of source reduction, recycling, combustion, and land disposal [4].

Among municipal solid waste components, packaging and containers are the largest part. For plastic packaging wastes, recycling is an appropriate option to disposal. HDPE is one of the top recycled plastics. However, the recycled HDPE often contains relatively high levels of PP contaminant. It is known that immiscible blends of HDPE/PP cause reduction in the mechanical performance of the materials, despite the similarity of their chemical structures [5]. In attempting to improve the mechanical properties of these materials, a number of researchers have studied the effect of addition of wood fiber or paper fiber into recycled HDPE, PP and HDPE/PP blends [6-17]. It has been shown that some mechanical properties of these composites could be improved, such as tensile modulus and stiffness, by addition of wood fiber [8, 12], but the impact strength [6, 8, 13], toughness [6], elongation at break [8, 16], tensile strength [8, 9, 13, 16, 18] and yield strength [16] were reduced. The low strength properties of polyolefin/wood fiber composites may result from poor interfacial adhesion between hydrophilic wood fiber and the hydrophobic polymer matrix [6, 12, 19], as well as poor dispersion of wood fibers in the polymer matrix due to the strong interactions between fibers by intermolecular hydrogen bonding [6, 12]. Moreover, the lower toughness and impact strength of these composites compared to unfilled plastics may be caused by the addition of high modulus wood fiber [6].

Many researchers tried to improve the strength of polyolefin/wood fiber composites by using coupling agents to enhance the interfacial adhesion between wood

and plastics [9-12, 15, 18-22]. Addition of coupling agent into these composites resulted in enhancing the tensile strength [9, 11, 15, 18, 19], creep resistance [11] and yield strength [15], but decreased impact strength [11]. In addition, the density of polyolefin/wood fiber composites is higher than that of pure polymers and wood fiber themselves due to the compression of the cellular structure of wood fibers during processing, and the polymers filling the lumen of the fiber as well as between fibers [23]. The microcellular foaming technique has been employed to improve the impact strength and reduce the density of PVC/wood-fiber composites by Matuana *et al.* [24-28].

Recently, Doroudiani *et al.* [29] demonstrated that the microcellular foam technique (which amounts to treating the plastic to produce a foam like structure) could be used to improve the impact strength and reduce the weight of HDPE/isotactic PP blends. However, they demonstrated these results for only some processing conditions and mechanical properties. There is very limited information about the critical processing parameters of microcellular foam of HDPE/PP which control the cell structure and impact strength. In this research, the effects of critical processing parameters such as solubility and diffusivity of gas, foaming conditions (foaming time, foaming temperature), blend composition, crystallinity, crystalline morphology and wood fiber content on void fraction and cell morphology (cell size and cell density) of HDPE/PP blends and their composites with wood fiber were investigated and the relationship between cellular morphology and mechanical properties such as impact strength is reported.

There are many potential applications for microcellular foam plastics such as food packaging, airplane, automotive mirror brackets, cable, sport equipment, etc.

Scope of this study

Objectives

The main goal of this study was to investigate microcellular foams of HDPE/PP blends and their composites with wood fiber produced by a batch process. The specific objectives were:

- i. to determine the effects of processing conditions (foaming time and temperature), blend composition, and wood fiber content on the void fraction and cell morphology (average cell size and cell-population density) and impact strength of the sample materials;
- ii. to investigate the effects of blend composition, and wood content, crystallinity on the solubility and diffusion of CO₂ and consequently on the void fraction;
- iii. to investigate the effects of blend composition on miscibility and crystalline morphology of the HDPE/PP blends and correlate them to cell morphology of foamed samples;
- iv. to identify suitable processing conditions and/or blend compositions for microcellular foamed HDPE/PP blends;
- v. to establish the relationship of the cell morphology to impact strength of microcellular foamed samples;
- vi. to investigate the effect of HDPE melt index on the foamability of HDPE/PP blends.

References:

1. R. J. Hernandez, S. E. M. Selke, and J. D. Culter, "Plastic Packaging Properties, Processing, Application and Regulations", Hanser Gardner Publications, Inc., Cincinnati, Ohio (2000).
2. J. F. Hanlon, R. J. Kelsey, "Handbook of Package Engineering", 3rd ed., Technomic Publishing Co., Inc., Lancaster, Pennsylvania (1998).
3. *Plastics Handbook*, edited by Modern Plastics, McGraw-Hill, Inc., New York, 1994.
4. Basic Facts Municipal Solid Waste (MSW), [Online] Available at <http://www.epa.gov/epaoswer/non-hw/muncpl/facts.htm>, March 2003.
5. K. Solc (Ed.), *Polymer Compatibility and Incompatibility, Principles and Practices*, Harwood, New York (1982).
6. R. T. Woodhams, G. Thomas and D. K. Rodgers, "Wood Fibers as Reinforcing Fillers for Polyolefins", *Polym. Eng. Sci.*, **24** (15), 1166-1171 (1984).
7. I. K. Yam, V. Kalyankar, S. Selke, and C. Lai, "Mechanical Properties of Wood Fiber/Recycled HDPE Composites", *SPE ANTEC Tech. Papers*, 1809-1811 (1988).
8. V. Kalyankar, "Mechanical Characteristics of Composites Made from Recycled HDPE Obtained from Milk Bottles", M. S. Thesis, Michigan State University, East Lansing, MI, USA (1989).
9. K. A. Nieman, "Mechanical Property Enhancement of Recycled HDPE and Wood Fiber Composites Due to the Inclusion of Additives", M. S. Thesis, Michigan State University, East Lansing, MI, USA (1989).

10. B. K. Gogoi, "Processing-Morphology-Property Relationships for Compounding Wood Fibers with Recycled HDPE Using a Twin-Screw Extruder", M. S. Thesis, Michigan State University, East Lansing, MI, USA (1989).
11. M. D. Keal, "Effect of Dual Additives Systems on the Mechanical Properties of Aspen Fiber/Recycled HDPE Composites", M. S. Thesis, Michigan State University, East Lansing, MI, USA (1990).
12. H. Chtourou, B. Riedl and A. Ait-kadi, "Reinforcement of Recycled Polyolefins with Wood Fibers", *J. Reinf. Plast Comps.*, **11**, 372-394 (1992).
13. T. Chotopatomwan, "Processing and Mechanical Property Testing of Paper Fiber and HDPE Composites", M. S. Thesis, Michigan State University, East Lansing, MI, USA (1998).
14. S. Rojanarungtawee, "Composite of Wood Fiber and Mixed Recycled Thermoplastics", M. S. Thesis, Michigan State University, East Lansing, MI, USA (1998).
15. J. J. Ricciardi, "High Density Polyethylene/Paper Fiber Composites: Measuring the Impact of Additives on Their Physical and Mechanical Properties", M. S. Thesis, Michigan State University, East Lansing, MI, USA (1999).
16. N. Thepwiwatjit, "Composite of Wood Fiber and Recycled HDPE Bottles from Household Use", M. S. Thesis, Michigan State University, East Lansing, MI, USA (2000).
17. K. Vanichvarod, "Composite Material of Mixed Low Density Polyethylene/Polypropylene and Wood Fiber", M. S. Thesis, Michigan State University, East Lansing, MI, USA (2002).

18. R. G. Raj, B. V. Kokta, G. Grouleau, and C. Daneault, "The Influence of Coupling Agents on Mechanical Properties of Composites Containing Cellulosic Fillers", *Polymer.-Plast. Technolo. Eng.*, **29** (4), 339-353 (1990).
19. K. Oksman and C. Clemons, "Mechanical Properties and Morphology of Impact Modified Polypropylene-Wood Flour Composites", *J. Appl. Polym. Sci.*, **67**, 1503-1513 (1998).
20. M. Kazayawoko, J.J. Balatinez, R. T. Woodhams, and S. Law, "Effect of ester linkages on the mechanical properties of wood fiber-polypropylene composites", *J. Reinf. Plast. Comps.*, **16** (15), 1383-1406 (1997).
21. M. Kazayawoko, J. J. Balatinez, and L. M. Matuana, "Surface Modification and Adhesion Mechanisms in Woodfiber-Polypropylene Composites", *J. Mater. Sci.*, **34**, 6189-6199 (1999).
22. J. Wu, D. Yu, C. Chan, J. Kim, and Y. Mai, "Effect of Fiber Pretreatment Condition on the Interfacial Strength and Mechanical Properties of Wood Fiber/PP Composites", *J. Appl. Polym. Sci.*, **76**, 1000-1010 (2000).
23. R. L. Geimer, C. M. Clemons, and J. E. Jr. Wood, "Density range of compression molded polypropylene-wood composites", *Wood Fiber Sci.*, **25** (2), 163-169 (1993).
24. L. M. Matuana, C. B. Park, and J. J. Balatinez, "Characterization of Microcellular PVC/Cellulosic-Fibre Composites", *J. Cellular Plast.*, **32** (5), 449-467 (1996).
25. L. M. Matuana, C. B. Park, and J. J. Balatinez, "Processing and Cell Morphology Relationships for Microcellular Foamed PVC/Cellulosic-Fiber Composites", *Polym. Eng. Sci.*, **37** (7), 1137-1147 (1997).

26. L. M. Matuana, C. B. Park, and J. J. Balatinecz, "Cell Morphology and Property Relationships of Microcellular Foamed PVC/Wood-Fiber Composites", *Polym. Eng. Sci.*, **38** (11), 1862-1872 (1998).
27. L. M. Matuana, C. B. Park, and J. J. Balatinecz, "Structures and Mechanical Properties of Microcellular Foamed Polyvinyl Chloride", *Cellular Polym.*, **17** (1), 1-16 (1998).
28. L. M. Matuana and F. Mengelglu, "Microcellular Foaming of Impact-Modified Rigid PVC/Wood-Flour Composites", *J. Vinyl Addit. Technol.*, **7** (2), 67-75 (2001).
29. S. Doroudiani, C. B. Park, and M. T. Kortschot, "Processing and Characterization of Microcellular Foamed High-Density Polyethylene/Isotactic Polypropylene Blends", *Polym. Eng. Sci.*, **38** (7), 1205-1215 (1998).

Chapter 2

LITERATURE REVIEW

Polyolefins and Their Composites

Low density polyethylene (LDPE), the first of the polyolefins, was discovered in 1933 by Reginald O. Gibson and Eric W. Fawcett at the British industrial giant Imperial Chemical Industries (ICI) [1-6]. LDPE is produced by free radical bulk polymerization under high pressure and temperature conditions. Molecules of LDPE (molecular weight (M_w) = 6,000-40,000) contain highly branched structures with 30-500 monomer units in the long branches [2]. In the early 1950s, high density polyethylene (HDPE) with high molecular weight (M_w = 50,000-250,000) [5], high crystallinity, high melting temperature and a low concentration of branches in the molecular structure was produced at low pressure and temperature using special catalysts, by Professor Karl Ziegler at the Planck Institute in Germany [1]. In 1954, Professor Giulio Natta, a consultant with Montecatini Co. in Italy [1], showed that the Ziegler catalyst could be used to produce stereoregular polymerization of polypropylene (PP). In 1957, highly isotactic polypropylene (M_w 150,000-1,500,000) [2] first became commercial. Linear low-density polyethylene (LLDPE) is considered to be the third generation of hybrid polyethylene. The polymerization process using co-monomer alkenes such as butene, hexene and octene at low pressure and temperature results in a linear polymer with short branch groups [2, 3]. In 1963, Ziegler and Natta were jointly awarded the Nobel Prize for Chemistry for their contributions in the development of new polymerization catalysts [1].

Polyolefins are the most-used commercial polymers with 53 billion pounds (24 million tonnes), accounting for around 60% of total polymer manufacture in the U.S.

(1999) [1]. The most important categories of polyolefins are high density polyethylene (HDPE), low density polyethylene (LDPE), linear low density polyethylene (LLDPE) and polypropylene. Polyolefins such as HDPE, LLDPE, LDPE and PP are major plastics used as packaging materials because they have excellent chemical and physical properties, easy processability and low cost, as well as good recyclability.

Low density polyethylene (LDPE) is a branched homopolymer with moderate clarity, high flexibility, good heat seal and ease of processing. LDPE is the most-used packaging plastic. LDPE can be easily processed by extrusion blown film, cast film, extrusion coating, injection molding, and blow molding. The majority of LDPE is used as packaging materials such as containers, bags, shrink film, stretch wrap films, etc [3].

Linear low density polyethylene (LLDPE) is a linear polyethylene copolymer. Compared to LDPE, LLDPE has higher mechanical properties such as stiffness, tensile strength, puncture resistance, tear properties and elongation. Nevertheless, LDPE has better heat seal and clarity than LLDPE [3].

High density polyethylene (HDPE) produced by Ziegler-Natta or Phillips catalysts contains a low degree of branching, 0.5-3 methyl groups compared to LDPE's 15-30 methyl groups per 500 monomer units [5]. HDPE has a high crystallinity of 65-90% which contributes to good moisture-barrier properties and chemical resistance [3]. Compared to LDPE, HDPE has higher tensile strength, stiffness, chemical resistance, elongation, barrier, etc. [5]. Therefore, most HDPE used in packaging is in rigid containers. HDPE is the second most used packaging plastic. Products made of HDPE include containers for milk, detergent, juice, and water; industrial chemical drums; pharmaceutical bottles; shampoo and deodorant containers, etc. [3].

Polypropylene (PP) is the third most used polyolefin. Isotactic PP is produced by addition polymerization of propylene using Ziegler-Natta catalysts such as titanium trichloride (TiCl_3) with aluminum diethyl monochloride [$\text{Al}(\text{C}_2\text{H}_5)_2\text{Cl}$] or titanium tetrachloride (TiCl_4) with triethyl aluminum [$\text{Al}(\text{C}_2\text{H}_5)_3$] to control its stereochemical configuration [5], with molecular weight in the range of 200,000-600,000 [3]. Isotactic PP has low density (0.89-0.92 g/cm^3) and possesses good chemical resistance and mechanical fatigue resistance [3]. Typical uses for PP include battery cases, semi-rigid packaging (yogurt and margarine containers, caps and closures for medicine), shrink wrap film; and packaging for bakery products, produce, and other foods [3, 5].

The widespread use of plastic packaging materials has created serious public concerns because landfill space is less and less available and more and more expensive. One way to reduce disposal of postconsumer packaging plastics is to recycle these packages. The plastic fraction in U.S. municipal solid waste (MSW) in 1996 was 9.4% by weight, but was considerably higher by volume (25.3%) because of the relatively low density of plastic materials compared to other materials [3]. The plastic fraction in MSW contains 25.3% LLDPE and LDPE, 20.9% HDPE, and 13.1% PP [3]. Recycling of LDPE and PP in the U.S. is relatively low compared to HDPE. In 2000, the recycling rates for LDPE and PP packaging were only 5.2% and 0.8%, respectively, but the recycling rate for HDPE packaging was 11.5% [7]. In 1998, the recycling rate for HDPE bottles was even higher than for PET bottles, 25.2% (734 million pounds) [3]. Markets for recycled HDPE bottles are pallets & lumber, drainage pipe, and films as well as containers [3].

In general, recycled HDPE bottles contain PP contamination, which can deteriorate their mechanical properties. Many investigators used wood fiber as a reinforcement filler in polyolefin resins [8-19]. Wood fiber is an attractive reinforcement fiber because it is a naturally plentiful organic fiber. In 2000, there was about 42.9% by weight of wood, paper and paperboard generated in MSW [7]. Wood fiber offers several benefits such as low cost (about 5 cents per pound), ease of processing, low equipment abrasion, ease of surface modification, high strength to weight ratio, renewability, lack of toxicity, recyclability, and improved tensile modulus and stiffness of composites [8]. However, the drawbacks of wood fiber are poor mechanical properties such as tensile strength (from the poor interfacial adhesion between hydrophobic plastics and hydrophilic wood fibers), poor dispersion of wood, and decomposition of lignocellulosics at relatively moderate elevated temperature (180-200°C) [8-10].

Several researchers have investigated the mechanical properties of composites of polyolefin matrices with reinforcements from different natural fibers. In addition, chemical treatments such as coupling agents have been studied in order to enhance the interfacial adhesion between the fiber and polyolefin matrix. Kalyankar [11] reported that the tensile modulus of composites of recycled HDPE (from milk bottles) with aspen wood fiber increased with wood fiber content, but the tensile strength, elongation at break and impact strength decreased. Addition of bonding agent (ethylene vinyl acetate) into the composite enhanced the impact strength. Woodhams *et al.* [12] and Chotipatoomwan [13] found that addition of wood fiber and paper fiber into HDPE caused a reduction in tensile and impact strength, but an increase in tensile modulus. Composites of PP with paper fiber (pulp) behaved similarly [12]. Raj *et al.* [14] showed

that the addition of wood fiber to HDPE increased the stiffness of the composites, but decreased the tensile strength. Thepwiwatjit [15] found similar results. She studied the mechanical properties of composites of recycled HDPE bottles from household use with wood fiber. She found that the tensile strength, yield strength and elongation decreased with an increase in the wood fiber fraction, but the modulus and impact strength slightly increased. Rojanarungtawee [16] conducted research on the effect of mixed HDPE and PP with aspen wood fiber (40% by weight) on the mechanical properties of plastic/wood fiber composites compounded at two different sets of processing temperatures, 150°C and 180°C, by a co-rotating twin screw extruder. The PP/HDPE ratios varied from 0% to 100% by weight. She found that at a processing temperature of 180°C, the ultimate tensile strength and modulus of elasticity were highest at 30:70 and 10:90 PP/HDPE, respectively. Only the ratios 0:100 and 30:70 PP/HDPE were processible at 150°C, as the processing temperature was lower than the melting temperature of PP, so the higher PP content in the polymer matrix caused the matrices to be too viscous to process. The tensile strength of 0:100 PP/HDPE was higher than that of 30:70 PP/HDPE but the difference in modulus was not statistically significant [16].

Substantial research has studied the surface modification of wood fiber using coupling agents to enhance the mechanical properties of polyolefin/wood fiber composites by improving the interfacial adhesion between the wood and polymer matrix. Nieman [10] reported that addition of maleic anhydride modified polypropylene (MAPP) into the recycled HDPE/wood fiber composites slightly improved the tensile strength and modulus by enhancing the adhesion between the recycled HDPE and wood fibers. Keal [17] studied the effect of dual coupling agent systems on the mechanical properties of

composites of recycled HDPE from milk containers and wood fiber. The coupling agent systems were sets of two of stearic acid, maleic anhydride modified polypropylene (MAPP) and ionomer modified polyethylene (IPE). The use of additives improved the tensile properties and creep of the composites, but the use of stearic acid/MAPP, and MAPP/IPE systems decreased the impact strength. Only the stearic acid/ionomer system did not reduce impact strength. The improvement of mechanical properties of composites with dual coupling systems compared to single additives was not significant. Raj *et al.* showed [14] that the reduction of tensile strength by addition of wood fiber in the HDPE/wood fiber composites could be improved by pretreating the wood fibers with a silane coupling agent/polyisocyanate before manufacturing. The increase of tensile strength resulted from improving the adhesion between the HDPE matrix and wood fibers. Kazayawoko *et al.* [18] reported that addition of maleated polypropylene (MAPP) improved the tensile strength of PP/wood fiber composites because MAPP may reduce the total wood fiber surface free energy, decreased the attractive forces among the fibers, improved fiber dispersion and fiber orientation, as well as enhanced the interfacial adhesion through mechanical interlocking. Kazayawoko *et al.* [19] attributed the improvement of the strength properties of PP/wood fiber composites to the esterification of the anhydride carbonyl groups of MAPP and the hydroxyl group of the wood fibers. However, the ductility and impact strength of the composites did not improve and the density of the composites did not reduce upon the chemical coupling of the polymer matrix and wood fiber. Recently, the microcellular foaming technique has shown the potential to reduce the density [20, 21] and enhance the impact strength of the materials [22-24].

In this study, the microcellular foaming technique was applied to improve the impact strength and reduce the density of HDPE/PP blends and their composites with wood fiber. The critical processing parameters affecting the foamability of the materials were investigated.

Microcellular Foam

Microcellular foam plastics are innovative cellular polymeric materials. They are characterized by cell sizes in the range of 0.1 to 10 μm in diameter and cell densities in the range of 10^9 to 10^{15} cells/ cm^3 and specific density reduction in the range of 5 to 98% [20, 21]. The idea to introduce microvoids into plastics was created by Professor Nam P. Suh of the Massachusetts Institute of Technology around 1980 in order to reduce the amount of plastic usage and reduce the cost of products without compromising the mechanical properties [20, 21]. It was hypothesized that if the voids (bubbles) were sufficiently small (smaller than the critical flaws pre-existing in polymers), the mechanical properties could be maintained or sometimes improved.

When the microcellular foam plastic materials are forced to break, the energy will dissipate around the small bubbles, therefore, it needs more energy to break. Crack propagation is inhibited by blunting the crack tip and increasing the amount of energy needed to propagate (Figure 1).

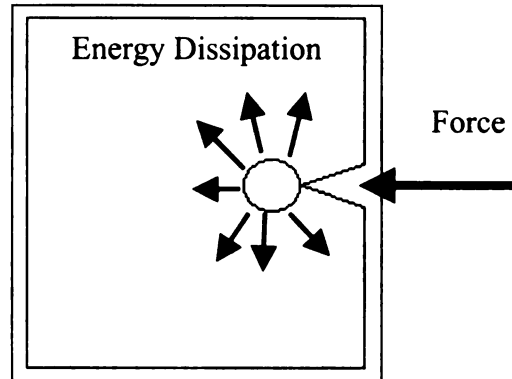


Figure 1: Energy dissipation around the bubbles (microvoids)

The microcellular foam is produced by using the thermodynamic instability of gas in a polymer system [20, 21, 25-29], and involves three steps: a) polymer/gas solution formation, b) microcellular nucleation, and c) cell growth [27, 28]. A microcellular foam can be produced in either a batch process, a semi-continuous process or a continuous process. A semi-continuous process was recently patented by Kumar and Schirmer [30]. A microcellular foam continuous process was demonstrated using extrusion by Park *et al.* [27-29]. However, in this thesis research we used the microcellular foam batch process; therefore, we will discuss only that process. In the microcellular foam batch process, in the first step, the plastic samples are placed in a pressure vessel under high pressure of a non-reacting gas such as CO₂ or N₂ at room temperature. Both CO₂ and N₂ are normally used as foaming agents in microcellular foam batch processes because both gases are low cost and have high solubility in most plastics [31]. The samples absorb gas over time until they are saturated. This step takes a long period of time, from hours to several days [25-28]. However, the saturation time can be reduced by decreasing the sample thickness, increasing the saturation temperature

and/or increasing the gas pressure [26]. In the next step, the saturated samples are removed from the pressure vessel and then are heated in a hot bath at the specified foaming temperature for the desired time to induce foaming. In this step, a large number of bubbles are nucleated and grown by inducing a large thermodynamic instability, which is related to quickly changing the solubility of the gas in the samples by decreasing pressure and increasing temperature [26]. The microcellular plastics are characterized by their void fraction, cell size, and cell density. The calculation of void fraction (VF) is determined by [32, 33]:

$$VF = 1 - \frac{\rho_f}{\rho} \quad (1)$$

where ρ is density of the unfoamed sample and ρ_f is density of the foamed sample.

The densities of the samples were measured by a water displacement technique (ASTM D-792) using the following equation:

$$Density = 0.9975 \left(\frac{M_a}{M_w} \right), \text{ (g/cm}^3\text{)} \quad (2)$$

where M_a is the weight of unfoamed or foamed samples measured in air and M_w the weight of unfoamed or foamed samples measured in distilled water.

The cell-population density per unit volume of the original unfoamed polymer (N_o) is characterized from the environmental scanning electron microscope (ESEM) micrographs by using the following equation [32, 33]:

$$N_o = \left(\frac{nM^2}{A} \right)^{3/2} \left[\frac{1}{1-VF} \right] \quad (3)$$

where n , A and M are the number of cells, area and the magnification factor of the micrograph, respectively. From the calculated VF (from equation 1) and equation 3, the average cell size, d , can be determined as [32]

$$d = \sqrt[3]{\frac{6VF}{\pi N_o(1-VF)}} \quad (2)$$

Microcellular foam plastics have received increasing attention in recent years because of their unique properties such as lower material usage per unit part, enhanced toughness [34], impact strength [21-24], fatigue life [35], and thermal stability [36]. Therefore, microcellular foam has potential applications in food packaging with reduced material costs, airplane and automotive parts with high strength-to-weight ratios, sports equipment with reduced weight and high-energy absorption, etc. [37, 38]. Recently, Jacobsen and Pierick [39] presented the advantages and examples of applications of microcellular foam such as automotive mirror brackets and nylon cable. They claimed

that the microcellular foam process could enhance product design, improve processing efficiency, and reduce product costs [39].

Research on microcellular foam polymers and their potential has been reviewed by Kumar [25] and Kumar and Weller [26]. Most research has centered on amorphous polymers such as polystyrene, polycarbonate, and polyvinyl chloride because they are much easier to foam compared to semi-crystalline polymers. However, some semi-crystalline polymers were studied such as polypropylene, polyethylene, and polyethylene terephthalate. Microcellular foam processing technology was first applied to semi-crystalline polymers by Colton [40] and Colton and Suh [41]. Colton [40] used high temperature gas saturation and foamed polymers above the melting temperature of pure resin. He studied microcellular foams of PP and found that microcellular foamed PP was successfully produced by adding appropriate nucleating agents to the formulation. He also reported that microcellular foamed ethylene-propylene copolymer could be produced without a nucleating agent at temperatures above the melting point because of the lower surface tension in the copolymer [40]. Doroudiani *et al.* [22] reported that the morphology of semi-crystalline polymers has a great influence on the solubility and diffusivity of the blowing agent as well as the cellular structure of the microcellular foams produced in a batch process. It is known that microcellular foaming of pure high density polyethylene (HDPE) and pure polypropylene (PP) is very difficult to achieve through a batch foaming process because of their high crystallinity [22, 42] except by quenching the polymer during cooling from the melt to achieve relatively low crystallinity [42] or by blending HDPE and PP [22]. However, the effects of critical processing parameters such as solubility and diffusivity of gas, foaming conditions

(foaming time, foaming temperature), blend composition, crystallinity, crystalline morphology and wood fiber content on void fraction and cell morphology (cell size and cell density) of HDPE/PP blends and their composites with wood fiber should be identified because these parameters can affect the foamability of materials, which is related to cellular morphology and mechanical properties such as impact strength.

Critical Processing Parameters in Microcellular Foaming

It is known that the foamability of polymers is affected by sorption of gas in the polymer matrix, the degree of supersaturation, the rate of gas diffusion into the cells, the stiffness of the gas/polymer matrix, the hydrostatic pressure or stress applied to the polymer matrix, the interfacial surface energy (i. e. surface tension), the viscoelastic properties of the polymer/gas solution and the amount of gas loss in the foaming process [21, 28, 32, 33], which are related to the degree of crystallinity [42], phase heterogeneity (i.e., additive, plasticizer, wood fiber content), blend morphology [21, 33, 43-45], interphase adhesion [33, 45], and foaming conditions [27, 28, 32, 37]. Substantial research has studied these parameters in different gas/polymer systems.

Kumar and Weller [46] reported that the cell density of foamed polycarbonate (PC) increases with saturation pressure but is independent of the foaming temperature over a wide temperature range (60-160°C). Weller and Kumar [47] studied the effect of saturation temperature on the polycarbonate-CO₂ system. They reported that foam density was not influenced by saturation temperature; however, the saturation temperature significantly affected the cell nucleation density and cell diameter. The cell nucleation density decreased and the average cell diameter increased when the saturation

temperature increased above approximately 80°C because of a change in free volume. Holl *et al.* [48] observed the change in cell geometry. They reported that cells with a high degree of spherical symmetry at sufficient foaming time begin as individual flat cracks produced in a solid polymer matrix.

Shimbo *et al.* [49] observed the relationship between foaming temperature and cell size and cell density for microcellular foamed poly(ethylene terephthalate) containing a polyolefin nucleating agent (CPET). They found that the cell size increased with increasing foaming temperature, but cell density was almost constant as foaming temperature increased. In addition, the relative density increased with decreasing average cell size. Baldwin *et al.* [27, 28] studied the effect of foaming conditions (saturation time, saturation pressure, foaming time and foaming temperature) on microcellular foam nucleation and cell growth of both amorphous and semi-crystalline poly(ethylene terephthalate) with and without a polyolefin nucleating agent in batch processing. They suggested that the saturation time should be selected as at least the minimum necessary to achieve a uniform gas concentration; therefore, the gas saturation time is not a suitable process variable. They found that cell density increased and cell size decreased with increasing saturation pressure in amorphous PET, resulting from the increase in gas concentration during saturation; however, the semicrystalline PET showed independence of cell density and cell size on saturation. Semicrystalline PET exhibited higher density and smaller cell size than amorphous PET, which contributed to heterogeneous nucleation in the amorphous/crystalline interphase regions [27, 28]. They also found that the foaming time had a relatively weak influence on cell density and cell size for both amorphous and semicrystalline PETs at foaming times larger than 2 and 10 sec,

respectively. For foaming temperature, they found that cell density increased with foaming temperature below 100°C and is relatively independent of foaming temperature above 100°C for amorphous PET. The cell size in amorphous PET is independent of foaming temperature. Semicrystalline PET and CPET showed no detectable cell structures when foamed at or below 100°C and 80°C, respectively. The cell density was constant over the foaming temperature, but cell size increased with foaming temperature for semicrystalline polymers. A bimodal structure could be observed in semicrystalline polymers at foaming temperatures above 150°C [27, 28].

Goel and Beckman [50, 51] studied microcellular foam of poly(methyl methacrylate) (PMMA). They found that cell size dropped sharply and cell density increased dramatically with increasing saturation pressure. The foam density decreased with increasing pressure because of a higher cell density and a reduced skin thickness. In addition, a lower cell density is generated at shorter saturation times due to the reduction in the rate of nucleation resulting from a lower amount of gas absorbed by the polymer at shorter times [50]. They further studied the effect of foaming temperature on the cell size. The cell size increased gradually with increasing foaming temperature, which they attributed to the decreasing viscosity of the system and increasing gas diffusivity in PMMA at higher temperatures [51].

Collias and Baird [52] found that cell size increased with foaming time for polystyrene using N₂ gas. Sumarno *et al.* [53] studied the production of microcellular foam polystyrene using N₂ gas by a quick-heating process (batch process) at high temperature. They found that at low temperature the cell size and volume expansion increased and cell density decreased with increased solubility of N₂ gas, but this was not

true for high temperature because of cell coalescence at high temperatures. The change in decompression rate influenced the dissolved gas in the sample, and affected the cellular structure. They [54] further investigated the effects of saturation temperature, saturation pressure, and late- and quick-heating processes on the cellular structure. The solubility of N_2 gas related to saturation pressure and temperature has a significant effect on the cellular structure. The results showed that the average cell size decreased and the cell-population density increased with increase in the gas solubility. They reported that the heating time could be used as a controlling parameter to achieve a desired cell structure and volume expansion ratio.

Lee *et al.* [55] studied the microcellular foam of styrene-co-acrylonitrile (SAN). They found that average cell size decreased with increasing saturation pressure and increasing swelling time. The average cell size increased with increased foaming temperature. The trend of cell density was opposite to that of cell size.

Murray *et al.* [31] investigated solid-state microcellular acrylonitrile-butadiene-styrene (ABS) foams using CO_2 as the blowing agent. They found that the rate of CO_2 sorption and desorption in acrylonitrile-butadiene-styrene was influenced by the gas concentration where concentration of gas at equilibrium increased as the saturation pressure was increased. They found that the rate of gas desorption increased with increasing saturation pressure and the higher saturation pressures allowed lower sorption times. They concluded that foam density decreased linearly with increasing foaming temperature until a minimum density is reached, since at higher foaming temperature, the cells begin to collapse, leading to a denser structure and poor morphology.

Matuana *et al.* [23, 24, 32, 33, 56] extensively studied microcellular foam of PVC and PVC/wood-fiber composites. They reported that void fraction increased with increasing foaming temperature. The void fraction of pure PVC was higher than composites and the void fraction of composites with silane-treated fibers was higher than that of composites with untreated wood fibers because a higher CO₂ concentration remained in the PVC and composite with treated fibers and the PVC with untreated wood fiber has weak interfaces allowing gas to escape quickly [56]. Foaming temperature did not influence the cell population density, and the cell population density of PVC is higher than that of the composite with treated fiber at a foaming time of 5 sec. The average cell size increased with foaming temperature as the gas diffused into the cells and then cells expanded [56]. They studied the effects of cellulosic-fiber content and fiber surface treatment in the PVC composite [33]. They concluded that the addition of cellulosic-fiber into the composite decreased the gas solubility, regardless of the surface treatment; however, the composite with treated fiber had higher gas concentration than the composite with untreated fiber. The diffusivity of CO₂ increased with increasing fiber content for untreated fiber, but the reverse tendency was observed in composites with treated fiber. The high diffusion in composites with untreated fiber might be attributed to a poorly bonded interface between the wood and the polymer matrix. They also reported that the cell density is strongly dependent on the dissolved gas in the material and the void fraction is influenced by the addition of wood fiber in the composite [33]. They showed that the void fraction is dependent on foaming time and foaming temperature and average cell size depends on foaming temperature, but the cell population density is independent of the foaming temperature [23, 24]. However, a high void fraction (above

20%) could not be achieved due to the increase of stiffness and melt viscosity of the composite from adding the wood fiber. They further studied adding dioctyl phthalate (DOP) as a plasticizer and coupling agent to improve the void fraction. They found that the plasticizer content in the composite with untreated fiber had no effect on the void fraction because of low gas concentration from the materials due to rapid gas escape via the poor interface between the polymer and the wood, but the void fraction of PVC and composites with treated fiber increased with plasticizer up to 20 parts per hundred resin (phr). They observed that the void fraction, cell size and cell density are strongly dependent on the foaming time and temperature. They concluded that the desired cell density, cell size and void fraction (above 20%) could be achieved by controlling the concentration of plasticizer, the surface treatment of wood fiber, foaming time and foaming temperature [32]. Holl *et al.* [57] studied the effect of additives on microcellular foam PVC. They found that the additives and processing aids helped lower the foaming temperature and reduced the density of PVC. Matuana and Mengelolu [58] studied the effect of impact modification on pure PVC and PVC/wood-flour composites. They reported that impact modification accelerated gas loss, regardless of the modification type. A similar void fraction to unmodified samples could not be achieved when impact modifiers were presented. Therefore, they concluded that the addition of impact modifiers is not necessary for microcellular foam samples.

Effect of Crystallinity on Microcellular Foam

Little research has been found in the literature for microcellular foamed semicrystalline polymers by a batch process. In general, for the microcellular foaming

batch process, semicrystalline polymers are difficult to control compared to amorphous polymers and the cellular structures of foamed semicrystalline polymers are not uniform due to the heterogeneity of the polymers [42]. Colton studied nucleation phenomena in polypropylene with and without nucleating agent and copolymer of polyethylene-propylene [40]. He stated that there are three major obstacles for microcellular foaming of polypropylene and polyethylene:

- 1) Low gas solubility in the gas/polymer solution because gas cannot dissolve in the crystalline regions, causing widely scattered microvoids.
- 2) Foaming temperature should be above the melting temperature.
- 3) The crystalline morphology.

He overcame these problems by foaming above the melting point and adding appropriate nucleating agents in the polymer or by using polypropylene/ethylene copolymer.

Baldwin *et al.* [37] studied the effects of crystallinity in semicrystalline and amorphous PET on microcellular foam batch processing. They observed that crystallization in polymers resulted in lower solubility, higher polymer matrix stiffness, and lower diffusivity. They reported that an increase in saturation pressure increased gas concentration in the polymers and induced crystallinity resulting from the plasticizing nature of gas at high concentrations, but decreased the glass transition temperature due to the plasticizing effect. They also found that it is more difficult to produce a microcellular foam with semicrystalline PET than with amorphous PET. The semicrystalline polymer is more difficult to foam because it requires relatively high temperatures to foam.

However, the foamed semicrystalline PET had higher cell density and smaller cell size than amorphous PET [37]. They concluded that the crystallinity of the polymer matrix

plays a major role in the microcellular foaming process. The cell growth process in semicrystalline PET foams tended to be governed by the viscoelastic behavior of the CO₂/PET solution, but the amorphous PET foams tended to be governed by the diffusion of gas. The cell nucleation process could occur throughout the materials or at high energy regions of heterogeneous interphases. In semicrystalline PET, cells nucleated at the interface of amorphous and crystalline regions because of lower local activation energy. The cell size of foamed semicrystalline polymers decreased because of the increased stiffness of the matrix from crystallites. Moreover, a bimodal structure was observed. This was caused by the variation of crystallinity across the sheet thickness or perhaps because gas concentration across the sheet was not uniform. They found that increasing the foaming time and foaming temperature increased the cell size for semicrystalline PET.

Doroudiani *et al.* [42] studied the effect of crystallinity and morphology on the microcellular foam structure of semicrystalline polymers such as HDPE, polybutylene (PB), PP, and PET. They varied the crystallinity of the polymers by changing the cooling rate. They found that the solubility and diffusivity decreased with increasing crystallinity. With a fast cooling rate, the samples had low crystallinity and high gas solubility, and produced foams with a more uniform and finer cell structure, but with a slow cooling rate, the samples had high crystallinity and produced nonuniform cell structures. They concluded that the morphology of foamed semicrystalline polymers was strongly dependent on the solubility and diffusivity of gas.

Therefore, in order to achieve microcellular structure in semicrystalline polymers, these polymers have to cool down fast to lower crystallinity and increased gas solubility.

Moreover, the foaming temperature should be relatively high (above T_m), but it was limited by strength of the materials.

Microcellular Foams of Polymer Blends

Colton and Suh [59] studied nucleation phenomena in microcellular foams. They investigated the cell nucleation of microcellular foams of polystyrene using N_2 gas with and without nucleating agent. They hypothesized that if the additive concentration is very low, the additive did not exist as distinct second-phase particles in the matrix; therefore, those particles did not provide sites for heterogeneous nucleation. But if additives did exist as a second phase, they would act as nucleation sites for cell nucleation. In the case of homogeneous nucleation, it will occur in the free volume of the polymer, but in heterogeneous nucleation (distinct second-phase particles), these particles provide advantageous nucleation sites for heterogeneous nucleation to occur. Baldwin *et al.* [27, 28, 37] showed that nucleated PET (containing a polyolefin additive) had a higher cell density than homopolymer PET, because the presence of the nucleating polyolefin particles acts like heterogeneous sites for cell nucleation. In the interface region between nucleating particles and the polymer matrix, the activation energy necessary to nucleate a cell is less than in the homopolymer PET, resulting in the preferential nucleation of bubbles at the interface.

Ramesh *et al.* [60, 61] investigated polystyrene (PS) and high impact polystyrene (HIPS) using N_2 and CO_2 gas as blowing agents. They reported that the elastomeric inclusions in HIPS act as nucleation sites. They observed that elastic inclusions around 2

μm in size provided excellent nucleation sites. Below a critical radius of elastic inclusions, the inclusions were not effective as nucleation sites.

Siripurapu *et al.* [44] studied microcellular foam of poly(vinylidene fluoride) (PVDF), a semicrystalline polymer, with the amorphous polymer poly(methyl methacrylate) (PMMA) in a continuous process. They reported that microcellular foamed PVDF had poor cellular morphology because PVDF has a high degree of crystallinity (>40%) and low CO_2 solubility, only 2% (maximum). Moreover, the melting temperature (T_m) is high, 170°C , whereas the glass transition temperature (T_g) is low (-40°C). Because of the large T_g and T_m difference, foaming could not be produced near the T_g of the polymer, which is necessary to reduce cell coalescence. They blended PVDF with PMMA, and found that addition of PMMA dramatically improved the cellular morphology of materials relative to pure PVDF. They also observed that the crystallinity of PVDF decreased and the T_g of PVDF increased with increasing PMMA content. The blend viscosity decreased as the PMMA content increased. Additionally, the CO_2 solubility in blends was higher than in pure PVDF; the higher CO_2 concentration increased the cell nucleation rate and the cell density.

Doroudiani *et al.* [22] studied the processing and characterization of microcellular foamed high-density polyethylene/isotactic polypropylene (HDPE/iPP) blends. They reported that the morphology of semi-crystalline polymers has a great influence on the solubility and diffusivity of the CO_2 gas as well as on the cellular structure of the microcellular foams produced in a batch process. They observed that blending decreased the crystallinity of iPP in the blends because it interfered with the growth of the PP spherulites. Blends of HDPE and iPP enhance the microcellular foam with uniform fine

cells compared to pure polymers, and the foamed HDPE/iPP 50:50 gave a very high volume expansion ratio and had a uniform cell structure. They concluded that introducing a microcellular foam structure into materials improved the impact strength which was deteriorated by blending.

It can be concluded that polymer blends improved microcellular structures by the inclusions acting as sites for cell nucleation because of lower activation energy at the interface. However, the inclusions must be above a critical radius to be effective as nucleation sites.

References:

1. T. C. Mike Chung, "Functionalization of Polyolefins", Academic Press, New York (2002).
2. J. R. Fried, "Polymer Science and Technology", Prentice Hall PTR, New Jersey (1995).
3. R. J. Hernandez, S. E. M. Selke, and J. D. Culter, "Plastic Packaging Properties, Processing, Application and Regulations", Hanser Gardner Publications, Inc., Cincinnati, Ohio (2000).
4. "An Introduction to the History of Plastics", [Online] Available at <http://www.packagingtoday.com/introplasticexplosion.htm>, March 2003.
5. G. Odian, "Principles of Polymerization", John Wiley & Sons, Inc., New York (1991).
6. T. O. J. Kresser, "Polyolefin Plastics", Van Nortrand Reinhold Company, New York (1969).
7. EPA, "Municipal Solid Waste in the United States: 2000 Facts and Figures, the U.S. Environmental Protection Agency, EPA530-R-02-001., [Online] Available at <http://www.epa.gov/epaoswer/non-hw/muncpl/report-00/report-00.pdf>, March 2003.
8. K. Vanichvarod, "Composite Material of Mixed Low Density Polyethylene/Polypropylene and Wood Fiber", M. S. Thesis, Michigan State University, East Lansing, MI, USA (2002).
9. R. T. Woodhams, G. Thomas and D. K. Rodgers, "Wood Fibers as Reinforcing Fillers for Polyolefins", *Polym. Eng. Sci.*, **24** (15), 1166-1171 (1984).
10. K. A. Nieman, "Mechanical Property Enhancement of Recycled HDPE and Wood Fiber Composites Due to the Inclusion of Additives", M. S. Thesis, Michigan State

- University, East Lansing, MI, USA (1989).
11. V. Kalyankar, "Mechanical Characteristics of Composites Made from Recycled HDPE Obtained from Milk Bottles", M. S. Thesis, Michigan State University, East Lansing, MI, USA (1989).
 12. R. T. Woodhams, G. Thomas and D. K. Rodgers, "Wood Fibers as Reinforcing Fillers for Polyolefins" *Polym. Eng. Sci.*, **24** (15), 1166-1171 (1984).
 13. T. Chotopatomwan, "Processing and Mechanical Property Testing of Paper Fiber and HDPE Composites", M. S. Thesis, Michigan State University, East Lansing, MI, USA (1998).
 14. R. G. Raj, B. V. Kokta, G. Grouleau, and C. Daneault, "The Influence of Coupling Agents on Mechanical Properties of Composites Containing Cellulosic Fillers", *Polymer.-Plast. Technolo. Eng.*, **29** (4), 339-353 (1990).
 15. N. Thepwiwatjit, "Composite of Wood Fiber and Recycled HDPE Bottles from Household Use", M. S. Thesis, Michigan State University, East Lansing, MI, USA (2000).
 16. S. Rojanarungtawee, "Composite of Wood Fiber and Mixed Recycled Thermoplastics", M. S. Thesis, Michigan State University, East Lansing, MI, USA (1998).
 17. M. D. Keal, "Effect of Dual Additives Systems on the Mechanical Properties of Aspen Fiber/Recycled HDPE Composites", M. S. Thesis, Michigan State University, East Lansing, MI, USA (1990).
 18. M. Kazayawoko, J. J. Balatinecz, and L. M. Matuana, "Surface Modification and Adhesion Mechanisms in Woodfiber-Polypropylene Composites", *J. of Mater. Sci.*,

- 34, 6189-6199 (1999).
19. M. Kazayawoko, J.J. Balatinez, R. T. Woodhams, and S. Law, "Effect of ester linkages on the mechanical properties of wood fiber-polypropylene composites", *J. of Reinf. Plast. Comps.*, **16** (15), 1383-1406 (1997).
 20. J. Martini, F. A. Waldman, and N. P. Suh, Patent U.S.4,473,665 (1984).
 21. J. Martini, F. A. Waldman, and N. P. Suh, "The Production and Analysis of Microcellular Thermoplastic Foams", *SPE ANTEC Tech. Papers*, **28**, 674-672 (1982).
 22. S. Doroudiani, C. B Park, and M. T. Kortschot, "Processing and Characterization of Microcellular Foamed High-Density Polyethylene/Isotactic Polypropylene Blends", *Polym. Eng. Sci.*, **38** (7), 1205-1215 (1998).
 23. L. M. Matuana, C. B. Park, and J. J. Balatinez, "Cell Morphology and Property Relationships of Microcellular Foamed PVC/Wood-Fiber Composites", *Polym. Eng. Sci.*, **38** (11), 1862-1872 (1998).
 24. L. M. Matuana, C. B. Park, and J. J. Balatinez, "Structures and Mechanical Properties of Microcellular Foamed Polyvinyl Chloride", *Cellular Polym.*, **17** (1), 1-16 (1998).
 25. V. Kumar, "Microcellular Polymers: Novel Materials for the 21st Century", *Cellular Polymers*, **12** (3), 207-223 (1993).
 26. V. Kumar and J. E. Weller, "Microcellular Foams", ACS Symposium Series 669, Polymeric Foams Science and Technology, Kishan C. Khemani, Editor, Eastman Chemical Company Developed from A Symposium Sponsored by the Division of Polymer Chemistry, Inc, American Chemical Society, Washington D. C., pp 101-114 (1997).

27. D. F. Baldwin, C. B. Park, N. P. Suh, "A Microcellular Processing Study of Poly(Ethylene Terephthalate) in the Amorphous and Semicrystalline States. Part I: Microcell Nucleation", *Polym. Eng. Sci.*, **36** (10), 1425-1435 (1996).
28. D. F. Baldwin, C. B. Park, N. P. Suh, "A Microcellular Processing Study of Poly(Ethylene Terephthalate) in the Amorphous and Semicrystalline States. Part II Cell Growth and Process Design", *Polym. Eng. Sci.*, **36** (11), 1446-1453 (1996).
29. C. B. Park, A. H. Behraves, and R. D. Venter, "A Strategy for The Suppression of Cell Coalescence in the Extrusion of High-Impact Polystyrene Foams", ACS Symposium Series 669, Polymeric Foams Science and Technology, Kishan C. Khemani, Editor, Eastman Chemical Company Developed from A Symposium Sponsored by the Division of Polymer Chemistry, Inc, American Chemical Society, Washington D. C., pp115-129 (1997).
30. V. Kumar and H. G. Schirmer, Patent U.S. 5,684,005 (1997).
31. R. E. Murray, J. E. Weller, and V. Kumar, "Solid-State Microcellular Acrylonitrile-Butadiene-Styrene Foams", *Cellular Polymers*, **19** (6), 413-425 (2000).
32. L. M. Matuana, C. B. Park, and J. J. Balatinez, "Processing and Cell Morphology Relationships for Microcellular Foamed PVC/Cellulosic-Fiber Composites", *Polym. Eng. Sci.*, **37** (7), 1137-1147 (1997).
33. L. M. Matuana, C. B. Park, and J. J. Balatinez, "Characterization of Microcellular PVC/Cellulosic-Fibre Composites" *J. Cellular Plast.*, **32** (5), 449-467 (1996).
34. D. I. Collias, D. G. Baird, and R. J. M. Borggreve, "Impact Toughening of Polycarbonate by Microcellular Foaming", *Polymer*, **35** (18), 3978-3983 (1994).
35. K. A. Seeler, and V. Kumar, "Tension-Tension Fatigue of Microcellular

- Polycarbonate: Initial Results”, *J. Reinforced Plast. Comp.*, **12**, 359-376 (1993).
36. M. Shimbo, D. F. Baldwin, and N. P. Suh, “Viscoelastic Behavior of Microcellular Plastics”, *Proc. of Polymeric Materials: Science and Engineering, Amer. Chem. Soc. Conference*, **67**, 512-513 (1992).
37. D. F. Baldwin, N. P. Suh, and M. Shimbo, “Gas Dissolution and Crystallization in Microcellular Thermoplastic Polyesters”, *Cellular Polymers*, **38**, 109-128 (1992).
38. L. M. Matuana, “Wood Fiber/Polyvinyl Chloride Composites and Their Microcellular Foams”, Ph. D Thesis, Faculty of Forestry, University of Toronto, Toronto, Ontario, Canada, (1997).
39. K. Jacobsen and D. Pierick, “Microcellular Foam Molding: Advantages and Application Examples”, *SPE ANTEC Papers*, **2**, 28-32 (2000).
40. J. S. Colton, “The Nucleation of Microcellular Foams in Semi-Crystalline Thermoplastics”, *Materials & Manufacturing Processes*, **4**, 253-262 (1989).
41. J. S. Colton and N. P. Suh, U.S. Patent 5,160,674 (1992).
42. S. Doroudiani, C. B. Park, and M.T. Kortschot, “Effect of the Crystallinity and Morphology on the Microcellular Foam Structure of Semicrystalline Polymers”, *Polym. Eng. Sci.*, **36** (21), 2645-2662 (1996).
43. M. R. Holl, M. Ma, and V. Kumar, “Effects of Additives on Microcellular PVC Foams: Part I – Effect on Processing and Microstructure”, *Cellular Polymers*, **17** (4), 271-283 (1998).
44. S. Siripurapu, Y. J. Gay, J. R. Royer, J. M. DeSimone, S. A. Khan, and R. J. Spontak, “Microcellular Polymeric Foams (MPFs) Generated Continuously in Supercritical Carbon Dioxide”, *Mat. Res. Soc. Symp.* **629**, 991-996 (2000).

45. S. Doroudiani, M. T. Kortschot, and C. B. Park, "Structure and Mechanical Properties Study of Foamed Wood Fiber/Polyethylene Composites", *SPE ANTEC Papers*, **541**, 2046-2050 (1997).
46. V. Kumar and J. E. Weller, "Bubble Nucleation in Microcellular Polycarbonate Foams", *Polymeric materials, science and engineering, proceedings of the ACS Division of Polymeric Materials, Science and Engineering, American Chemical Society*, 501-502 (1992).
47. J. E. Weller and V. Kumar, "The Effect of Elevated Sorption Temperature on Cell Nucleation in the Polycarbonate-CO₂ System", *SPE ANTEC Papers*, **857**, 1947-1978 (1997).
48. M. R. Holl, V. Kumar, J. L. Garbini and W. R. Murray, "Cell Nucleation in Solid-State Polymeric Foams: Evidence of A Triaxial Tensile Failure Mechanism", *J. Mater. Sci.*, **34**, 637-644 (1999).
49. M. Shimbo, D. F. Baldwin, and N. P. Suh, "The Viscoelastic Behavior of Microcellular Plastics with Varying Cell Size", *Polym. Eng. Sci.*, **35** (17), 1387-1393 (1995).
50. S. K. Goel and E. J. Beckman, "Generation of Microcellular Polymeric Foams Using Supercritical Carbon Dioxide. I: Effect of Pressure and Temperature on Nucleation", *Polym. Eng. Sci.*, **34** (14), 1137-1147 (1994).
51. S. K. Goel and E. J. Beckman, "Generation of Microcellular Polymeric Foams Using Supercritical Carbon Dioxide. I: Cell Growth and Skin formation", *Polym. Eng. Sci.*, **34** (14), 1148-1156 (1994).
52. D. I. Collias and D. G. Baird, "Impact Behavior of Microcellular Foams of

- Polystyrene and Styrene-Acrylonitrile Copolymer, and Single-Edge-Notched Tensile Toughness of Microcellular Foams of Polystyrene, Styrene-Acrylonitrile Copolymer, and Polycarbonate”, *Polym. Eng. Sci.*, **35** (14), 1167-1177 (1995).
53. Sumarno, T. Sunada, Y. Sato, S. Takishima, and H. Masuoka, “ Polystyrene Microcellular Plastic Generation by Quick-Heating Process at High Temperature”, *Polym. Eng. Sci.*, **40** (7), 1510-1521 (2000).
54. Sumarno, T. Sunada, Y. Sato, S. Takishima, and H. Masuoka, “Production of Polystyrene Microcellular Foam Plastics and a Comparison of Late- and Quick-Heating”, *J. Appl. Polym. Sci.*, **77**, 2383-2395 (2000).
55. K. N. Lee, H. J. Lee, and J. H. Kim, “Preparation and Morphology Characterization of Microcellular Styrene-Co-Acrylonitrile (SAN) Foam Processed in Supercritical CO₂ *Polymer International*, **49**, 712-718 (2000).
56. L. M. Matuana, C. B. Park, and J. J. Balatinecz, “Effect of Cell Morphology on the Properties of Microcellular PVC/Wood-Fiber Composites”, *Cellular and Microcellular Materials*, V. Kumar and K.A. Seeler, Eds., ASME, New York, MD- Vol. **76**, pp.1-16 (1996).
57. M. R. Holl, M. Ma, V. Kumar, and R. R. Kwapisz, “The Effect of Additives on Microcellular PVC Foams: Part 1-Effect on Processing and Microcellular Structure”, *Cellular Polymers*, **17** (4), 271-283 (1998).
58. L. M. Matuana and Fatih Mengeloglu, “Microcellular Foaming of Impact-Modified Rigid PVC/Wood-Flour Composites”, *J. Vinyl Addit. Technol.*, **7** (2), 67-75 (2001).
59. J. S. Colton and Suh, “The Nucleation of Microcellular Thermoplastic Foam with Additives: Part II: Experimental Results and Discussion”, *Polym. Eng. Sci.*, **27** (7),

500-503 (1987).

60. N. S. Ramesh, J. A. Kweeder, D. H. Rasmussen, and G. A. Campbell, "The Heterogeneous Nucleation of Microcellular Foams Assisted by the Survival of Microvoids in Polymers Containing Low Glass Transition Particles. Part I: Mathematical Modeling and Numerical Simulation", *SPE ANTEC Tech Papers*, **38**, 1078-81 (1992).
61. N. S. Ramesh, D. H. Rasmussen, and G. A. Campbell, "Nucleation of Microcellular Foam", *SPE ANTEC Tech. Papers*, **37**, 1398-1400 (1991).

Chapter 3

Microcellular Foam of Polymer Blends of HDPE/PP and Their Composites with Wood Fiber

This chapter is slightly modified from *Journal of Applied Polymer Science*, **88** (12), 2842-2850 (June 2003). It is co-authored by P. Rachtanapun¹, S. Selke¹ and L. M. Matuana²

¹School of Packaging, Michigan State University, East Lansing, Michigan, 48824

²Department of Forestry, Michigan State University, East Lansing, Michigan, 48824

ABSTRACT

In this study, the effects of batch processing conditions (foaming time and temperature) and blend composition as well as the effect of incorporating wood fiber into the blends on the crystallinity, sorption behavior of CO₂, void fraction and cellular morphology of microcellular foamed HDPE/PP blends and their composites with wood fiber were studied. Blending decreased the crystallinity of HDPE and PP and facilitated microcellular foam production in blend materials. The void fraction was strongly dependent on the processing conditions, and on blend composition. Foamed samples with a high void fraction were not always microcellular. The addition of wood fiber inhibited microcellular foaming.

INTRODUCTION

The U.S. Environmental Protection Agency reported that containers and packaging are the largest category of plastic in municipal solid waste (MSW). Recycling reduces the impact of this waste on limited landfill space. Polyolefins are the largest group of polymers used as packaging materials such as water bottles, milk bottles, juice bottles, rigid bottle packaging for household detergents, and other cleaners. High-density polyethylene (HDPE) is commonly used as the body of the bottle and polypropylene (PP) is commonly used as the cap. These rigid bottles are easy to separate and collect, thus making them one of the top recycled materials. However, separation of plastic waste into individual parts and sorting is costly and time consuming, and separation of HDPE and PP is difficult because of their similar density. Moreover, it is well known that blends of HDPE/PP decrease the material's mechanical properties such as impact strength because HDPE and PP are immiscible and incompatible, despite the similarity of their chemical structures [1]. Substantial research has concentrated on improving the mechanical properties by adding compatibilizer to the polyolefins to improve the interfacial adhesion [2-4].

Not long ago, microcellular foaming was proposed as an effective technique to toughen plastics [5]. Microcellular foamed polymer is a new class of materials characterized by cell densities larger than 10^9 cells per cubic centimeter of unfoamed materials and cell sizes in the range of 0.1 to 10 μm . Microcellular polymers are produced through the utilization of the thermodynamic instability of gas in a polymer system. Three main steps are involved [6]: 1) polymer/gas solution formation by

saturating a polymer with a high pressure gas, 2) microcellular nucleation, and 3) cell growth and density reduction. Microcellular polymers offer a reduction in material usage and are light weight. They also exhibit enhanced impact strength [7-10], toughness [5], fatigue life [11], and thermal stability [12]. Therefore, this method could be applied to improve the mechanical properties of HDPE/PP blends. However, the research on microcellular foams has been mainly directed at amorphous polymers. Very little work has been done on the foaming of semicrystalline polymers because microcellular foaming of semicrystalline polymers is difficult to achieve because of the high crystallinity and the size of the crystallites [13]. Only one report of research on microcellular foamed HDPE/ isotactic PP blends was found [8].

In this study, microcellular foams of polymer blends of HDPE and PP as well as composites with wood fiber were investigated to determine the effects of processing conditions, blend composition, and wood fiber content on the void fraction and cell morphology of the materials. The effects of blend composition and crystallinity on solubility and diffusion of CO₂ and consequently on the void fraction were also investigated.

METHODOLOGY

Sample Preparation

Injection-molding-grade HDPE [Dow HDPE 00452N, melt index 4g/10min (ASTM D1238), density 0.952 g/cc] and extrusion and injection-molding-grade PP [INSPIRE H704-04, melt index 4 g/10min (ASTM D1238), density 0.90 g/cc from Dow Plastics Cooperation, Midland, MI] were used as polymeric matrices. Commercial grade carbon dioxide was used as a blowing agent. Aspen hardwood fiber at 30 parts wood fiber per hundred parts resin was used as the reinforcement (Abitibi Corporation, Alpeno, MI). This ratio was chosen in accord with previous work on microcellular foamed wood/plastic composites [9]. The mesh size of wood fiber was in the range of 30-200.

In this study, the effects of blend composition, foaming time and temperature and wood fiber content on void fraction and cell morphology of foamed samples were investigated. HDPE/PP blends (100:0, 70:30, 50:50, 30:70 and 0:100 % w/w) and composites with wood fiber were manufactured using a Baker Perkins Model ZSK-30, 30 mm, 26:1 co-rotating twin-screw extruder (Werner & Pfleiderer Corporation, Ramsey, New Jersey), at 100 rpm. Two different temperature profiles were used. For neat HDPE, temperatures were set at 155°C for all six control zones. For PP and HDPE/PP blends, temperatures were set at 180°C in the first two zones and 155°C in the remaining four.

Six-inch lengths of extrudate were compression-molded (Carver Laboratory Press, Model M, Menomenee Falls, WI) at 30,000 psi for 5 minutes, temperature 160°C for HDPE and HDPE composites and 185°C for samples containing PP. The 2 mm thick panels were cut to 0.5 × 1 inch test specimens.

Sorption Experiments

Saturation of the samples with CO₂ [room temperature (23-25°C), 800 psi for 24 hours] was used to determine the diffusion and solubility of CO₂ in the samples. CO₂ uptake (solubility) was measured by weight gain immediately after pressure release. Weight loss as a function of $t^{1/2}/l$ was used to determine the diffusion coefficient [14-16].

Microcellular Foaming Experiments

In batch microcellular foaming experiments, the CO₂ saturated samples were immediately immersed in a hot glycerin bath [14-16] at various foaming temperatures (135°C, 160°C and 175°C) for foaming times of 5 s, 10 s, 20 s or 30 s and then were immediately quenched in cold water.

Characterization of Foams

The densities of the samples were measured by a water displacement technique (ASTM D-792). The weights of unfoamed and foamed samples were measured in air (M_a) and in distilled water (M_w), and the density determined by:

$$\text{Density} = 0.9975 \left(\frac{M_a}{M_w} \right), (\text{g/cm}^3) \quad (1)$$

The reported density is the average of five replicates.

The void fraction (VF) was calculated by [14-16]:

$$VF = 1 - \frac{\rho_f}{\rho} \quad (2)$$

where ρ is density of the unfoamed sample and ρ_f is density of the foamed sample. Sample morphology was investigated through an environmental scanning electron microscope ESEM (ElectroScan 2020 system with a LaB6 filament, Electro Scan Company, Boston, MA.) at acceleration voltages of 10 and 20 kV. The samples were immersed in liquid nitrogen and fractured, to ensure that the microstructure remained clean and intact [14].

Differential Scanning Calorimetry (DSC)

DSC was performed using 3-5 mg samples (DSC 2010, TA Instruments, New Castel, Del.) to investigate the crystallinities of the HDPE, PP and their blends. Three to five replicates were heated from room temperature to 200°C at 10°C/min. Nitrogen was used as a purge gas with a flow rate of 50 mL/minute. The heats of fusion of HDPE and PP used in the calculation of the crystalline fractions were 293 and 209 J/g, respectively [17]. The calculation of crystallinity (χ) of the HDPE, PP and their blends, and total crystallinity are described in detail in Chapter 6.

RESULTS AND DISCUSSION

Effect of Blending on Crystallinity

The effects of blending on crystallinity are shown in Table 1. Blending decreased the crystallinity of both HDPE and PP. The crystallinity of HDPE decreased gradually with increase in the PP component. The melting temperature of HDPE decreased slightly with increase in the PP content. For PP, there were no statistically significant differences between the crystallinities in the three blend compositions; all were less than for pure PP. There was a similar pattern with the melt temperature; melting temperatures of all blends were slightly lower than that of pure PP, but there was no consistent pattern. The total amount of crystallinity of the blends decreased as PP content increased (Table 1). This behavior is expected because another phase interfered with crystalline growth and T_m decreased as crystallinity decreased.

Table 1: Melting temperature (T_m) and percent crystallinity (χ) of HDPE/PP blend samples

| Blends | $T_{m,HDPE}$ (°C) | χ_{HDPE} (%) | $T_{m,PP}$ (°C) | χ_{PP} (%) | Total % χ in Blends |
|--------|-------------------|-------------------|-----------------|-----------------|--------------------------|
| HDPE | 132.1 | 73.3 | - | - | 73.3 |
| 70:30 | 130.0 | 68.6 | 163.4 | 43.4 | 61.1 |
| 50:50 | 130.0 | 63.5 | 162.4 | 40.1 | 51.8 |
| 30:70 | 128.8 | 61.9 | 163.8 | 43.8 | 49.2 |
| PP | - | - | 164.3 | 49.2 | 49.2 |

Effects of Polymer Blend Composition and Wood Fiber Content on Solubility and Diffusivity of Carbon Dioxide

It is known that the foamability of polymers is affected by the sorption of gas in the polymer, and that the mechanisms of cell nucleation and cell growth are influenced by the amount of gas dissolved in the polymer and the rate of gas diffusion [5, 9, 11-13]. Figure 1 shows that the amount of CO₂ gas dissolved decreased as the ratio of HDPE increased in the blends without wood fibers. The measured solubility of gas was strongly dependent on the total crystallinity of the polymer (Table 1). When the HDPE component increased, the total crystallinity increased and the solubility of gas decreased. The measured solubility of gas decreased with the addition of wood fiber into the polymer matrix, perhaps due to the high crystallinity of the fiber, as suggested by Matuana *et al.* [10, 14]. However, the measured solubility of gas in composites tended to increase as the HDPE component increased. The reason for this behavior is not fully understood.

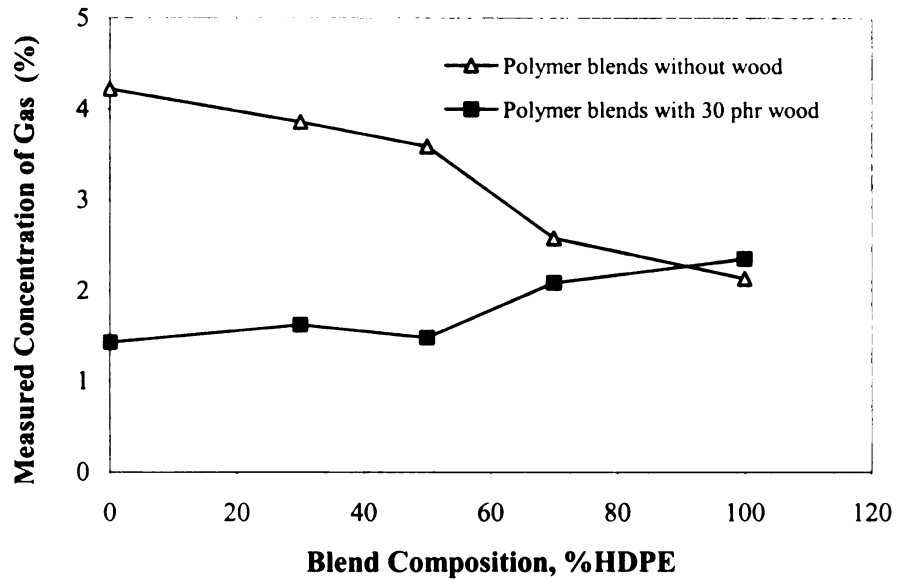


Figure 1: Measured solubility of CO₂ in the polyolefin blends as a function of blend composition.

Desorption isotherm curves for the polymer blends and composites with wood fiber are illustrated in Figure 2. As expected, gas diffusion rates were higher in the composites than in the polymers. In general, the addition of fiber to the polymer without pretreating the wood surface leads to poor adhesion between the wood fiber and the polymer matrix. The poor surface adhesion of the polar wood to the non-polar polymer provides a channel through which gas can quickly escape from the composite [10-14].

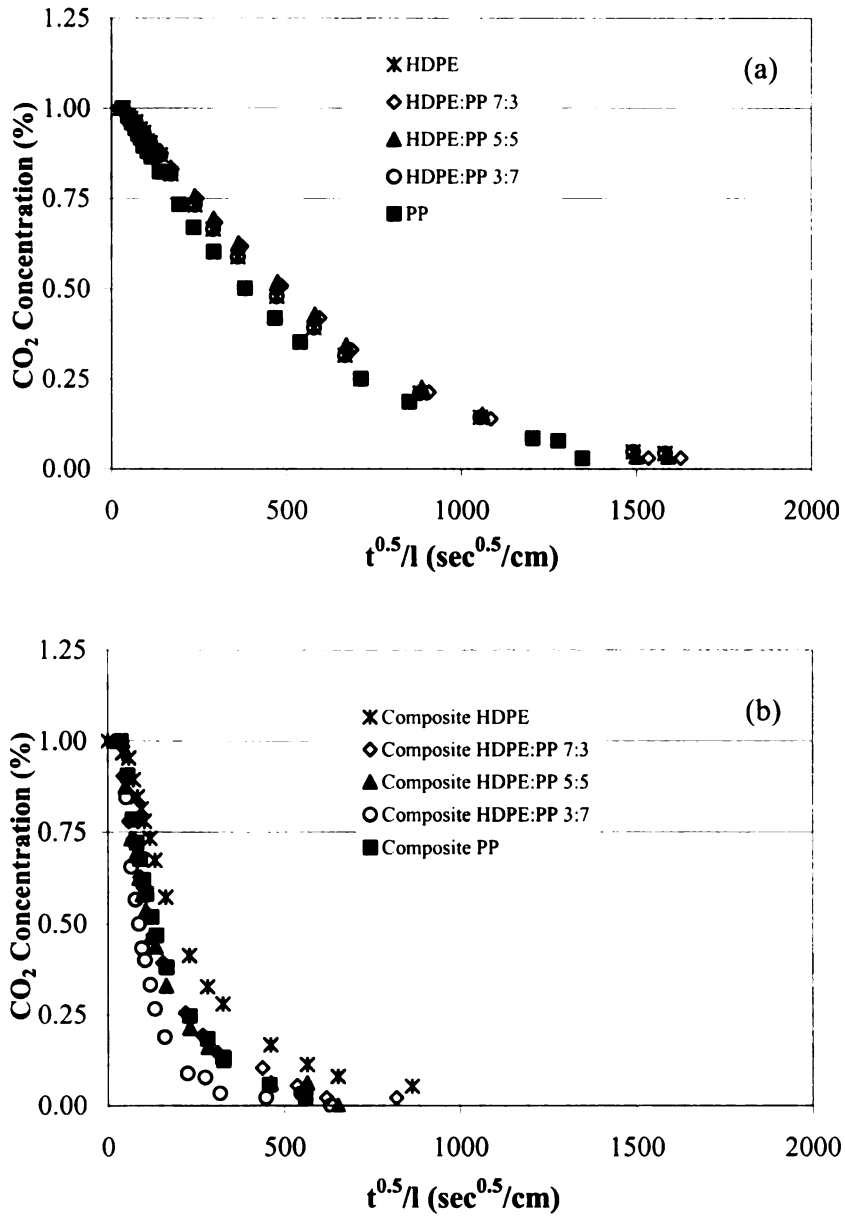


Figure 2: Desorption curves of polymer blends and composites with wood fiber (a) polymer blends, (b) composites with wood fiber.

Effects of Foaming Conditions, Blend Composition, and Wood Fiber Content on Void Fraction of Foamed Samples

The effects of foaming time, foaming temperature, and blend composition on the void fractions of both unfilled HDPE/PP blends and HDPE/PP blends filled with 30 phr wood fiber are shown in Figures 3 and 4, respectively.

Figure 3 shows that at the lowest foaming temperature (135°C), and at short foaming times (5 and 10 seconds), a high void fraction (above 20%) was not achieved for any conditions. However, when the foaming temperature was well above the melting temperature of the sample and foaming time was long enough (20 and 30 seconds), the void fraction increased dramatically as foaming time and temperature increased. Thus, when the foaming temperature of HDPE at 30 seconds increased from 135 to 160 and 175°C, the void fraction increased from 5.8% to 35.4% and 43.9%, respectively.

The ability to use high temperature to achieve high void fraction is limited by the rapid decrease of strength of the polymer at temperatures above the melting point. This results in substantial deformation of the polymer matrix, even though the softened polymer matrix is favorable to bubble growth [14, 15]. For example, foaming HDPE samples at 175°C for 30 seconds provided a high void fraction, but the high temperature and long foaming time resulted in deformation of the samples.

The void fraction of the foamed polymer blends was strongly dependent on the blend compositions. Polymer blends of 70:30 and 30:70 HDPE/PP resulted in a higher void fraction, but 50:50 HDPE/PP behaved strangely. Its void fraction was lower than that of the other blends at all foaming times and temperatures, and generally was even

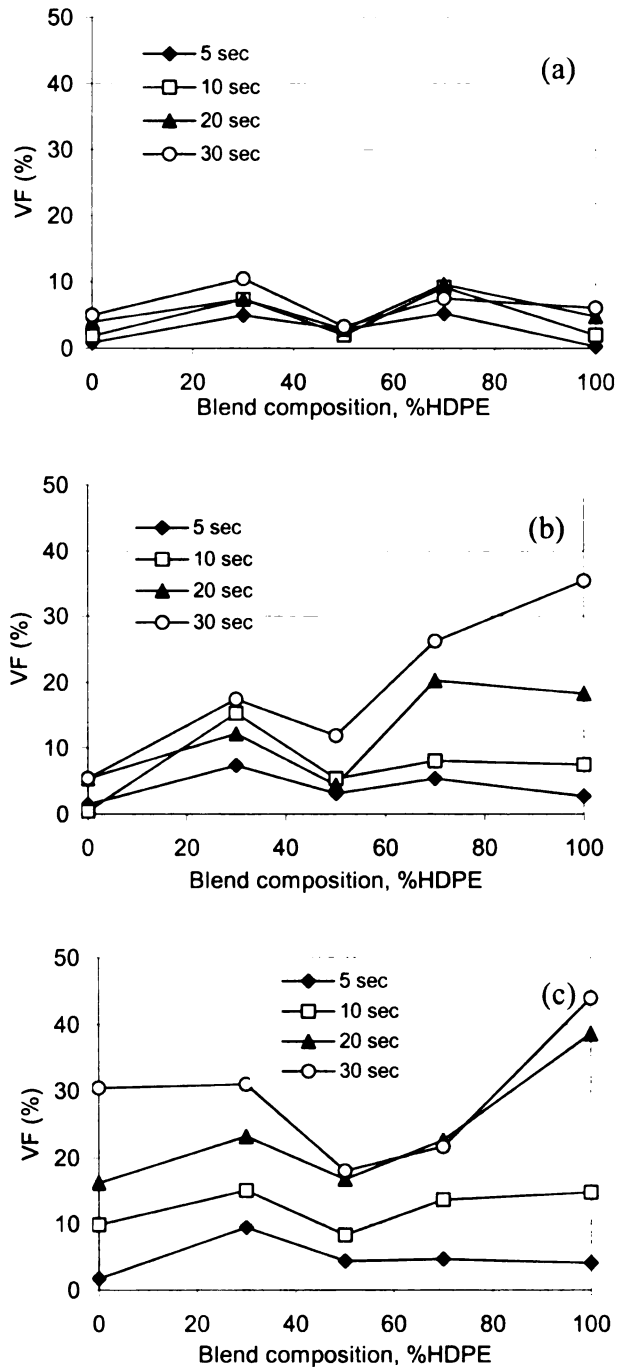


Figure 3: Effects of foaming time and blend composition on the void fraction of unfilled HDPE/PP blends foamed at (a) 135°C, (b) 160°C, (c) 175°C.

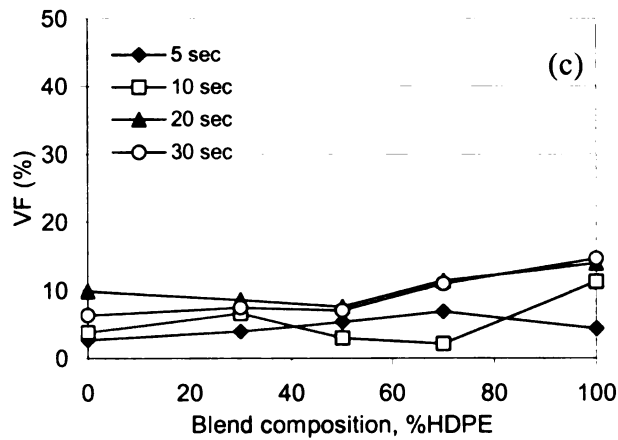
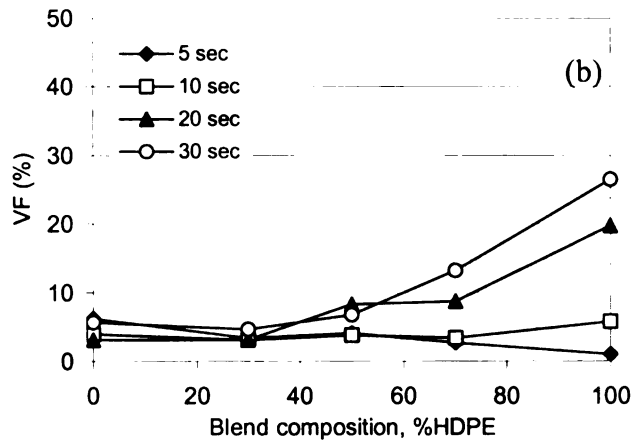
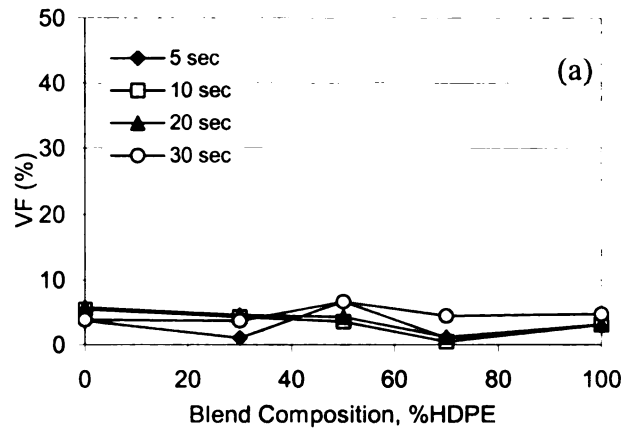


Figure 4: Effects of foaming time and blend composition on the void fraction of HDPE/PP blend filled with 30 phr wood fibers foamed at (a) 135°C, (b) 160°C, (c) 175°C.

lower than pure HDPE and PP. By the rule of mixing, the void fraction of 50:50 HDPE/PP would be expected to be between the void fractions of HDPE and PP. For instance, the void fraction of 50:50 HDPE/PP blend was less than 20% for a foaming time of 30 seconds at 175°C, whereas the void fraction of HDPE was above 40% and PP was around 30%. This was especially surprising in view of the results of Doroudiani *et al.* [8], who achieved the highest void fraction at this composition. This behavior should be investigated further.

As shown in Figure 4, the addition of wood fiber decreased the void fraction because of lower CO₂ uptake (Figure 1); microcellular foams with a high void fraction were not achieved. HDPE composites had a reasonably high void fraction at high foaming temperatures and times, but were not microcellular, as will be discussed in the next section. The mechanism of cell growth is governed by the stiffness of the gas/polymer matrix, the rate of gas diffusion, and the amount of gas loss [14, 15]. The void fraction decreased dramatically with the addition of wood fiber as it increased both matrix stiffness and the rate of gas loss (Figure 2).

Cell Morphology of Foamed HDPE/PP Blends

ESEM micrographs of unfoamed polymer blends are shown in Figure 5. Both HDPE and PP exhibited a single phase, while the blends showed phase separation. In the 70:30 HDPE/PP blend, HDPE was the continuous phase and PP the dispersed phase. The size of the PP regions increased with increasing PP content. Interpenetrating inversion structures were observed in 50:50 HDPE/PP. Phase inversion was observed in 30:70 HDPE/PP; PP became the continuous phase and HDPE the dispersed phase [18].

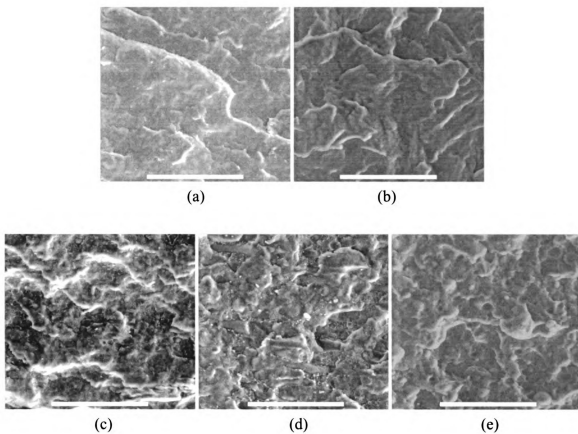


Figure 5: ESEM micrographs of unfoamed polymers and their blends: (a) HDPE, (b) PP, (c) HDPE/PP 70:30, (d) HDPE/PP 50:50, and (e) HDPE/PP 30:70 (all scale bars 45 μm).

The effect of blend composition on cell morphology at fixed foaming time and foaming temperature (30 s, 175°C) is shown in Figure 6. In both HDPE and PP, a high void fraction could be achieved but cell morphology was not favorable. HDPE had a large-celled structure on the surface (Figure 6a) and a microcellular structure toward the middle of the samples (Figure 6b). For foamed PP, cellular structures developed only locally near the surface of the samples (Figure 6c), and the center of the sample could not be foamed (Figure 6d). When HDPE and PP were blended, the microcellular structures were significantly improved and more uniformly distributed (Figure 6f, g). However, the void fraction of 70:30 HDPE/PP blend did not increase at this condition (Figure 3c) because of cell coalescence (Figure 6e). Foaming 50:50 HDPE/PP gave uniform structures but a high void fraction was not achieved for reasons not understood.

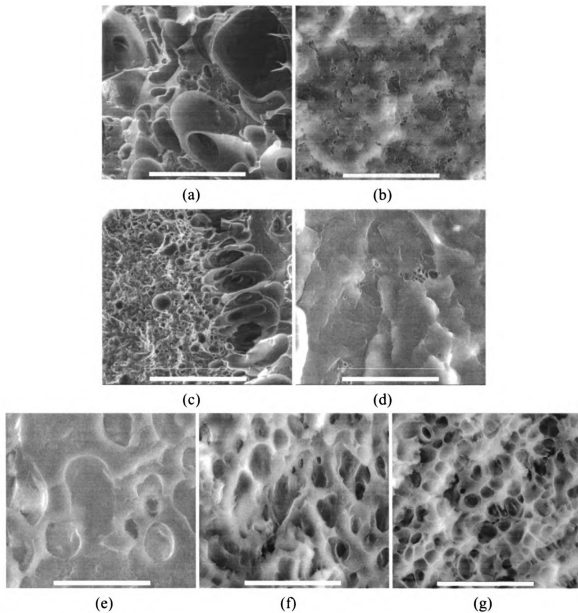
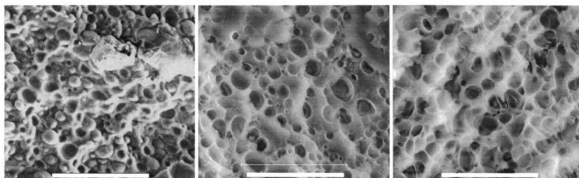


Figure 6: ESEM micrographs of foamed polymer blends at 175°C for 30 sec
 (a) HDPE (surface) (scale bar 450 μm), (b) HDPE (center) (scale bars 45 μm),
 (c) PP (surface) (scale bar 450 μm); (d) PP (center) (e) HDPE/PP 70:30,
 (f) HDPE/PP 50:50, and (g) HDPE/PP 30:70 (all scale bars 45 μm).

The effect of foaming temperature on cell morphology is shown in Figure 7. It is known that the poorly bonded interfacial regions of immiscible polymer blends have a lower activation energy for bubble nucleation [19]. Therefore, the interfaces of the immiscible HDPE/PP blends could be favorable as nucleating sites for bubble growth. Therefore, the blend of 30:70 HDPE/PP was investigated at a low foaming temperature (135°C) and short time (10 seconds). Bubbles nucleated between the HDPE globules and PP matrix (Figure 7a); however, a high void fraction was not achieved. It is difficult to distinguish marks of the pull-out of HDPE globules from true microcellular bubbles. When the foaming time and temperature increased, the void fraction increased (Figure 3), resulting in a uniformly distributed microcellular foamed structure (Figure 7b, c).



(a)

(b)

(c)

Figure 7: ESEM micrographs of foamed HDPE/PP 30:70 samples at (a) 135°C for 10 sec, (b) 160°C for 30 sec, (c) 175°C for 30 sec (scale bar 45 µm).

The effect of foaming time on the cell morphology was studied by maintaining the blend composition at 30:70 HDPE/PP and the foaming temperature at 175°C and varying the foaming times (5, 10, 20 and 30 sec). The void fraction increased when the foaming time increased (Figure 3c) and ESEM micrographs showed the development of cell growth (Figure 8). When the foaming time increased, the average cell size increased, as shown in Figure 8.

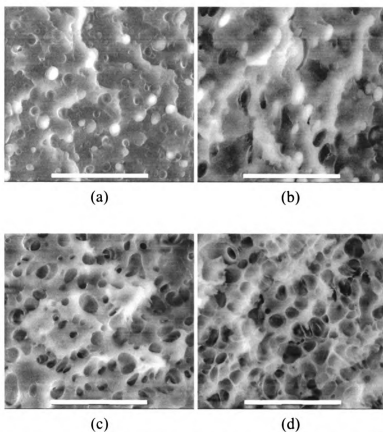


Figure 8: ESEM micrographs of foamed HDPE/PP 30:70 samples at 175°C for (a) 5 sec, (b) 10 sec, (c) 20 sec, (d) 30 sec (all scale bars 45 µm).

The effect of wood fiber on the cell morphology was studied by maintaining the foaming conditions at 175°C for 30 seconds. The void fraction decreased when wood fiber was added to the polymer matrix. Some cellular structures could be found in HDPE composites, but these features were not evident in the PP or the blends (Figure 9). Addition of wood fiber to the polymers decreased the solubility and increased the rate of CO₂ gas diffusion in the samples, accelerating the gas loss during foaming. Only a small portion of gas remained for nucleation and cell growth. Therefore, development of microcellular structures and a high void fraction were inhibited by adding the wood fiber.

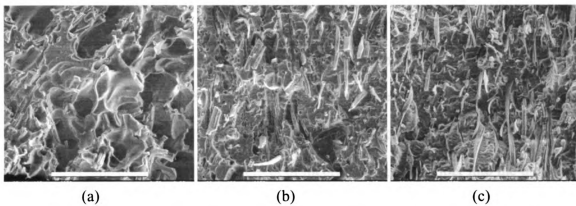


Figure 9: ESEM micrographs of foamed composite with wood fiber at 175°C for 30 sec
(a) HDPE (b) HDPE /PP 70:30 (c) PP (all scale bars 450 μm).

CONCLUSIONS

In this chapter, the microcellular foams of polymer blends of HDPE and PP as well as composites with wood fiber were studied to produce foamed samples with high void fraction. The effects of batch processing conditions (foaming time and temperature) and blend composition as well as the effect of incorporating wood fiber into the blends on the crystallinity, sorption behavior of CO₂, void fraction and cellular morphology of microcellular foamed HDPE/PP blends and their composites with wood fiber were investigated.

Solubility of CO₂ in polymer blends decreased with increased HDPE content, as expected from the increase in total crystallinity. Measured solubility of CO₂ in the composites was lower than in polymer blends because of the crystallinity of the wood fiber. A trend of increasing solubility of CO₂ in composites with increasing HDPE content was observed; the reason for this is not well understood. In blends, the crystallinity of both HDPE and PP decreased.

A high void fraction was dependent more on the rate of gas loss (diffusivity) than on the solubility of gas in the polymers or composites. The amount of crystallinity affected the cell structure. Blending facilitated the formation of microcellular foam structures in polyolefins. All polymer blends foamed with a uniform fine cellular structure, while large-celled structures were observed near the surface in pure HDPE and PP. Blend composition, foaming time and temperature strongly affected the void fraction and cell morphology. To achieve a high void fraction the foaming temperature had to be well above the melting temperature of the polymer, and the foaming time had to be long

enough. Addition of wood fiber to the polymers inhibited the foaming ability, related to less total gas and fast gas loss.

REFERENCES

1. K. Solc (Ed.), *Polymer Compatibility and Incompatibility, Principles and Practices*, Harwood, New York (1982).
2. U. Niebergall, J. Bohse, S. Seidler, W. Grellmann, and L. Schümann, "Relationship of Fracture Behavior and Morphology in Polyolefin Blends", *Polym. Eng. Sci.*, **39** (6), 1109-1118 (1999).
3. H. P. Blom, J. W. Teh, and A. Rudin, "iPP/HDPE Blends. II. Modification with EPDM and EVA", *J. Appl. Polym. Sci.*, **60**, 1405-1417 (1996).
4. C. M. C. Bonelli, A. F. Martins, E. B. Mano, and C. L. Beatty, "Effect of Recycled Polypropylene on Polypropylene/High-Density Polyethylene Blends", *J. Appl. Polym. Sci.*, **80**, 1305-1311 (2001).
5. D. I. Collias, D. G. Baird, and R. J. M. Borggreve, "Impact Toughening of Polycarbonate by Microcellular Foaming", *Polymer*, **35** (18), 3978-3983 (1994).
6. J. Martini, F. A. Waldman, and N. P. Suh, Patent U.S.4,473,665 (1984).
7. J. Martini, F. A. Waldman, and N. P. Suh, "The Production and Analysis of Microcellular Thermoplastic Foams", *SPE ANTEC Tech. Papers*, **28**, 674-676, (May 1982).
8. S. Doroudiani, C. B. Park, and M. T. Kortschot, *Polym. Eng. Sci.*, "Processing and Characterization of Microcellular Foamed High-Density Polyethylene/Isotactic Polypropylene Blends", **38** (7), 1205-1215 (1998).

9. L. M. Matuana, C. B. Park, and J. J. Balatinecz, "Cell Morphology and Property Relationships of Microcellular Foamed PVC/Wood-Fiber Composites", *Polym. Eng. Sci.*, **38** (11), 1862-1872 (1998).
10. L. M. Matuana, C. B. Park, and J. J. Balatinecz, "Structures and Mechanical Properties of Microcellular Foamed Polyvinyl Chloride", *Cellular Polym.*, **17** (1), 1-16 (1998).
11. K. A. Seeler, and V. Kumar, "Tension-Tension Fatigue of Microcellular Polycarbonate: Initial Results", *J. Reinforced Plast. Comp.*, **12**, 359-376 (1993).
12. M. Shimbo, D. F. Baldwin, and N. P. Suh, "Viscoelastic Behavior of Microcellular Plastics", *Proc. of Polymeric Materials: Science and Engineering, Amer. Chem. Soc. Conference*, **67**, 512-513 (1992).
13. S. Doroudiani, C. B. Park, and M. T. Kortschot, "Effect of the Crystallinity and Morphology on the Microcellular Foam Structure of Semicrystalline Polymers", *Polym. Eng. Sci.*, **36** (21), 2645-2662 (1996).
14. L. M. Matuana, C. B. Park, and J. J. Balatinecz, "Processing and Cell Morphology Relationships for Microcellular Foamed PVC/Cellulosic-Fiber Composites", *Polym. Eng. Sci.*, **37** (7), 1137-1147 (1997).
15. L. M. Matuana and F. Mengeloglu, "Microcellular Foaming of Impact-Modified Rigid PVC/Wood-Flour Composites", *J. Vinyl Addit. Technol.*, **7** (2), 67-75 (2001).
16. L. M. Matuana, C. B. Park, and J. J. Balatinecz, "Characterization of Microcellular PVC/Cellulosic-Fibre Composites", *J. Cellular Plast.*, **32** (5), 449-467 (1996).

17. B. Wunderlich, *Macromolecular physics, Vol. 1, Crystal Structure, Morphology, Defects*, Academic Press, New York (1973).
18. M. Fujiyama and Y. Kawasaki, "Rheological Properties of Polypropylene/High Density Polyethylene Blend Melts. I Capillary Flow Properties", *J. Appl. Polym. Sci.*, **42**, 467-480 (1991).
19. J. S. Colton and N. P. Suh, "The Nucleation of Microcellular Thermoplastic Foam with Additives: Part II: Experimental Results and Discussion", *Polym. Eng. Sci.*, **27**, 493 (1987).

Chapter 4

Cell Morphology and Impact Strength of Microcellular Foamed HDPE/PP Blends

This chapter is slightly modified from *SPE ANTEC Tech paper* currently in press (2003). It is co-authored by P. Rachtanapun¹, L. M. Matuana² and S. Selke¹

¹School of Packaging, Michigan State University, East Lansing, Michigan, 48824

²Department of Forestry, Michigan State University, East Lansing, Michigan, 48824

ABSTRACT

Polymer blends such as result from recycling of postconsumer plastics often have poor mechanical properties. Microcellular foams have been shown to have the potential to improve properties, and permit higher value uses of mixed polymer streams. In this study, the effects of microcellular batch processing conditions (foaming time and temperature) and HDPE/PP blend compositions on the cell morphology (the average cell size and cell-population density) and impact strength were studied. Optical microscopy was used to investigate the miscibility and crystalline morphology of the HDPE/PP blends. Pure HDPE and PP did not foam well at any processing conditions. Blending facilitated the formation of microcellular structures in polyolefins due to the poorly bonded interfaces of immiscible HDPE/PP blends which favored cell nucleation. The experimental results indicated that well-developed microcellular structures are produced in HDPE/PP blends at ratios of 50:50 and 30:70. The cell morphology had a strong relationship with the impact strength of foamed samples. Improvement in impact strength was associated with well-developed microcellular morphology.

INTRODUCTION

Containers and packaging are the largest category of plastics in municipal solid waste. Recycling reduces the impact of this waste on limited landfill space. Polyolefins, including high density polyethylene (HDPE) and polypropylene (PP), are the cheapest and most-used plastics for short-term packaging. HDPE is commonly used in blow-molding applications such as water bottles, milk bottles, juice bottles, and household detergent bottles and PP is commonly used as the spout or the closure on these bottles. A problem is the difficulty of separating HDPE and PP from each other in recycling processes because of their similar density. It is well known that the incompatibility and immiscibility of HDPE and PP blends will lead to poorer mechanical properties such as impact strength [1, 2] and tensile properties [2] compared to the pure components. Substantial research has concentrated on improving the mechanical properties by adding compatibilizer to the polyolefins to improve the interfacial adhesion [3-6].

Microcellular plastics are foamed polymers characterized by cell densities larger than 10^9 cells/cm³ per unit volume of the original unfoamed polymer and cell sizes in the range of 0.1 to 10 μ m [7]. They have shown the potential to improve impact strength [8-10] and permit higher value uses of mixed polymer streams. Microcellular foam processing technology was first applied to semi-crystalline polymers by Colton [11] and Colton and Suh [12]. Colton [11] used high temperature gas saturation and foamed polymers above the melting temperature of pure resin. He studied microcellular foams of PP and found that microcellular foamed PP was successfully produced by adding appropriate nucleating agents in the formulation. He also reported that microcellular foamed ethylene-propylene copolymer could be

produced without a nucleating agent at temperatures above the melting point because of the lower surface tension in the copolymer [11]. Doroudiani *et al.* [13] reported that the morphology of semi-crystalline polymers has a great influence on the solubility and diffusivity of the blowing agent as well as the cellular structure of the microcellular foams produced in a batch process. It is known that microcellular foaming of pure high density polyethylene (HDPE) and pure polypropylene (PP) is very difficult to achieve through a batch foaming process due to their high crystallinity [13, 14] except by quenching the polymer during cooling from the melt to achieve relatively low crystallinity [13]. It has been reported that microcellular foams were greatly enhanced by using HDPE/isotactic PP blends [14].

Our recent study has shown that void fraction and cell morphology of microcellular foams of HDPE/PP blends and their composites with wood fiber were strongly dependent on processing conditions (foaming time and foaming temperature) and blend composition as well as wood fiber content (Chapter 3). The solubility of CO₂ in HDPE/PP blends related to total crystallinity. Blends decreased in crystallinity of both HDPE and PP, and facilitated microcellular foam production with a uniform microcellular structure, while foamed pure HDPE and pure PP had a large-celled structure on the surface and were unfoamed at the center with high void fraction (Chapter 3).

In this paper, the microcellular foaming of HDPE/PP blends is investigated further to determine the effects of batch processing conditions (foaming time and temperature) and blend composition on the cell morphology (average cell size and cell-population density) and impact resistance of foamed materials. The effects of blend composition on miscibility and crystalline morphology of the HDPE/PP blends were investigated and correlated to cell morphology of foamed samples.

METHODOLOGY

Materials

Injection molding grade HDPE [Dow HDPE 00452N, melt index 4g/10min (ASTM D1238), density 0.952 g/cc] and extrusion and injection molding grade PP [INSPIRE H704-04, melt index 4 g/10min (ASTM D1238), density 0.90 g/cc from Dow Plastics] were blended in different ratios (100:0, 70:30, 50:50, 30:70 and 0:100 % w/w). Commercial grade carbon dioxide was used as a blowing agent.

Blends and Sample Preparation

Blends of HDPE/PP at various HDPE to PP weight ratios were prepared using a Baker Perkins Model ZSK-30, co-rotating twin-screw extruder (Werner & Pfleiderer Corporation, Ramsey, New Jersey) at 100 rpm. The compounding conditions and test specimens are described in Chapter 3.

Optical Microscopy (OM)

The morphologies of the unfoamed samples were examined to determine the effects of blending on the miscibility and crystalline morphology of the samples. Specimens were cut from unfoamed samples. First, the samples were cut perpendicular to the long axis to obtain bars with width about 5 mm. Second, thin sections (1-2 μm) were cut perpendicular to the width of those bars. For the pure HDPE and HDPE/PP 70:30 blend, the sections were cut by microtome RMC MT-7-CRX with a diamond knife at -120°C under liquid nitrogen. The HDPE/PP 50:50 blend was cut at -100°C , and the HDPE/PP 30:70 blend and pure PP were cut at -30°C . The change of cutting temperature was required because all samples were too

soft and viscous to be cut at room temperature [15]. An Olympus BH-2 polarizing microscope at crossed and parallel polars (light and polarized light) was used to obtain optical micrographs.

Microcellular Foaming Experiments and Property Characterization

In batch microcellular foaming experiments, the samples were saturated with CO₂ [room temperature (23-25°C), 800 psi for 24 hours]. The CO₂-saturated samples were microcellular foamed by immersing them in a hot glycerin bath [16, 17] at different foaming temperatures (135°C, 160°C and 175°C) for various foaming times of 5 s, 10 s, 20 s or 30 s. Foamed samples were immediately quenched in cold water to prevent cell deterioration. The void fraction, average cell diameter, and the cell-population density of foamed samples were determined following the approach described in references [16-18].

The Izod impact strengths of unfoamed and foamed samples were determined using a Tinius Olsen model 92 Impact Tester. Notched samples were tested at room temperature following ASTM D 256-97 [19]. At least five to ten foamed samples and 20 unfoamed samples were tested. All foamed samples were allowed to desorb gas for at least two weeks before property testing [20, 21].

Statistical Analysis

Data were analyzed by ANOVA and Tukey's Studentized Range (HSD) test using the SAS software program ($\alpha = 0.05$).

RESULTS AND DISCUSSION

Optical Microscopy Observations

Our previous study reported the effect of HDPE/PP blend composition on crystallinity (Chapter 3). Crystallinities of pure HDPE and PP were 73.3% and 49.2%, respectively; blending decreased the crystallinity of both the HDPE and PP phases (Chapter 3). In this study, optical microscopy with light and polarized light was used to study the miscibility and crystalline morphologies of pure HDPE and PP as well as their blends.

Phase separation was evident in optical micrographs of HDPE/PP blends (Figure 1), as expected since blending of immiscible polymers usually leads to multiphase systems. Micrographs of pure PP showed regular spherulite patterns with well-developed positive radius (type I) α -spherulites [22-24] (size around 20-30 μm) (Figure 1b). HDPE did not exhibit the spherulite structure (Figure 1a). The blending of HDPE with PP dramatically changed the crystalline morphology of the samples (Figures 1c, d, e). The regular spherulite patterns of PP became more irregular as HDPE content increased. The large dispersed spherical HDPE particles appear to have hindered the regular growth of the spherulites [22]. The observed trend agrees with earlier results published by several authors. Lovinger and Williams [25] and Teh [26] reported that the addition of LDPE to PP resulted in a drastic decrease in the spherulite size of the PP. The HDPE has also an irregular spherulite pattern with high crystallinity (Chapter 3). In our previous work, ESEM micrographs of pure HDPE and pure PP showed a single phase, but their blends exhibited two phases (Chapter 3). These results agree with the morphology seen in optical microscopy (Figure 1).

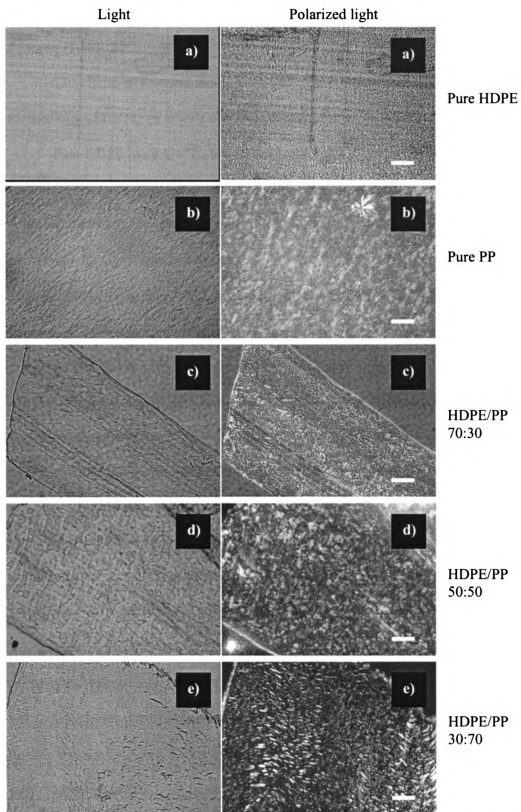


Figure 1: Optical micrographs of HDPE/PP blends (Left column is light and right column is polarized light) a) Pure HDPE, b) Pure PP, c) HDPE/PP 70:30, d) HDPE/PP 50:50 and e) HDPE/PP 30:70 (all scale bars 25 μm).

Effects of Foaming Conditions and Blend Composition on Cell Morphology of Foamed HDPE/PP Blends

The effects of foaming temperature and blend composition on the cell morphology of HDPE/PP blends at a fixed foaming time (30 s) are shown in Figure 2.

Pure HDPE has a low T_m with high crystallinity (Chapter 3). At 135°C, pure HDPE did not foam (Figure 2a). It is believed that at this foaming temperature, the polymer matrix remained too stiff and viscous to allow the polymer to move sufficiently for significant cell growth (Chapter 3). At 160°C, foamed pure HDPE had large cells near the surface, a microcellular structure in subsurface layers and no foaming at the core (Figure 2a).

At 175°C, pure HDPE samples were well foamed (Figure 1a). However, foamed samples had large cells at the surface and a microcellular structure at the subsurface and the center (Figure 2a). Foaming at high temperature softened the matrix and reduced the resistance for bubble growth. In general, the viscoelastic behavior of the semicrystalline polymer matrix is a strong function of temperature and time. Large cells developed at the surface of the sample because exposure to higher temperature for longer time at the surface led to the relaxation of the cell structure, which achieved a lower free energy state through cell coalescence [17, 27].

Pure PP did not foam at 135 and 160°C (Figure 2b) because the foaming temperature was too low. At 175°C, foamed pure PP had a non-uniform structure. Large cells developed close to the surface of the samples while the center of the sample was not foamed (Chapter 3) and a microcellular structure developed in the subsurface (Figure 2b).

It should be noted that pure HDPE and pure PP are not suited for microcellular foam batch processing.

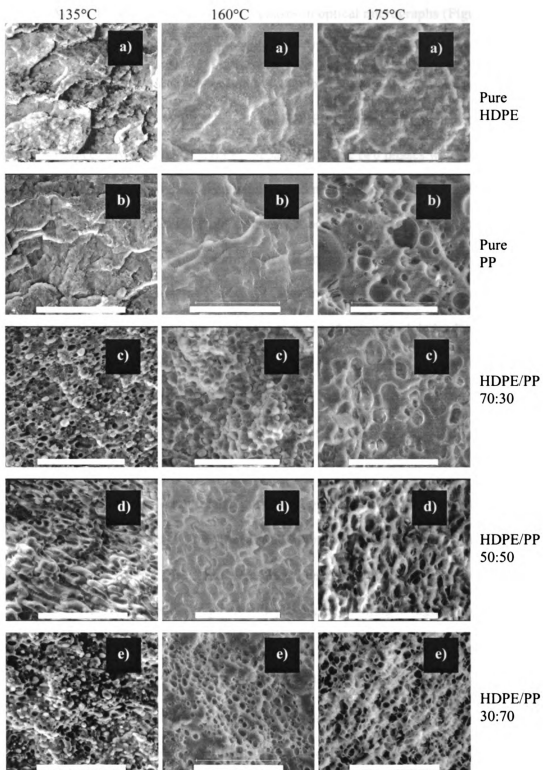


Figure 2: ESEM micrographs of foamed polymer blends for 30 sec (at 135°C, left column), (at 160°C, middle column) and (at 175°C, right column) a) Pure HDPE, b) Pure PP, c) HDPE/PP 70:30, d) HDPE/PP 50:50, and e) HDPE/PP 30:70 (all scale bars 100 μ m).

All HDPE/PP blends showed two phases in optical micrographs (Figures 1c, d, e). The interfacial regions of immiscible HDPE/PP blends have a lower activation energy for cell nucleation with poor bonding (Chapter 3) [8]. At 135°C, pure HDPE and pure PP could not be foamed, but for the HDPE/PP blends, cell nucleation started at the interface between HDPE and PP. Separation of the two phases was observed (Figure 2c, d, e), which was not seen in unfoamed polymer blends (Chapter 3). The cells could nucleate in HDPE/PP blends at this condition, but the polymer matrix was still too stiff and viscous to allow significant cell growth. Therefore, blends did not achieve a high void fraction (above 20%) (Chapter 3). At this processing condition, it is difficult to distinguish marks left by the pull-out of polymer globules from the true microcellular bubbles. Therefore, the average cell size and cell-population density are not reported.

The 70:30 HDPE/PP blend at 160°C (Figure 2c) obviously showed gaps (voids) between the HDPE matrix and PP domains. However, it was again difficult to distinguish between marks left by the pull-out of PP globules and true microcellular voids. At 175°C, the morphology transformed from two phases to one phase with a cellular structure. The stiffness and viscosity of the matrix dramatically decreased due to high HDPE content causing cell collapse during foaming at high temperature with long foaming time (Figure 2c).

At 160°C, the 50:50 and 30:70 HDPE/PP blends (Figure 2d, e middle column) showed a change in morphology compared with foaming at 135°C for 30 sec (Figure 2d, e left column). Cell growth dramatically increased. Cell size increased with increased foaming temperature. The cell size of the 50:50 HDPE/PP blend was larger than in the 30:70 HDPE/PP blend, and cell-population density was lower (Figure 2d, e)

At a foaming temperature of 175°C, for 50:50 and 30:70 HDPE/PP blends, ESEM showed that morphology was uniform and cells fully grown (Figure 2d, e right column). The microcellular structure was well developed. The void fraction also increased with increasing foaming temperature and time (Chapter 3). Both the 50:50 and 30:70 HDPE/PP blends seem to be appropriate blending ratios for microcellular foaming. They provide adequate nucleation and viscosity in the correct range for adequate cell growth without cell coalescence.

The effects of blend composition on average cell size and cell-population density at the optimum foaming condition (175°C for 30 sec) are summarized in Table 1. Pure HDPE and pure PP had a non-uniform structure with large cells on the surface and a microcellular structure toward the middle of the sample (Figure 2a, b). HDPE had a bigger average cell size and lower cell-population density on the surface due to its lower T_m ; the lower viscosity led to cell coalescence. For HDPE/PP blends, the average cell size increased and cell-population density decreased with increased HDPE content. The 70:30 HDPE/PP blend had poor morphology (Figure 2c) with large cell size and low cell-population density (Table 1) compared to the other blends (Figure 2d, e); the high HDPE content resulted in too low viscosity of the matrix.

Table 1: Effect of blend composition on average cell size and cell-population density of samples foamed at 175°C for 30 sec.

| | HDPE/PP ratio in the blends | | | | |
|--|---|----------|----------|----------|--|
| | HDPE | 70:30 | 50:50 | 30:70 | PP |
| Cell Size (μm) | 1.30 (Center) 65.9 (Surface) | 15.2 | 5.2 | 4.0 | Not foamed (Center) 9.1 (Subsurface) 36.23 (Surface) |
| Cell Density (Cell/ cm^3) | 6.84E+10 (Center) 5.22E+05 (Surface) | 1.51E+07 | 3.05E+08 | 1.37E+09 | Not foamed (Center) 1.12E+08 (Subsurface) 1.76E+06 (Surface) |

The 50:50 and 30:70 HDPE/PP blends seemed to be the best blending ratios; therefore, the remaining discussion focuses primarily on the 50:50 and 30:70 HDPE/PP blends foamed at 175°C.

The effects of foaming time (5, 10, 20 and 30 sec) and blend composition on cell morphology at a foaming temperature of 175°C are shown in Figures 3 and 4. ESEM micrographs of pure HDPE and pure PP (Figure 3) showed poor morphology. Pure HDPE and PP were hard to foam because they had a single phase (Figure 1) with high crystallinity (Chapter 3). The 70:30 HDPE/PP blend had poor morphology (Figure 3) as discussed in the previous section.

At foaming times of 5 and 10 sec, ESEM micrographs of 50:50 and 30:70 HDPE/PP blends (Figures 4a, b) show the cells starting to grow at the interface of the polymer blends. The poorly bonded interfaces of immiscible HDPE/PP blends have a lower activation energy, which allows the cells to start nucleating (Chapter 3) [8], but the foaming time was too short to permit significant cell growth. The results agree with our previous study; all HDPE/PP blends at this processing condition did not achieve a high void fraction (Chapter 3). As mentioned in the previous section, it is difficult to distinguish marks left by the pull-out of polymer globules from true microcellular foaming. Thus, the average cell size and cell-population density could not be determined.

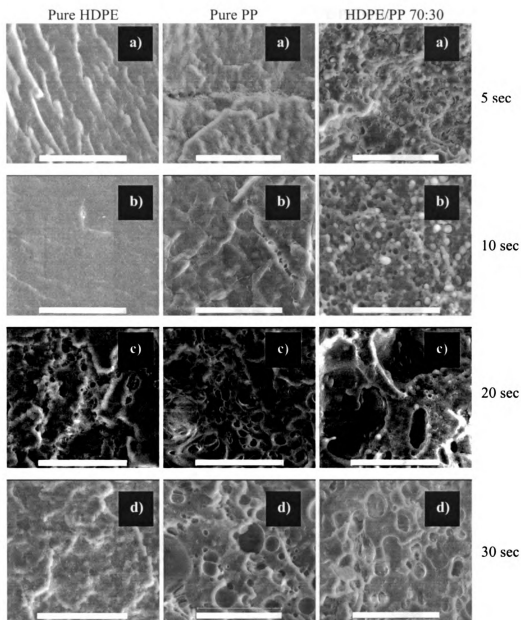


Figure 3: ESEM micrographs of foamed polymer blends at 175°C (Pure HDPE, left column), (Pure PP, middle column) and (HDPE/PP 70:30, right column) a) 5 sec, b) 10 sec, c) 20 sec, and d) 30 sec (all scale bars 100 μ m).

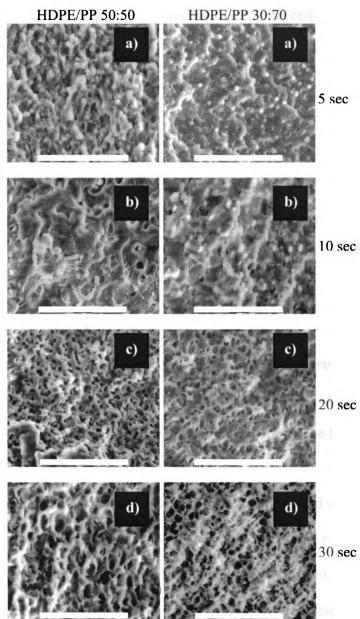


Figure 4: ESEM micrographs of foamed polymer blends at 175°C (HDPE/PP 50:50, left column) and (HDPE/PP 30: 70, right column) a) 5 sec, b) 10 sec, c) 20 sec and d) 30 sec (all scale bars 100 μ m).

At a foaming time of 20 sec, the 50:50 and 30:70 HDPE/PP blends (Figure 4c, d) showed a well-developed microcellular structure, except that cell-population density in the core was lower than near the surface. The microcellular structure grew better near the surface than in the middle, likely due to insufficient time for heat transfer. Therefore, the foaming time must be longer to permit heat transfer to the sample core.

The effects of foaming for 30 sec were discussed in page 74-78.

From this study, we can conclude that 50:50 and 30:70 HDPE/PP blends were the best blending ratios, and 175°C for 30 sec was the best foaming condition.

Impact Strength of Foamed Samples

To understand the effect of blend composition on the impact strength of foamed samples, unfoamed HDPE/PP blends were investigated first. As discussed in the previous section, blending decreased the crystallinities of both the HDPE and PP fractions (Chapter 3). Optical micrographs showed phase separation in HDPE/PP blends (Figure 1c, d, e). It is well known that the incompatibility and immiscibility of HDPE and PP blends will lead to poor impact strength [1, 2]. The average impact strengths of unfoamed pure HDPE and pure PP were 176.9 ± 47.2 and 26.8 ± 9.6 J/m, respectively. No statistically significant differences between the average impact strengths of unfoamed PP and the three blend compositions were found; all were significantly lower than the impact strength of unfoamed pure HDPE (Figure 5). These results are in agreement with the observations made by Blom *et al.* [2].

The effects of foaming temperature on impact strength at a fixed foaming time (30 sec) are shown in Figure 5. The notched Izod impact strengths of all HDPE/PP blends tended to increase with increasing foaming temperature. However, the impact

strength of pure HDPE decreased with increasing foaming temperature. Impact strengths of foamed HDPE at 135, 160 and 175°C, foamed for 30 sec, were 147.2 ± 36.5 , 135.5 ± 75.2 and 77.6 ± 26.1 J/m, respectively. At 135 and 160°C, the decrease in impact strength of foamed HDPE and unfoamed HDPE was not statistically significant, but was significant at 175°C, where large cells were observed on the surface of the samples. A microcellular structure was found in the middle of the sample (Figure 2a), but large cells on the surface apparently had more effect on the impact strength.

At 135 and 160°C, pure PP did not foam (Figure 2b). At 175°C, which is above T_m , the foamed PP had a high void fraction (Chapter 3) with large cells on the surface, and a microcellular structure in subsurface layers, but no foaming at the center. The impact strength did not improve significantly, likely due to this poor morphology.

While foaming was not successful in improving the impact strength of the pure polymers, blending facilitated the formation of a microcellular structure in HDPE/PP blends (Chapter 3). The impact strength of the blends tended to increase with increased foaming temperature.

The impact strength of the 70:30 HDPE/PP blend tended to increase with increased foaming temperature, but the differences were not statistically significant. At 135 and 160°C, cells started nucleating but did not grow because the foaming temperature was too low. At 175°C, cells coalesced.

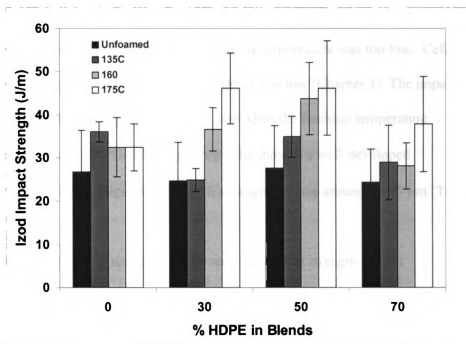


Figure 5: Effects of foaming temperature and blend composition on notched Izod impact strength of HDPE/PP blend samples foamed for 30 sec. The notched impact strength of unfoamed HDPE is 176.9 ± 47.2 J/m.

The impact strength of the foamed 50:50 and 30:70 HDPE/PP blends at 135°C did not significantly improve because the foaming temperature was too low. Cells did not grow well (Figure 2d, e) and the void fraction was low (Chapter 3). The impact strength of these blends significantly improved when the foaming temperature increased to 160 and 175°C. ESEM micrographs showed a well-developed microcellular structure (Figures 2d, e) with average cell size around 4 to 5 μm (Table 1).

At lower foaming times (5, 10, 20 sec), the impact strength did not significantly improve, because no uniform well-developed microcellular morphology was achieved.

The notched Izod impact strengths increased with increased foaming temperature at high foaming time. Improvement in impact strength was associated with a well-developed microcellular morphology.

CONCLUSIONS

In this paper, the microcellular foam batch processing of HDPE/PP blends was investigated to determine the effects of batch processing conditions (foaming time and temperature) and blend composition on cell morphology of the materials. The effects of blend composition on miscibility and the crystalline morphology of the HDPE/PP blends were also investigated. A relationship of the cell morphology to impact strength was reported.

- Optical micrographs of pure HDPE and PP showed a single phase and HDPE/PP blends exhibited phase separation. PP had a regular spherulite structure. HDPE did not show the spherulite structure. HDPE particles hindered the regular growth of the spherulites of PP and the crystalline morphology showed an irregular pattern in blends.
- Blending facilitated the formation of microcellular structures in polyolefins as the poorly bonded interfaces of immiscible HDPE/PP blends have a lower activation energy and allow the cell to start nucleating. However, to achieve a well-developed microcellular structure, foaming temperature and foaming time had to be relatively high. The foaming condition 175°C for 30 sec was best.
- Pure HDPE and PP did not foam well under any conditions.
- The 70:30 HDPE/PP blend had poor morphology because the higher HDPE content caused the matrix to be too soft and less viscous, causing cell coalescence.

- The 50:50 and 30:70 HDPE/PP blends were the best blending ratios, with viscosity and stiffness value appropriate for a well-developed microcellular structure.
- The cell morphology had a strong relationship to the impact strength. To improve the impact strength, the cell morphology had to consist of a well-developed uniform microcellular structure with small cell size and high cell-population density.

REFERENCES

1. K. Solc (Ed.), *Polymer Compatibility and Incompatibility, Principles and Practices*, Harwood, New York (1982).
2. H. P. Blom, J. W. Teh, and Rudin, "i-PP/HDPE Blends: Interactions at Lower HDPE Contents", *J. Appl. Polym. Sci.*, **58**, 995 (1995).
3. H. P. Blom, J. W. Teh, and A. Rudin, "iPP/HDPE Blends. II. Modification with EPDM and EVA", *J. Appl. Polym. Sci.*, **60**, 1405-1417 (1996).
4. H. P. Blom, J. W. Teh, and A. Rudin, "i-PP/HDPE Blends. III. Characterization and Compatibilization at Lower i-PP contents", *J. Appl. Polym. Sci.*, **61**, 959-968 (1996).
5. U. Niebergall, J. Bohse, S. Seidler, W. Grellmann, and L. Schümann, "Relationship of Fracture Behavior and Morphology in Polyolefin Blends", *Polym. Eng. Sci., Polym. Eng. Sci.*, **39** (6), 1109-1118 (1999).
6. C. M. C. Bonelli, A. F. Martins, E. B. Mano and C. L. Beatty, "Effect of Recycled Polypropylene on Polypropylene/High-Density Polyethylene Blends", *J. Appl. Polym. Sci.*, **80**, 1305-1311 (2001).
7. J. Martini, F. A. Waldman and N. P. Suh, U.S. Patent 4,473,665 (1984).
8. F. Waldman, "The Processing of Microcellular Foam", MS thesis, Mechanical Engineering Department, MIT, Cambridge, Mass. (1982).
9. L. M. Matuana, C. B. Park, and J. J. Balatinez, "Cell Morphology and Property Relationships of Microcellular Foamed PVC/Wood-Fiber Composites", *Polym. Eng. Sci.*, **38** (11), 1862-1872 (1998).

10. L. M. Matuana, C. B. Park, and J. J. Balatinez, "Structures and Mechanical Properties of Microcellular Foamed Polyvinyl Chloride", *Cellular Polym.*, **17** (1), 1-16 (1998).
11. J. S. Colton, "The Nucleation of Microcellular Foams in Semi-Crystalline Thermoplastics", *Materials & Manufacturing Processes*, **4**, 253-262 (1989).
12. J. S. Colton and N. P. Suh, U.S. Patent 5,160,674 (1992).
13. S. Doroudiani, C. B. Park, and M.T. Kortschot, "Effect of the Crystallinity and Morphology on the Microcellular Foam Structure of Semicrystalline Polymers", *Polym. Eng. Sci.*, **36** (21), 2645-2662 (1996).
14. S. Doroudiani, C. B. Park, and M. T. Kortschot, "Processing and Characterization of Microcellular Foamed High-Density Polyethylene/Isotactic Polypropylene Blends", *Polym. Eng. Sci.*, **38** (7), 1205-1215 (1998).
15. N. Kukaleva, F. CSER, M. Jollands, and E. Kosior, "Compression of Structure and Properties of Conventional and "High Crystallinity" Isotactic Polypropylenes and Their Blends with Metallocene-Catalyzed Linear Low Density Polyethylene. II. Morphology Studies", *J. Appl. Polym. Sci.*, **80** (6), 831-840 (2001).
16. L. M. Matuana, C. B. Park, and J. J. Balatinez, "Processing and Cell Morphology Relationships for Microcellular Foamed PVC/Cellulosic-Fiber Composites", *Polym. Eng. Sci.*, **37** (7), 1137-1147 (1997).
17. L. M. Matuana and F. Mengelglu, "Microcellular Foaming of Impact-Modified Rigid PVC/Wood-Flour Composites", *J. Vinyl Addit. Technol.*, **7** (2), 67-75 (2001).
18. L. M. Matuana, C. B. Park, and J. J. Balatinez, "Characterization of Microcellular PVC/Cellulosic-Fibre Composites", *J. Cellular Plast.*, **32** (5), 449-467 (1996).

19. ASTM D 256-97, "Standard Test Methods for Determining the Izod Pendulum Impact Resistance of Plastics", Annual Book of ASTM Standards, Philadelphia, P.A., Vol 8.01, pp. 1-12 (2000).
20. D. I. Collias and D. G. Baird, "Tensile Toughness of Microcellular Foams of Polystyrene, Styrene-Acrylonitrile Copolymer, and Single-Edge-Notched Tensile Toughness of The Same Polymer Matrices and Microcellular Foams", *Polym. Eng. Sci.*, **35** (14), 1167-1177 (1995).
21. D. I. Collias and D. G. Baird, "Impact Behavior of Microcellular Foams of Polystyrene and Styrene-Acrylonitrile Copolymer, and Single-edge-Notched Tensile Toughness of Microcellular Foams of Polystyrene, Styrene-Acrylonitrile Copolymer, and Polycarbonate", *Polym. Eng. Sci.*, **35** (14), 1178-1183 (1995).
22. I. Smit and G. Radonjic, "Effects of SBS on Phase Morphology of iPP/aPS Blends", *Polym. Eng. Sci.*, **40** (10), 2144 (2000).
23. F. J. Padden and H. D. Keith, "Spherulite Crystallization in Polypropylene", *J. Appl. Phys.*, **30**, 1479 (1959).
24. J. Varga, *J. Mater. Sci.*, "Review Supermolecular Structure of Isotactic Polypropylene", **27**, 2557 (1992).
25. A. J. Lovinger and M. L. Williams, "Tensile Properties and Morphology of Blends of Polyethylene and Polypropylene", *J. Appl. Polym. Sci.*, **25**, 1703-1713 (1980).
26. J. W. The, "Structure and Properties of Polyethylene-Polypropylene Blend", *J. Appl. Polym. Sci.*, **28**, 605 (1983).
27. D. F. Baldwin, C. B. Park, and N. P. Suh, "A Microcellular Processing Study of Poly(Ethylene Terephthalate) in the Amorphous and Semicrystalline States. Part II Cell Growth and Process Design", *Polym. Eng. Sci.*, **36** (11), 1446-1453 (1996).

Chapter 5

Characterization of Microcellular Foamed Polyolefin Blend Composites with Wood Fiber

This chapter has been submitted to *International Journal of Polymeric Materials* (Feb 2003). It is co-authored by P. Rachtanapun¹, S. E. M. Selke² and L. M. Matuana³

¹Department of Packaging Technology, Faculty of Agro-Industry, Chiang Mai University, Muang, Chiang Mai, Thailand 50100

²School of Packaging, Michigan State University, East Lansing, Michigan 48824

³Department of Forestry, Michigan State University, East Lansing, Michigan 48824

ABSTRACT

The effects of wood fiber content on the void fraction, cell morphology and notched Izod impact strength of microcellular foamed HDPE/PP blend composites with wood fiber were studied. The influence of wood fiber content on the carbon dioxide adsorption and desorption in the samples was also examined. Adsorption of carbon dioxide decreased with increased wood fiber content. Gas diffusion rates were faster as wood fiber content increased. The void fraction decreased dramatically when wood fiber was introduced in the blend. Environmental scanning electron microscopy (ESEM) was used to investigate the effects of wood fiber content on cell morphology. The 30:70 HDPE/PP polymer blend without wood fiber resulted in a high void fraction, with a uniform and well-developed microcellular structure, but when wood fiber was introduced, a uniform and well-developed microcellular structure could not be produced. The effects of foaming on Izod impact strength were dependent on wood fiber content.

INTRODUCTION

Microcellular plastics are foamed polymers characterized by cell densities larger than 10^9 cells/cm³ per unit volume of the original unfoamed polymer, and cell sizes in the range of 0.1 to 10 μm [1]. They have shown the potential to improve impact strength [2-4]. Research on microcellular polymers has been reviewed in references [5, 6]. Most research has centered on amorphous polymers because they are much easier to foam compared to semicrystalline polymers. It is known that microcellular foaming of neat high density polyethylene (HDPE) and neat polypropylene (PP) is very difficult to achieve through a batch foaming process, due to their high crystallinity (Chapter 3 and 4) [2, 7]. However, a microcellular structure can be developed in a semi-crystalline polymer by quenching the polymer during cooling from the melt to achieve relatively low crystallinity [7] or by blending with a suitable ratio of an immiscible polymer (Chapter 3 and 4) [2]. Many studies on microcellular foaming of composites with wood fiber in batch processes have been done by Matuana *et. al* [3, 4, 8-10] on PVC, which is an amorphous polymer. Very little work has been done on microcellular foams containing wood fiber prepared by extrusion [11-14] or injection molding [15]. Only one report of research on foamed wood fiber/polyethylene composites made by a batch process was found in the literature [16]. Microcellular foams of HDPE/PP blend composites with wood fiber made by a batch process have not been extensively studied.

Our recent investigation has shown that the void fraction and cell morphology of microcellular foams of HDPE/PP blends and their composites with wood fiber were strongly dependent on processing conditions (foaming time and foaming temperature)

and blend composition as well as wood fiber content (Chapter 3). The solubility of CO₂ in HDPE/PP blends was related to total crystallinity. Blends decreased in crystallinity of both HDPE and PP (Chapter 3) and facilitated the formation of a microcellular structure in HDPE/PP blends (Chapter 3 and 4). The cells start to grow at the interface of the polymer blends due to the poorly bonded interphases of immiscible HDPE/PP blends. However, to achieve a uniform and well-developed microcellular structure, foaming time and temperature had to be relatively high (175°C for 30 sec) with the appropriate blend ratio (HDPE/PP 50:50 or 30:70 by weight) (Chapter 4). Foamed neat HDPE and neat PP with a high void fraction had a large-celled structure on the surface and were unfoamed at the center (Chapter 3 and 4). Moreover, to improve impact strength, the microcellular structures had to be well developed and uniform with small cell size and high cell-population density (Chapter 4).

In this study, microcellular foaming of HDPE/PP blend composites with wood fiber is investigated. The effects of wood fiber content in HDPE/PP blend composites on the CO₂ adsorption and desorption was first investigated. The effects of wood fiber content on the void fraction of microcellular foams of HDPE/PP blend composites and cell morphology are examined. In addition, the results of Izod impact strength of the foamed samples are compared with those of unfoamed specimens.

MATERIALS

Injection molding grade HDPE [Dow HDPE 00452N, melt index 4 g/10min (ASTM D1238), density 0.952 g/cc] and extrusion and injection molding grade PP [INSPIRE H704-04, melt index 4 g/10min (ASTM D1238), density 0.90 g/cc] were used as polymeric matrices. Commercial grade carbon dioxide was used as a blowing agent. Aspen hardwood fiber was used as the reinforcement (Abitibi Corporation, Alpena, MI). The mesh size of wood fiber was in the range of 30-200.

METHODOLOGY

The effects of wood content on carbon dioxide adsorption and desorption, void fraction, and cell morphology, as well as notched Izod impact strength of microcellular foamed HDPE/PP blend composites with wood fiber were investigated. At a foaming condition of 175°C for 30 sec, the foamed 30:70 HDPE/PP blend (by weight) evidenced high void fraction (Chapter 3), and a well-developed uniform microcellular foam structure (Chapter 3 and 4) with a high cell population density and small cell size (Chapter 4). The impact strength significantly increased compared to unfoamed samples (Chapter 4). Therefore, the 30:70 HDPE/PP blend ratio and the foaming condition of 175°C for 30 sec were used in this study.

Sample Preparation

The 30:70 HDPE/PP polymer blend and composites with wood fiber [0, 5, 10, 15 and 30 per hundred parts of blend resins (phr)] were extruded using a Baker Perkins

Model ZSK-30, 30 mm, 26:1 co-rotating twin-screw extruder (Werner & Pfleiderer Corporation, Ramsey, New Jersey) as described previously (Chapter 3). Six-inch lengths of extrudate were compression-molded into panels (2 mm in thickness) in a hydraulic hot press at 185°C for 5 minutes using 30,000 psi. From these panels, ½ inch by 1 inch rectangular test specimens were cut for sorption experiments and microcellular foaming experiments and ½ inch by 2.5 inch rectangular specimens were cut for impact test experiments.

Sorption Experiments

The diffusion and concentration of absorbed CO₂ in the samples were measured in the sorption experiments following the approach described in references [3, 4, 9, 10] and Chapter 3. The samples were saturated in a pressure vessel with carbon dioxide at room temperature (23-25°C) and 800 psi for 24 hours (Chapter 3) [3, 4, 9]. This length of time was determined to be sufficient for saturation based on our previous work (Chapter 3).

The solubility of CO₂ in the HDPE/PP blend composite can be estimated in terms of mass fractions using the following equation [2]:

$$S_c = \{ [S_{am,HDPE}(1 - \chi_{HDPE}) + S_{cr,HDPE}(\chi_{HDPE})][x_{HDPE}] + [S_{am,PP}(1 - \chi_{PP}) + S_{cr,PP}(\chi_{PP})][x_{PP}] + [S_{wood}][x_{wood}] \} \quad (1)$$

where S_c , $S_{am,HDPE}$, $S_{am,PP}$, $S_{cr,HDPE}$, $S_{cr,PP}$ and S_{wood} are the solubilities of CO₂ in the composite, in the amorphous regions of HDPE and PP, in the crystalline regions of HDPE and PP, and in wood fiber, respectively. The quantities χ_{HDPE} and χ_{PP} are the

crystalline fractions of HDPE and PP in the HDPE/PP blends, respectively, and x_{HDPE} and x_{PP} are the weight fractions of HDPE and PP, respectively.

If the solubility of CO₂ in the crystalline regions of the polymer matrix [3, 7] and in the wood fiber [9] are neglected, the theoretical solubility of CO₂ in the HDPE/PP blend composites (S_c), may be rewritten as [2]:

$$S_c = S_{am,HDPE}(1 - \chi_{HDPE})(x_{HDPE}) + S_{am,PP}(1 - \chi_{PP})(x_{PP}) \quad (2)$$

The solubilities of CO₂ in the amorphous regions can also be calculated from the measured solubilities of CO₂ in pure HDPE ($S_{measured\ HDPE}$) and PP ($S_{measured\ PP}$) from the sorption experiments (Chapter 3), and the crystallinities of pure HDPE and PP from DSC experiments (Chapter 3) using the following equations [2].

$$S_{measured\ HDPE} = S_{am,HDPE}(1 - \chi_{HDPE}) \quad (3)$$

$$S_{measured\ PP} = S_{am,PP}(1 - \chi_{PP}) \quad (4)$$

From our previous study, the crystallinities of the HDPE and PP were found to be 73.2 % and 49.2 %, respectively (Chapter 3). The measured solubilities of CO₂ in the pure HDPE and PP were 2.1 and 4.2 wt %, respectively (Chapter 3). The calculated $S_{am, HDPE}$ and $S_{am, PP}$ are 8.0 and 8.3 wt %, respectively, and these values were substituted into Equation 2. Therefore, the solubility of CO₂ in the HDPE/PP blend composites can be calculated from:

$$S_c = 7.99(1 - \chi_{HDPE})(x_{HDPE}) + 8.30(1 - \chi_{PP})(x_{PP}) \quad (5)$$

The measured crystalline fractions of HDPE (61.9%) and PP (43.8%) in the 30:70 HDPE/PP blend (Chapter 3) were substituted in equation 5. The predicted solubility of CO₂ in the HDPE/PP blend composites can be estimated by the following equation:

$$S_c = 3.04(x_{HDPE}) + 4.67(x_{PP}) \quad (6)$$

Weight loss as a function of $t^{1/2}/l$ was used to determine the diffusion coefficient (Chapter 3) [8-10]. The diffusivity of gas (D) was determined following the approach described elsewhere [9].

Microcellular Foaming Experiments and Foam Characterization

In batch microcellular foaming experiments, the samples were saturated with CO₂ at a high pressure (800 psi) and room temperature for 1 day. Next the CO₂ saturated samples were immediately immersed in a hot glycerin bath (Chapter 3 and 4) [8-10] for foaming and then were immediately quenched in cold water [19] to freeze the foam structures and minimize cell coalescence [17]. The void fractions (VF) may be calculated by $VF = 1 - \rho_f / \rho$, where ρ_f and ρ are the density of the foamed and unfoamed samples (Chapter 3) [8-10]. The average cell diameter and the cell-population density of foamed samples were determined following the approach described in references [8-10].

The notched Izod impact strengths of unfoamed and foamed samples were determined using a Tinius Olsen model 92 Impact Tester following ASTM D 256-97 [18]. At least eight foamed samples and 14 unfoamed samples were tested. All foamed samples were allowed to desorb gas for at least two weeks before property testing to eliminate the effects of the remaining gas in the samples [19, 20].

Statistical Analysis

Data were analyzed by ANOVA and Tukey's Studentized Range (HSD) test using the SAS software program ($\alpha = 0.05$).

RESULTS AND DUSCUSSION

Effect of Wood Fiber Content on Sorption Behaviors of CO₂

It is known that the foamability of polymers is affected by the sorption of gas in the polymer, and that the mechanisms of cell nucleation and cell growth are influenced by the solubility of gas in the polymer and the rate of gas loss [7-10]. It has been well demonstrated that solubility of gas is reduced and the diffusivity of CO₂ increased by the addition of wood fiber into the PVC matrix [9, 10], but no work has been found on HDPE/PP blend composites. Therefore, the effect of wood fiber content on the sorption behaviors of CO₂ in HDPE/PP blend composite with wood fiber was first investigated. The results are summarized in Table 1, and Figure 1 shows the desorption curves for CO₂ used to calculated the diffusivity of CO₂ in the samples. The data clearly show trends similar to those reported in previous research [9, 10].

Table 1: The solubility and diffusivity of CO₂ in HDPE/PP 30:70 blends and their composites with wood fiber, and percent void fraction in foamed samples as a function of wood fiber content.

| Wood Content (phr) | Solubility of CO ₂ (wt%) | | Diffusivity of CO ₂ (cm ² /s) | VF (%) |
|-----------------------|-------------------------------------|------------------|---|--------|
| | Measured | Predicted (Eq.6) | | |
| 0 | 3.9 | 4.2 | 1.1E-04 | 31.1 |
| 5 | 3.8 | 4.0 | 1.4E-04 | 17.1 |
| 10 | 3.1 | 3.8 | 2.1E-04 | 10.4 |
| 15 | 2.8 | 3.6 | 2.6E-04 | 9.1 |
| 30 | 1.6 | 3.2 | 5.6E-04 | 7.7 |

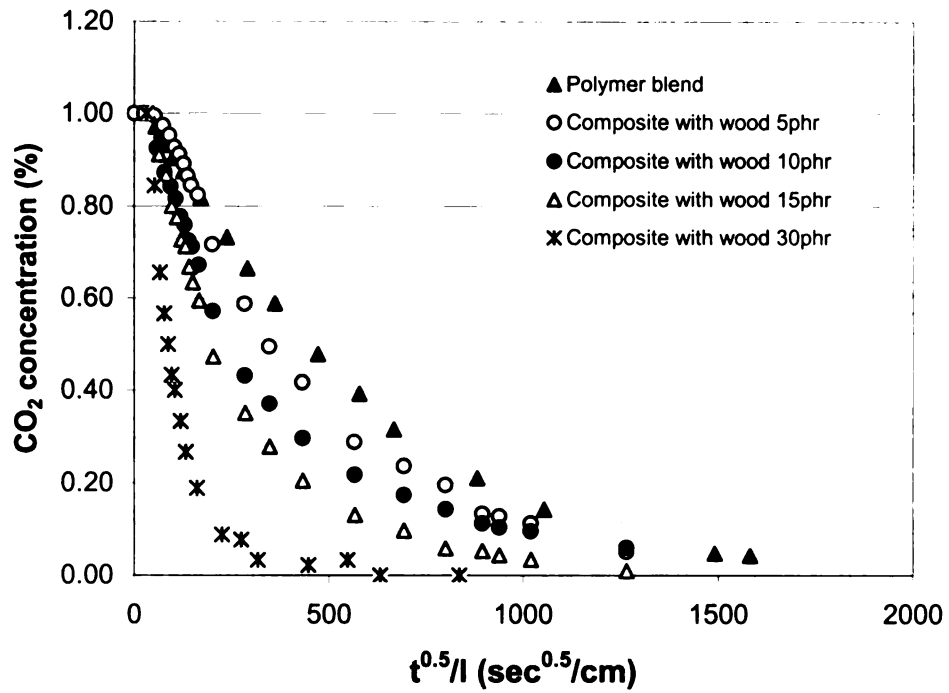


Figure 1: Effect of wood fiber content on desorption curves of 30:70 HDPE/PP blend with wood fiber.

As expected, the solubility of CO₂ in HDPE/PP blend composites was affected by the addition of wood fiber in the blend. The measured solubility of gas decreased as the ratio of wood fibers increased [10]. Since the solubility of gas in the crystalline regions of the polymer blend and wood fibers is negligible, increasing wood fiber content in the blend reduces the volume of the amorphous portion of the polymer in the HDPE/PP blends available for gas solution [10, 17]. Consequently, the gas uptake by the HDPE/PP blend with wood fibers is much lower than that absorbed by the unfilled HDPE/PP blend. It should also be mentioned that the predicted solubility of gas was higher than the measured values, regardless of wood fiber content. The lower measured solubility values might be due to significant gas loss occurring during CO₂ uptake measurement [10, 17].

The diffusivity (D) of CO₂ in HDPE/PP blends was also affected by the incorporation of wood fiber in the blends. As expected, the diffusivity of CO₂ increased with increasing wood fiber content (Table 1), due to the poor interfacial adhesion between the fiber and the blend matrix [10]. Matuana *et al.* [10] have reported that poor surface adhesion between components allows gas to diffuse quickly through channels in the composites, thus increasing gas diffusivity.

From our experimental data, it can be concluded that both the solubility and diffusivity of CO₂ in HDPE/PP blends are strongly dependent on the wood fiber content.

Effects of Wood Fiber Content on the Void Fraction and Cell Morphology of Foamed HDPE/PP Blend Composites

The variation of void fraction of microcellular foamed HDPE/PP blends as a function of wood fiber content is listed in Table 1. The void fraction of foamed HDPE/PP blends dramatically decreased with increasing wood fiber content. The nucleation of bubbles and their growth, which govern the void fraction during the foaming process, are strong functions of gas uptake in the material (solubility) and the rate of gas loss (diffusivity). The void fraction dramatically decreased with the addition of 5 phr wood fiber, despite the slight change in amount of CO₂ absorbed by the sample. This indicates that sorption parameters are not the only variable affecting the void fraction of filled polymer blends. Void fraction is also affected by the viscoelastic properties of the matrix. Several investigators [8] have shown that high melt viscosity and high stiffness provide high resistance for cell growth. Since wood fiber increases the stiffness of the matrix [3, 11], it is believed that increasing wood fiber content into the HDPE/PP blend coupled with lower gas solubility and high diffusivity have prevented bubble growth. Thus blend composites with high void fractions could not be produced.

Figures 2-4 illustrate the cell morphology of microcellular foamed neat HDPE/PP blends and blend composites with wood fiber. The microcellular structure of the neat 30:70 HDPE/PP blend foamed at 175°C for 30 sec was uniform and well developed (Figure 2) with a high void fraction (above 20%) (Table 1). The average cell size and cell-population density are 4 μm and 1.37E+9 cell/cm³, respectively. Even though the HDPE/PP blend facilitated microcellular foaming (Figure 2), addition of wood fiber into HDPE/PP blend composites had a deleterious effect on the foamability of HDPE/PP

blends. A microcellular structure could be generated in HDPE/PP blend composites at low wood fiber content (5 phr), but the microcellular structure was not well developed and was non-uniform. The addition of 5 phr wood fibers in the HDPE/PP blend composites (Figure 3) resulted in reduction of average cell size ($3.5\mu\text{m}$) and cell-population density ($8.83\text{E}+8\text{ cell}/\text{cm}^2$), compared to the pure HDPE/PP blend (Figure 2).

With 10 phr wood fiber, the average cell size ($2\mu\text{m}$) and cell population density decreased further (Figure 4). The reduced cell size may be attributed to the fast diffusion of gas (gas loss) to the environment during the foaming process. Moreover, the ESEM micrographs (Figures 3 and 4) show clean surfaces of pockets due to the pull out of fibers, indicating poor interfacial adhesion between the polymer matrix and wood fibers. These pockets are channels for the gas to easily and quickly escape to the environment (Chapter 3).

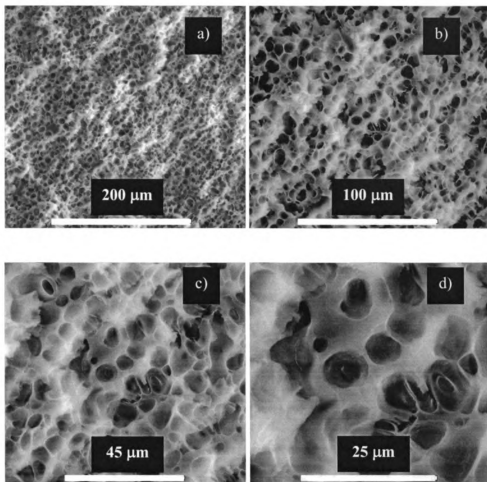


Figure 2: ESEM micrograph of foamed neat 30:70 HDPE/PP blend observed at different magnifications: (a) 250X, (b) 500X, (c) 1000X, and (d) 2000X.

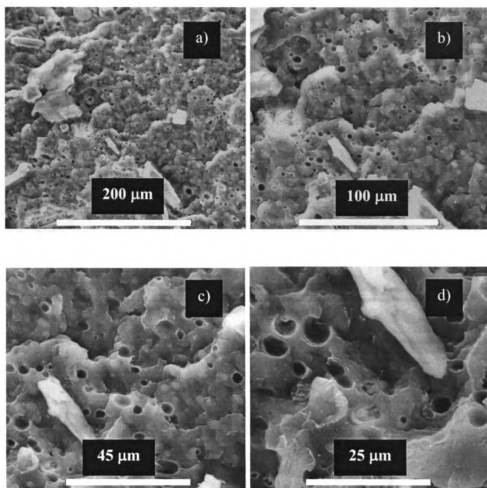


Figure 3: ESEM micrographs of foamed HDPE/PP 30:70 blend composite samples with 5 phr wood fiber observed at different magnifications: (a) 250X, (b) 500X, (c) 1000X, and (d) 2000X.

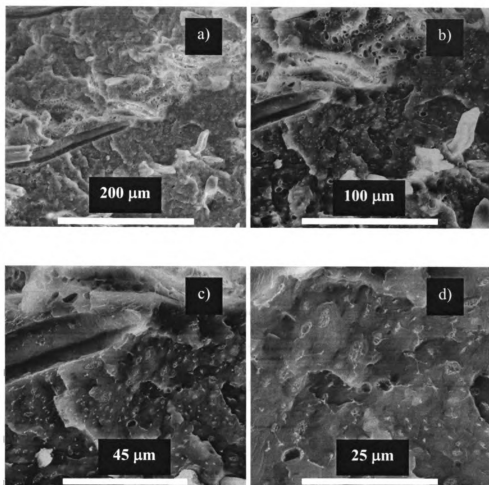


Figure 4: ESEM micrographs of foamed HDPE/PP 30:70 blend composite samples with 10 phr wood fiber observed at different magnifications: (a) 250X, (b) 500X, (c) 1000X, and (d) 2000X.

Effect of Wood Fiber Content on Impact Strength of Samples

The effects of foaming and wood fiber content on notched Izod impact strength of HDPE/PP blends are shown in Figure 5. The notched Izod impact strength of unfoamed samples tended to slightly decrease with increasing wood fiber content up to 10 phr. However, there are no statistically significant differences between the average impact strengths of unfoamed HDPE/PP blend composites between 0 phr and 15 phr. The impact strength of unfoamed HDPE/PP blend composites with 30 phr wood fiber (~23 % wood fiber content) was significantly higher than the impact strengths of other unfoamed samples. A similar observation was made by Raj *et. al* [21] in an early study on composites of LLDPE with aspen fiber. They found that the unnotched Izod impact strength of LLDPE composites with aspen increased with increasing wood content until around 20 % wood fiber content. The impact strength dramatically decreased with a further increase in wood fiber content [21]. They concluded that the impact strength decreased at higher filler content in the composites [21].

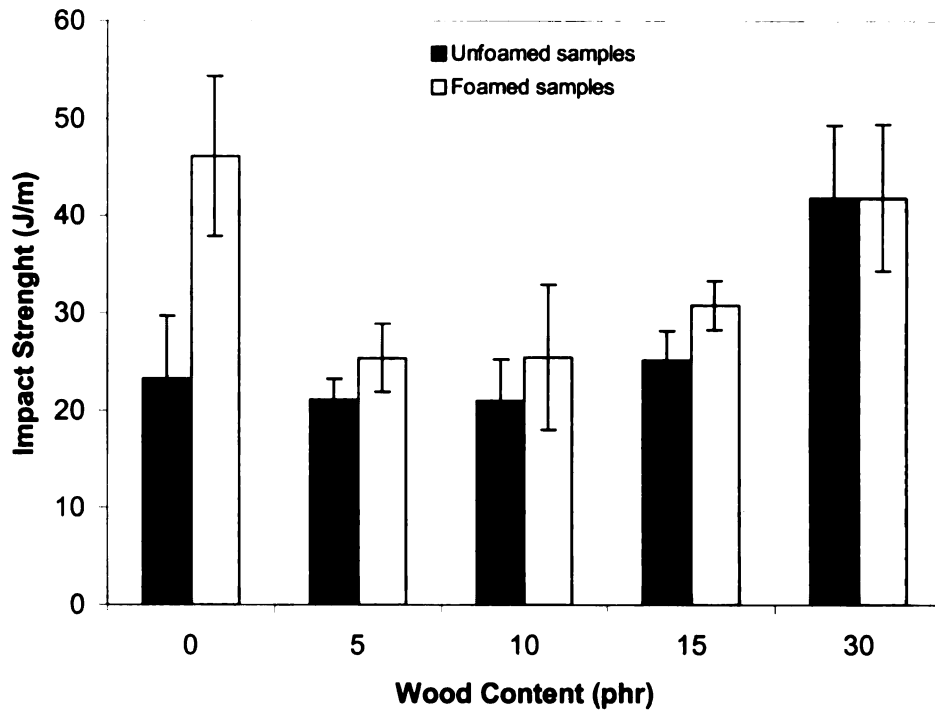


Figure 5: Effect of wood content on impact strength of microcellular foamed HDPE/PP 30:70 blend composites with wood fiber.

The impact strength of foamed neat HDPE/PP blend samples without wood fiber (0 phr) significantly improved, nearly doubling compared to unfoamed counterpart samples (Figure 5), because the microcellular structure was uniform and well developed (Figure 2) with a high void fraction (Table 1). Our previous study showed that the cell morphology has a strong relationship with the impact strength (Chapter 4). To improve the impact strength, the cell morphology has to be uniform with fully-grown cells (well-developed) (Chapter 4). For HDPE/PP blend composites with wood fiber (5, 10 and 15 phr), foaming tended to improve the impact strength. However, the differences were small and not statistically significant. ESEM micrographs (Figures 3 and 4) showed foamed HDPE/PP blend composites with low wood fiber content (5 and 10 phr) had a microcellular structure, but it was non-uniform and not well developed with a low void fraction (Table 1). Therefore, the impact strength of these HDPE/PP blend composites did not significantly improve. These results agree well with our previous study (Chapter 4). The foamed HDPE/PP blend composites with 30 phr wood fiber did not improve in impact strength at all because they did not foam well; the impact strength remained unchanged compared to the foamed counterpart samples.

CONCLUSIONS

The effects of wood fiber content on the sorption behavior of gas, cell morphology, and impact strength of microcellular foamed HDPE/PP blend were investigated.

The solubility of CO₂ in HDPE/PP blends decreased with increased wood fiber content due to the smaller volume of amorphous polymer in the composites, which meant less gas can be absorbed. The diffusion of CO₂ in HDPE/PP blends increased with increased wood fiber content, likely due to the poor interfacial adhesion between the polar wood fiber and non-polar polymer matrix providing channels through which gas can rapidly diffuse from the composites.

The addition of wood fiber to HDPE/PP blends affected the void fraction and cell morphology of microcellular foamed HDPE/PP blends. The void fraction of foamed HDPE/PP blends dramatically decreased with the addition of wood fiber content, due to the decreased solubility of CO₂ gas, increased rate of CO₂ gas diffusion, increased matrix stiffness and acceleration of gas loss during foaming. Foaming of a 30:70 blend of HDPE/PP resulted in a uniform and well developed microcellular morphology. Addition of wood fiber tended to reduce the average cell size and cell-population density.

The impact strength of HDPE/PP blends and their composites was related to wood fiber content and cell morphology. The impact strength of foamed HDPE/PP blends with a uniform and well-developed cell morphology improved significantly. The impact strengths of the foamed HDPE/PP blend composites with wood fiber were dependent on the cell morphology. There was little improvement if the microcellular structure was not well developed and uniform.

REFERENCES

1. J. Martini, F. A. Waldman and N. P. Suh, U.S. Patent 4,473,665 (1984).
2. S. Doroudiani, C. B. Park, and M. T. Kortschot, "Processing and Characterization of Microcellular Foamed High-Density Polyethylene/Isotactic Polypropylene Blends", *Polym. Eng. Sci.*, **38** (7), 1205-1215 (1998).
3. L. M. Matuana, C. B. Park, and J. J. Balatinecz, "Cell Morphology and Property Relationships of Microcellular Foamed PVC/Wood-Fiber Composites", *Polym. Eng. Sci.*, **38** (11), 1862-1872 (1998).
4. L. M. Matuana, C. B. Park, and J. J. Balatinecz, "Structures and Mechanical Properties of Microcellular Foamed Polyvinyl Chloride", *Cellular Polym.*, **17** (1), 1-16 (1998).
5. V. Kumar, "Microcellular Polymers: Novel Materials for the 21st Century", *Cellular Polymers*, **12** (3), 207-223 (1993).
6. V. Kumar and J. E. Weller, ACS Symposium Series 669, Polymeric Foams Science and Technology, Kishan C. Khemani, Editor, Eastman Chemical Company
Developed from A Symposium Sponsored by the Division of Polymer Chemistry, Inc, American Chemical Society, Washington D. C. (1997).
7. S. Doroudiani, C. B. Park, and M.T. Kortschot, "Effect of the Crystallinity and Morphology on the Microcellular Foam Structure of Semicrystalline Polymers", *Polym. Eng. Sci.*, **36** (21), 2645-2662 (1996).

8. L. M. Matuana, C. B. Park, and J. J. Balatinez, "Processing and Cell Morphology Relationships for Microcellular Foamed PVC/Cellulosic-Fiber Composites", *Polym. Eng. Sci.*, **37** (7), 1137-1147 (1997).
9. L. M. Matuana and F. Mengelglu, "Microcellular Foaming of Impact-Modified Rigid PVC/Wood-Flour Composites", *J. Vinyl Addit. Technol.*, **7** (2), 67-75 (2001).
10. L. M. Matuana, C. B. Park, and J. J. Balatinez, "Characterization of Microcellular PVC/Cellulosic-Fibre Composites", *J. Cellular Plast.*, **32** (5), 449-467 (1996).
11. L. M. Matuana, R. T. Woodhams, J. J. Balatinez, C. B. Park, "Influence of Interfacial Interactions on the Properties of PVC/Wood-Fiber Composites", *Polym. Compos.*, **19** (4), 446-455 (1998).
12. X. Cheng, J. Wang, M. Yuan and J. He, "Preparation of Microcellular Composites with Biomimetic Structure via Supercritical Fluid Technology", *Chinese Science Bulletin*, **46** (11), 909-911 (2001).
13. L. M. Matuana and F. Mengelglu, "Studies on the Foamability of Rigid PVC/Wood-Flour Composites", *SPE ANTEC Tech. Papers*, **3**, 2997-3002 (2001).
14. H. Zhang, G. M. Rizvi, W. S. Lin, G. Guo, C. B. Park, "Development of an Extrusion System for Fine-Celled Foaming of Wood-Fiber Composites Using a Physical Blowing Agent", *SPE ANTEC Tech Papers*, **2**, 1746-1758 (2001).
15. A. K. Bledzki and O. Faruk, "Microcellular Foaming of Polypropylene Containing Wood Fibre in an Injection Moulding Process", *SPE ANTEC Tech Papers*, 154 (2002).

16. S. Doroudiani, M.T. Kortschot, and C. B Park, "Structure and Mechanical Properties Study of Foamed Wood Fiber/Polyethylene Composites, *SPE ANTEC Tech, Papers*, 2046-2050 (1997).
17. L. M. Matuana and Q. Li, "A Factorial Design Applied to the Extrusion Foaming of Polypropylene/Wood-Flour Composites", *Cellular Polym.*, **20** (2), 115-130 (2001).
18. ASTM D 256-97, "Standard Test Methods for Determining the Izod Pendulum Impact Resistance of Plastics", Annual Book of ASTM Standards, Philadelphia, P.A., Vol 8.01, pp. 1-12 (2000).
19. D. I. Collias and D. G. Baird, "Tensile Toughness of Microcellular Foams of Polystyrene, Styrene-Acrylonitrile Copolymer, and Single-Edge-Notched Tensile Toughness of the Same Polymer Matrices and Microcellular Foams", *Polym. Eng. Sci.*, **35** (14), 1167-1177 (1995).
20. D. I. Collias and D. G. Baird, "Impact Behavior of Microcellular Foams of Polystyrene and Styrene-Acrylonitrile Copolymer, and Single-edge-Notched Tensile Toughness of Microcellular Foams of Polystyrene, Styrene-Acrylonitrile Copolymer, and Polycarbonate", *Polym. Eng. Sci.*, **35** (14), 1178-1183 (1995).
21. R. G. Raj, B. V. Kokta, D. Maldas, and C. Daneault, "Use of Wood Fibers in Thermoplastics. VII. the Effect of Coupling Agents in Polyethylene-Wood Fiber Composites", *J. Appl. Polym. Sci.*, **37**, 1089-1103 (1989).

Chapter 6

Effect of Melt Index of HDPE on Microcellular Foaming of HDPE/PP Blends

This chapter will be presented at the 5th National Graduate Research Polymer Conference (June 2003). It is co-authored by P. Rachtanapun¹, S. Selke¹ and L. M. Matuana²

¹School of Packaging, Michigan State University, East Lansing, Michigan, 48824

²Department of Forestry, Michigan State University, East Lansing, Michigan, 48824

ABSTRACT

The effect of HDPE/PP blending on the crystallinity as a function of HDPE melt index was studied. The melting temperature and total amount of crystallinity in HDPE/PP blends were lower than those of pure polymers, regardless of blend composition and melt index. The effects of melt index, blending and foaming conditions (foaming temperature and foaming time) on the void fractions of various melt index HDPEs and their HDPE/PP blends were also investigated. The void fraction was strongly dependent on the foaming time, foaming temperature and blend composition as well as melt index of HDPE. The void fraction of the foamed 30:70 HDPE/PP blend was always higher than that of the foamed 50:50 HDPE/PP blend, regardless of melt index. The microcellular structure could be greatly enhanced by using a suitable ratio of HDPE/PP and foaming above the melting temperature for long enough; however, using high melt index HDPE in the HDPE/PP blend had a deleterious effect on both the void fraction and cell morphology of the blend.

INTRODUCTION

Currently, recycle of plastic materials is an important issue because of limitations in landfill space. Most attention has been concentrated on post-consumer waste, especially plastic packaging materials. Polyolefins are one of the most-used plastics by the packaging industry due to their good mechanical and processing properties as well as lower cost. However, in municipal solid waste (MSW), it is known that separation of the various polyolefins such as high density polyethylene and polypropylene is difficult and rarely cost-effective. Furthermore, the blends of high density polyethylene (HDPE) and polypropylene (PP) are immiscible and incompatible [1, 2] and lead to deterioration of some mechanical properties such as impact strength (Chapter 4) [1, 3].

In the last three decades, blending of HDPE/PP has been extensively studied. Substantial research on HDPE/PP blends has concentrated on rheological properties [4-11], water vapor transmission (WVT) [4], crystallization (Chapter 4) [12-22], structure and morphology (Chapter 3 and 4) [5, 14, 16, 18-25], mechanical properties (Chapter 4) [1, 3, 11, 14-19, 25-31], viscoelastic behavior and interfacial tension [25], surface modification [15, 29, 30] and thermodegradative properties [31]. Lovinger and Williams [18] studied the relationship between morphology and tensile properties of HDPE/PP blends. They found that an increase in the stress at yield and ultimate stress is related to the size reduction of spherulites, the increase in crystallinity, and the foaming of a permeating network. They also reported that the ultimate elongation of all HDPE/PP blends was lower than that of neat polymers due to the incompatibility of HDPE and PP. The tensile strength at yield increased gradually with increasing PP content [18]. Research about melt rheology of polyolefins has been reviewed by Gahleitner [32]. He

reported that melt flow rate is related to molecular weight (M_w) and molecular weight distribution (M_w/M_n), which also influence the Charpy impact strength [32]. When the M_w and M_w/M_n increased, melt flow rate decreased and Charpy impact strength increased. Kukaleva et al. [33] studied “high crystallinity” isotactic PP and conventional PP blended with metallocene-catalyzed linear low density polyethylene (LLDPE) blends. They found that melt flow rate decreased with increasing LLDPE content, but melt density was independent of blend composition and similar to the melt density of PP, regardless of the PP type. Moderated differential scanning calorimetry (MDSC) showed that the blends appeared to be miscible during processing and the phases separated during cooling, becoming immiscible in the solid state [33]. Furthermore, they reported that the level of crystallinity of PP in the blends was independent of PP/ LLDPE blend composition, and Young’s modulus and impact strength did not correlate with the level of crystallinity [33]. Liang [34] observed that crystallinity of HDPE increased with increasing melt density during processing. Nevertheless, little research has directly studied the effect of melt flow index on crystallization of HDPE/PP blends, in particular. The different melt flow index might have an effect on the crystallinity of blends which is related to the viscosity and stiffness of the polymer blend matrix. These properties might affect the foamability of HDPE/PP blends.

Our recent studies have shown that the deleterious effect of blending on impact strength can be overcome by creating a microcellular structure in HDPE/PP blends. However, successful production of cellular structure in the blends strongly depended on the foaming conditions and the viscoelastic behavior of the blends which control the cell growth and density reduction. To improve impact strength, the cell morphology had to

consist of a well-developed uniform microcellular structure which was achieved by foaming at relatively high temperature (175°C) for longer time (30 sec) with appropriate blend ratios (HDPE/PP 50:50 and 30:70 by weight) (Chapter 4). By contrast, the blend with the highest HDPE content, i.e., HDPE/PP of 70:30, had poor morphology because the matrix was too soft, causing cell coalescence (Chapter 4). These results implied that the viscosity of the blends is one of the critical variables for proper foamability.

Post-consumer polymers contain a mixture of resins with differing properties (e.g., M_w , viscosity or melt index), which can affect the processing and characteristics of microcellular foams. Therefore, it is imperative to examine the influence of melt index on the foamability of HDPE/PP blends and this was the goal of this study.

In this paper, the influence of HDPE melt flow index in the crystallinity of the neat polymers and HDPE/PP blends as well as the melt temperature was investigated first. Secondly, the effects of HDPE melt index and foaming conditions on the void fraction and cell morphology of HDPE/PP blends were examined.

METHODOLOGY

Sample Preparation

The materials used in this study were polypropylene (PP) [INSPIRE H704-04] and three HDPE grades differing in melt index: injection molding grade HDPE [Dow HDPE 00452N], DOWLEX IP 10262 and DOWLEX IP 40 polyethylene resins from Dow Plastics. These HDPEs are denoted HDPE1, HDPE2 and HDPE3, respectively, and their reported properties are summarized in Table 1. Commercial grade carbon dioxide was used as a blowing agent.

Samples of neat HDPE1, HDPE2, HDPE3, and PP and HDPE/PP blends (30:70 and 50:50 % w/w) were manufactured using a Baker Perkins Model ZSK-30, co-rotating twin-screw extruder (Werner & Pfleiderer Corporation, Ramsey, New Jersey). The compounding conditions are shown in Table 2.

Table 1: Typical properties of HDPE and PP, as supplied by manufacturer

| Physical Properties | HDPE1 Dow HDPE 00452N | HDPE2 DOWLEX IP 10262 | HDPE3 DOWLEX IP 40 | PP INSPRIE H704-04 |
|------------------------------|-----------------------------|--------------------------|-----------------------|-----------------------|
| Density (g/cm ³) | 0.9520 | 0.960 | 0.9520 | 0.90 |
| Melt Index (g/10 min) | 4.0 | 9.0 | 40 | 4.0 |
| DSC Melting Point (°C) | 133 | 133 | 128 | N/A |

Table 2: Compounding conditions

| Samples | Temperature (°C) | | | | | | Screw Speed (rpm) |
|------------------------------|------------------|--------|--------|--------|--------|--------------|----------------------|
| | Port 1(hopper) | Port 2 | Port 3 | Port 4 | Port 5 | Port 6 (die) | |
| PP and all HDPE/PP blends | 180 | 180 | 155 | 155 | 155 | 155 | 100 |
| Neat HDPE1 | 155 | 155 | 155 | 155 | 155 | 155 | 100 |
| Neat HDPE2 | 155 | 155 | 135 | 135 | 135 | 135 | 100 |
| Neat HDPE3 | 155 | 155 | 130 | 130 | 125 | 125 | 150 |

It was not possible to set the same compounding conditions for all polymers and their blends. For example, when the temperature was too high and screw speed was too slow, the HDPEs with the high melt flow index lost their melt strength, and the extrudate could not be cut into the desired length. Therefore, the temperature profiles and screw speed in the extruder were set differently for each polymer to get a continuous and consistent stream of flowing polymer. The extrudates were cut into six-inch lengths before they solidified at room temperature, and then were compression-molded (Carver Laboratory Press, Model M) at 30,000 psi for 5 minutes (Chapter 3). The compression molding temperatures were 160°C and 185°C for the pure HDPE samples and samples containing PP, respectively. Next, the system was cooled to room temperature using cooling water. The 2 mm thick panels were cut to 0.5 × 1 inch (1.27 × 2.54 cm) test specimens.

Differential Scanning Calorimetry (DSC)

DSC was performed using a DSC 2010 (TA Instruments) to investigate the crystallinities of the HDPE1, HDPE2, HDPE3, PP and the HDPE/PP blends, using 3-5 mg samples. The calibration for heat capacity was performed by running an indium reference standard. Three to five replicates were heated from room temperature to 200°C, using a heating rate of 10°C/min. Nitrogen was used as a purge gas with a flow rate of 50 ml/minute. The crystallinities of HDPE and PP were calculated as follows:

For the pure polymers

$$\chi_{HDPE}(\%) = \frac{\Delta H_{m,HDPE}}{\Delta H_{m,HDPE}^o} \times 100\% \quad (1)$$

$$\chi_{PP}(\%) = \frac{\Delta H_{m,PP}}{\Delta H_{m,PP}^o} \times 100\% \quad (2)$$

For each component in the blend

$$\chi_{HDPE}(\%) = \frac{\Delta H_{m,HDPE}}{\Delta H_{m,HDPE}^o(1-x)} \times 100\% \quad (3)$$

$$\chi_{PP}(\%) = \frac{\Delta H_{m,PP}}{\Delta H_{m,PP}^o(x)} \times 100\% \quad (4)$$

For the total sample:

$$\chi_{total} = (1-x)(\chi_{HDPE}) + (x)(\chi_{PP}) \quad (5)$$

where χ_{HDPE} and χ_{PP} are percent crystallinity of HDPE and PP, respectively.

Heats of fusion for HDPE ($\Delta H_{m,HDPE}^o$) and PP ($\Delta H_{m,PP}^o$) are 293 J/g and 209 J/g,

respectively [35]. Heats required for melting the HDPE phase ($\Delta H_{m,HDPE}$) and the PP

phase ($\Delta H_{m,PP}$) were measured by DSC (J/g), and x is the weight fraction of PP in the

blend.

Microcellular Foaming Experiments and Characterization of Foams

In batch microcellular foaming experiments, the samples were saturated with CO₂ [room temperature (23-25°C), 800 psi for 24 hours]. The CO₂-saturated samples were microcellular foamed by immersing them in a hot glycerin bath (Chapter 3) [36-38] at different foaming temperatures (160°C and 175°C) for foaming times of 20 s or 30 s. Foamed samples were immediately quenched in cold water to prevent cell deterioration. The void fraction of foamed samples was determined following the approach described in references (Chapter 3) [37-39]. Sample morphology was investigated using an environmental scanning electron microscope (ESEM) as described previously (Chapter 3).

RESULTS AND DISCUSSION

Effects of Blending on Crystallinity as a Function of Melt Index

Our previous study showed the effect of HDPE/PP blend composition on crystallinity; blending decreased the crystallinity of both HDPE and PP (Chapter 3). In this study HDPEs differing in melt index were blended with PP to study the effects of blending on the heat of fusion, crystallinity of the neat polymers and each component in the blends, and total crystallinity in the samples as well as the melting temperature, as a function of melt index. DSC thermograms of pure HDPE1, pure PP and the blends are presented in **Figure 1**. For the sake of clarity, the curves have been displaced from the baseline. Thermograms of pure HDPE2, pure HDPE3 and their blends were similar to those of HDPE1 and are not shown.

As can be seen in **Figure 1**, pure HDPE1 and pure PP showed a single peak. Two well-separated melting peaks were observed in the blends (the first melting peak is HDPE1 and second melting peak is PP), reflecting two crystalline phases in all blends. The results agree well with our previous studies (Chapter 4) investigating the crystallinity of HDPE/PP blends by optical microscopy, where we also found phase separation (Chapter 3 and 4). The results also agree well with those published by Teh [13] and Finlay *et al.* [27]. The blend composition strongly affected the heat of fusion (area under the peak). In all cases, the heat of fusion of HDPE and PP decreased in the blends. The HDPE peak decreased with increasing PP and the PP peak decreased with increasing HDPE content. The heat of fusion from the peaks was used to calculate the crystallinity of pure HDPE1 (using Equation 1), PP (using Equation 2) and each component in the blends (using Equations 3 and 4) as well as the total crystallinity (using Equation 5).

The effect of blending on the crystalline fraction of HDPE and PP as well as the total amount of crystallinity in HDPE/PP blends as a function of HDPE melt flow index are illustrated in Figures 2 and 3, and the percent crystallinity reduction for each component and melting temperature is presented in Table 3.

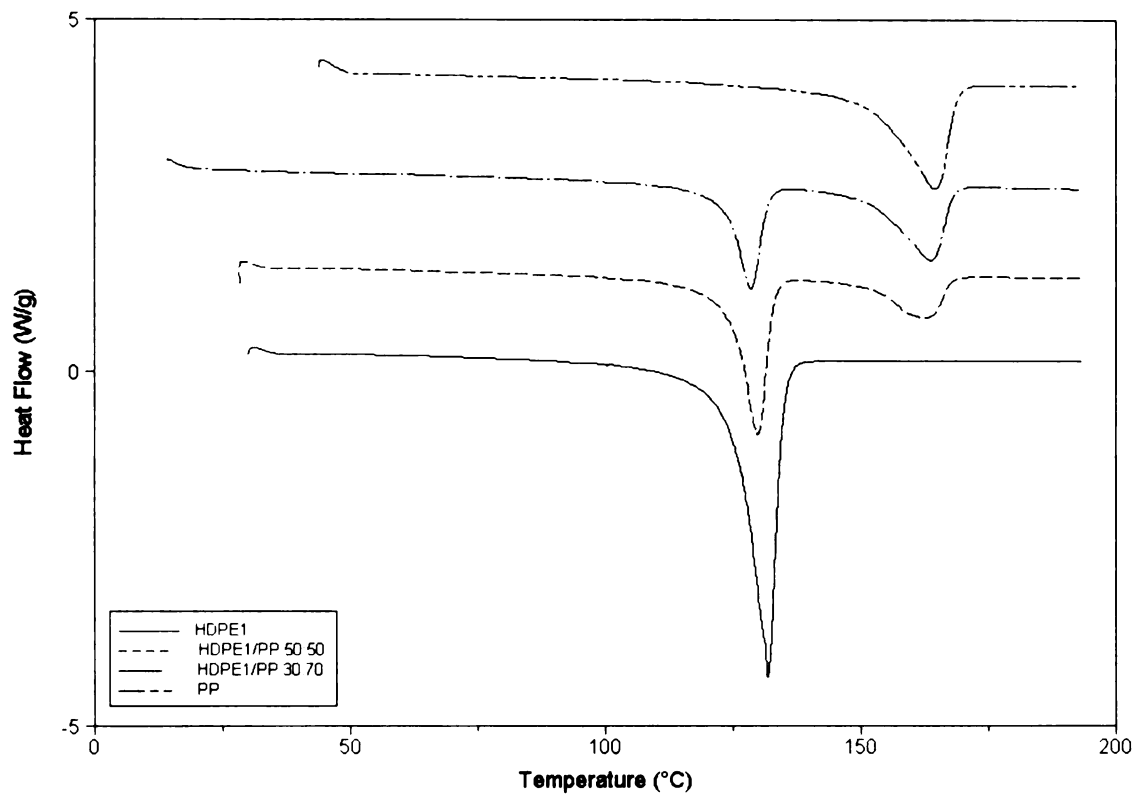


Figure 1: DSC thermograms of neat HDPE1, neat PP and HDPE1/PP blends.

Figure 2 shows that the crystalline fraction of both HDPE and PP in HDPE/PP blends tended to decrease as another component was introduced in the blends. As shown in **Figure 2**, the pure HDPE with lower melt index has higher crystallinity. Crystallinity of HDPE in blends decreased around 6-15% with added PP content (Table 3). The crystallinity of PP in the blends also decreased with added HDPE content (**Figure 2**). The percent crystallinity reduction of PP was around 10-20%, 40% and 30% in PP blended with HDPE1 (melt index 4 g/10 minutes), HDPE2 (melt index 9 g/ 10 minutes) and HDPE3 (melt index 40 g/ 10 minutes), respectively (Table 3). However, there was no consistent pattern for the percent of crystallinity reduction as a function of melt index; the effect of melt index on the percent reduction in crystallinity appears to be complex.

There was a similar trend with the melting temperatures of HDPE1, HDPE2, HDPE3 and PP in blends; the melting temperatures of blends were generally lower than those of the pure HDPE1, HDPE2, HDPE3 and PP (Table 3). The total amount of crystallinity of the blends also decreased with polymer blending, regardless of melt index (**Figure 3**).

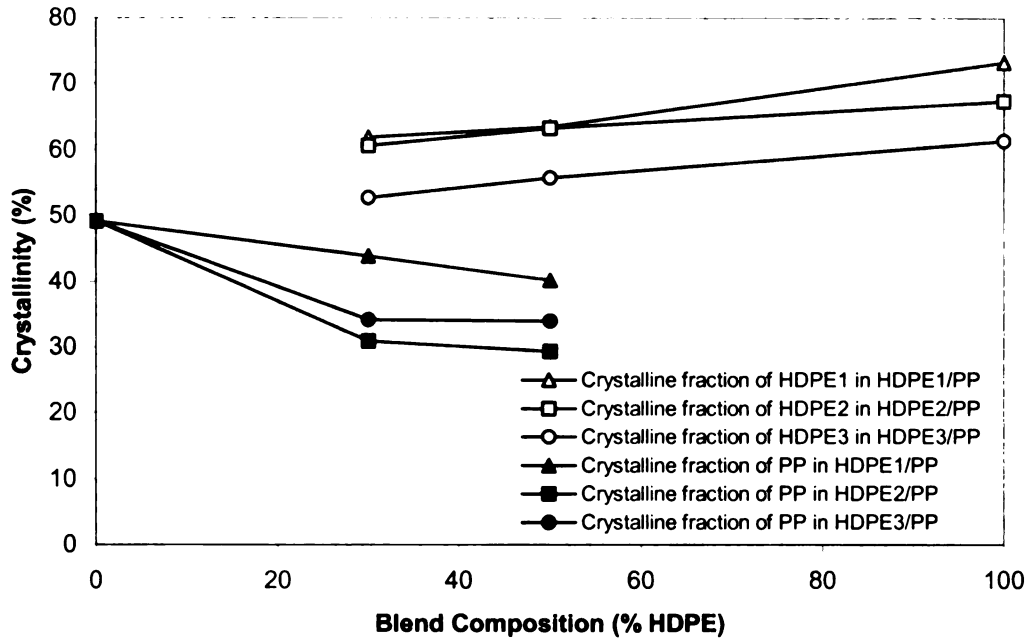


Figure 2: Effect of blending on the crystalline fraction of HDPE and PP in HDPE/PP blends as a function of melt index.

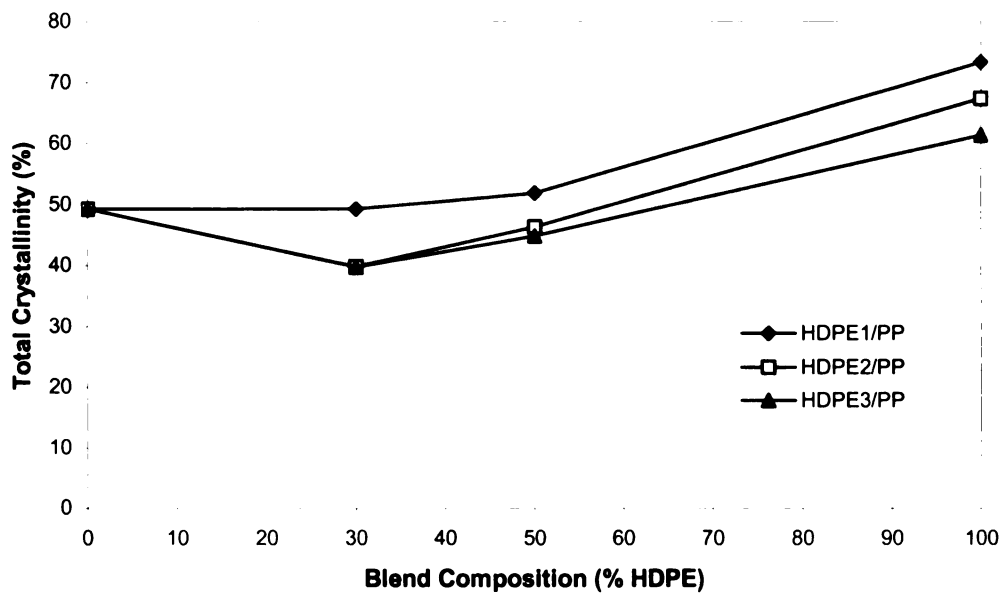


Figure 3: Effect of blending on the total amount of crystallinity in HDPE/PP blends as a function of melt index.

Table 3: Effects of blend composition on melting temperature (T_m) and percent crystallinity reduction of blend samples as a function of melt index.

| Samples | $T_{m, HDPE}$ (°C) | $T_{m, PP}$ (°C) | % χ reduction | |
|----------------------------------|-----------------------|---------------------|--------------------|------|
| | | | HDPE | PP |
| HDPE1 (Melt flow 4 g/ 10 min) | 132.1 | - | - | - |
| HDPE1/PP 50:50 | 130.0 | 162.4 | 13.4 | 18.4 |
| HDPE1/PP 30:70 | 128.6 | 163.8 | 15.5 | 11.0 |
| HDPE2 (Melt flow 9 g/ 10 min) | 134.1 | - | - | - |
| HDPE2/PP 50:50 | 132.8 | 162.5 | 6.0 | 40.5 |
| HDPE2/PP 30:70 | 132.2 | 162.0 | 9.9 | 37.2 |
| HDPE3 (Melt flow 40 g/10 min) | 129.3 | - | - | - |
| HDPE3/PP 50:50 | 128.1 | 161.4 | 9.1 | 31.0 |
| HDPE3/PP 30:70 | 128.5 | 164.5 | 14.0 | 30.5 |
| PP | - | 164.5 | - | - |

Effects of Melt Index, Polymer Blending, Foaming Time and Foaming Temperature on Void Fraction and Cell Morphology

The effects of foaming time and temperature on the void fraction of the pure HDPE1, pure HDPE2, pure HDPE3, pure PP and their HDPE/PP blends were investigated, with the results shown in Figures 4 and 5. Foaming times were 20 sec and 30 sec and foaming temperatures 160°C and 175°C.

As shown in **Figure 4**, at 160°C the void fraction is strongly dependent on the blend composition and the HDPE melt index. The void fraction of PP was not high (void fraction ~5%) because it was foamed below the melting temperature of PP [3, 16]. The effect of melt flow index is clear in neat HDPE, where the higher the melt flow, the higher the void fraction. The void fraction increased with foaming time, but the effect of differences in melt flow index on the void fraction decreased. The increased void fraction in foamed pure HDPE polymers resulted in large cells near the surface, as was found in our previous study (Chapter 3 and 4).

Polymer blends of 30:70 HDPE/PP always resulted in higher void fractions than those of 50:50 HDPE/PP, as was found in our previous work (Chapter 3). The reason for this is still not well understood, but is likely related to the blend morphology (Chapter 4). As 160°C was below the T_m of PP, the void fractions of all polymer blends were only around 10% at 160°C for 20 sec. The void fraction of HDPE1 and HDPE2 blends increased as foaming time increased from 20 to 30 sec, but the HDPE3 blends did not improve in void fraction. The foaming temperature may be too high for HDPE3 blends, causing the matrix to be too soft, resulting in cell collapse. Therefore, in foaming the blends with high melt flow index HDPE, the foaming temperature should not be too high.

At the foaming temperature of 175°C (Figure 5), the effect of HDPE melt flow index in the blends was more obvious. This foaming temperature is above the melting temperatures of both HDPE and PP. It is known that the ability to use high foaming temperatures and long foaming times in order to achieve a high void fraction is limited by the rapid decrease in strength of the polymer at temperatures above the melting point. This results in substantial deformation of the polymer matrix, even though the softened polymer matrix is favorable to bubble growth (Chapter 3) [39]. The void fraction of pure HDPE did not increase significantly with foaming time and higher temperature (175°C), and had large cells near the surface as discussed above. The void fraction of foamed pure PP did increase with foaming time, but had a non-uniform structure (Chapter 4). Large cells developed close to the surface of the samples while the center of the sample was not foamed and a microcellular structure developed in the subsurface (Chapter 3 and 4). The void fraction of the 30:70 HDPE/PP blend increased with foaming time but the blends with higher melt index HDPE resulted in a nearly unchanged or even lower void fraction when the foaming time increased from 20 sec to 30 sec. For all the 50:50 HDPE/PP blends, increased foaming time resulted in nearly unchanged void fraction.

It is known that blending increases the foamability of HDPE/PP blends when temperature and time are appropriate (Chapter 3 and 4). However, when the higher HDPE melt flow index was used in blends, the crystallinity of PP in the blends decreased dramatically (Figure 2 and Table 3), making the matrix too soft to maintain the cellular structure. Therefore, in order to foam HDPE/PP blends containing high melt flow index HDPE, it may be necessary to lower the foaming temperature and/or foaming time, along with using a suitable blend composition, to achieve a high void fraction.

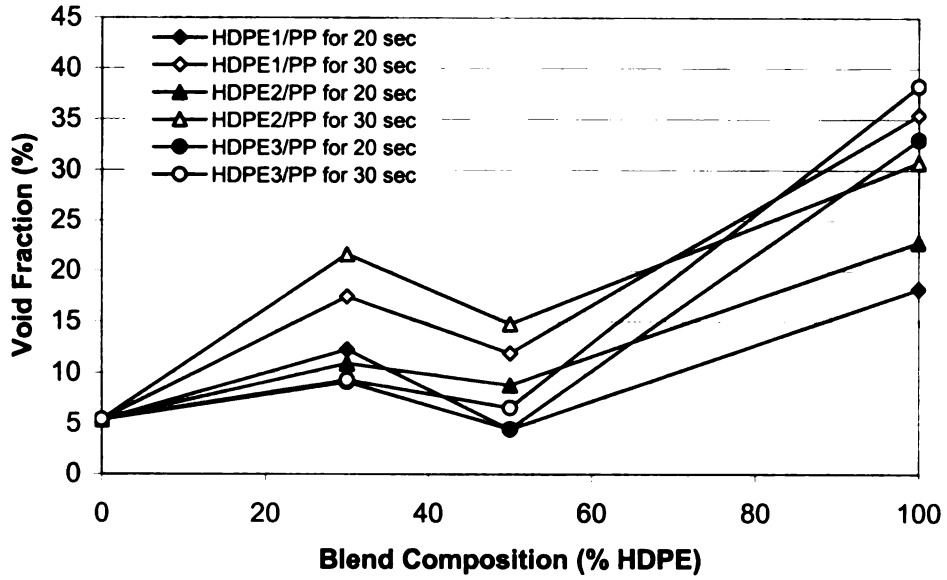


Figure 4: Effect of melt flow index, blending and foaming time on void fraction of samples foamed at 160°C.

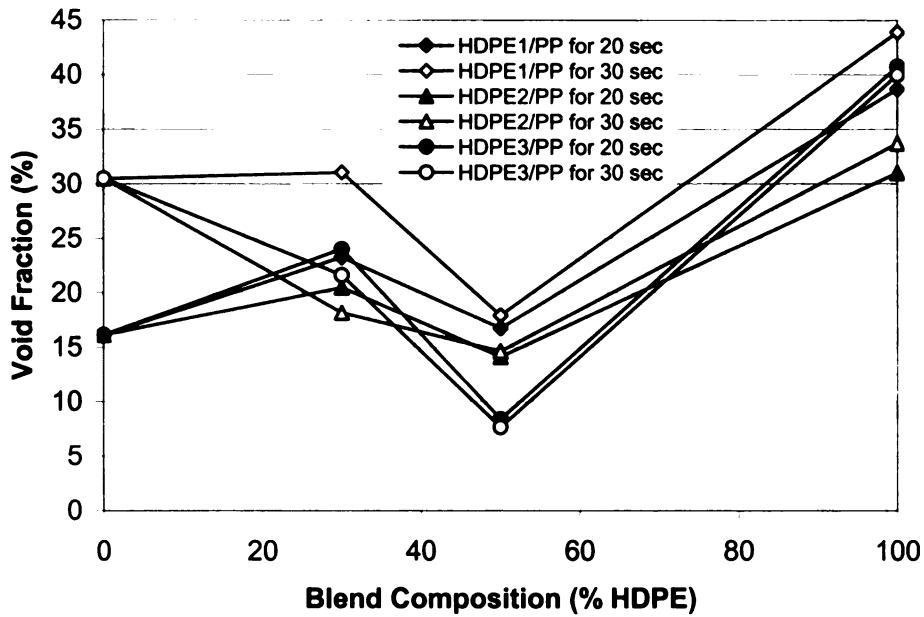
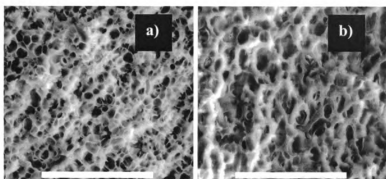


Figure 5: Effect of melt flow index, blending and foaming time on void fraction of samples foamed at 175°C.

Electron microscopy of blends foamed at 175°C for 30 sec revealed that the melt index of the HDPE also has a significant impact on cell morphology. For the HDPE1 resin, as shown in **Figure 6**, the microcellular structures in both the 30:70 and 50:50 HDPE1/PP blends were uniformly distributed and cells fully grown. The void fraction of the 30:70 blend was higher than that of the 50:50 blend, while the cell size was smaller (see **Figure 6**). The larger cell size of the 50:50 blend may be an indication of cell coalescence, perhaps due to the decreased viscosity at the higher HDPE content.

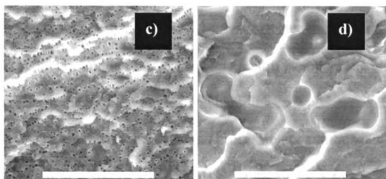
The 30:70 blends with the higher melt index HDPEs showed abundant cells, with the smallest cells in the intermediate HDPE2/PP blend, larger in the highest melt flow HDPE3/PP blend, and the largest in the low melt flow HDPE1/PP (**Figure 6a, c, e**). This corresponded with the void fractions (**Figure 5**), but not with the crystallinity, and is not yet well understood.

For the 50:50 blends, little if any microcellular structure was evident. The intermediate melt flow HDPE2 showed evidence of a few large cells that appeared (**Figure 6d**), from their irregular margins, to have collapsed. The high melt flow HDPE3 blend showed only a few isolated bubbles (**Figure 6f**). A possible explanation is that the coupling of lower viscosity in the HDPE regions with the greatly increased crystallinity loss in the PP regions (40% and 31% for HDPE2 and HDPE3 blend respectively, compared to 18% for HDPE1) (**Table 3**) resulted in material that was simply too soft to maintain the microcellular structure, resulting in massive cell coalescence and collapse. Physical deformation of the foamed samples was also observed. Therefore, it should be concluded that the melt flow index should be in a range that will not prevent nucleated cells from growing, but that will still maintain their structure.



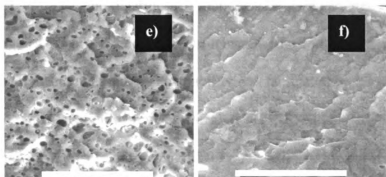
a) HDPE1/PP 30:70

b) HDPE1/PP 50:50



c) HDPE2/PP 30:70

d) HDPE2/PP 50:50



e) HDPE3/PP 30:70

f) HDPE3/PP 50:50

Figure 6: ESEM micrographs of foamed polymer blends for 30 sec at 175°C observed at 500X a) HDPE1/PP 30:70, b) HDPE1/PP 50:50, c) HDPE2/PP 30:70, d) HDPE2/PP 50:50 e) HDPE3/PP 30:70, and f) HDPE3/PP 50:50 (all scale bars 100µm).

CONCLUSIONS

The effects of melt index of HDPE on microcellular foaming of HDPE/PP blends, crystallinity reduction of HDPE and PP, the melting temperature and total amount of crystallinity as a function of melt index were studied. The neat HDPE with lower melt index had higher crystallinity. The crystallinity of HDPE and PP decreased in HDPE/PP blends regardless of blend composition and melt index. The total amount of crystallinity also decreased. Crystallinity reduction in HDPE was affected more by the melt index than crystallinity reduction in the PP fraction. The melting temperature also tended to decrease in blends regardless of melt index and blending.

The effects of blending, melt index, and processing conditions on void fraction and cell morphology were also investigated. The foamability is strongly dependent on blend composition. The 30:70 HDPE/PP blend always provided a higher void fraction than the 50:50 HDPE/PP blend regardless of foaming condition and melt index. At a foaming temperature of 160°C, the void fraction increased with foaming time regardless of blend composition and melt index. Foamability was facilitated by using a suitable HDPE/PP blend ratio at a high foaming temperature (175°C) and long enough foaming time (30 sec); however, the use of too high HDPE melt index in the blend had a negative effect on the void fraction and cell morphology because the polymer matrix lost strength during the foaming process. The void fraction and cell morphology of the blends were not only dependent on the foaming condition and blend composition, but also on stiffness or strength of the polymer matrix at the foaming conditions.

REFERENCES

1. S. Kraysem, *Polymer Blends*, Vol. 1 Academic Press, New York, p.15 (1978).
2. K. Solc, *Polymer Compatibility and Incompatibility Principles and Practices*, Harwood, New York, (1982).
3. D. W. Bartlett, J. W. Barlow, and D. R. Paul, "Mechanical Properties of Blends Containing HDPE and PP", *J. Appl. Polym. Sci.*, **27**, 2351-2360 (1982).
4. F. Oscar, III J. Noel, and F. Carley, " Properties of Polypropylene-Polyethylene Blends", *Polym. Eng. Sci.*, **15** (2) 117-126 (1975).
5. J. Z. Liang and J. N. Ness, "Material Characterization: Investigation on The Melt Flow Properties of Polyethylene and Polypropylene Blends", *Polymer Testing*, **16**, 379-389 (1997).
6. M. Fujiyama and Y. Kawasaki, "Rheological Properties of Polypropylene/High-Density Polyethylene Blend Melts. I. Capillary Flow Properties", *J. Appl. Polym. Sci.*, **42**, 467-480 (1991).
7. H. K. Chuang and C. D. Han, "Rheological Behavior of Polymer Blends", *J. Appl. Polym. Sci.*, **29**, 2205 (1984).
8. M. Levin and F. H. J. Maurer, "Morphology and Rheological Properties of Polypropylene-Linear Low Density Polyethylene Blends", *Polym. Eng. Sci.*, **28**, 670 (1988).
9. L. A Utracki. and P. Sammut, "Rheological Evaluation of Polystyrene/Polyethylene Blends", *Polym. Eng. Sci.*, **28**, 1405 (1988).

10. C. D. Han and H. K. Chuang, "Blends of Nylon 6 with An Ethylene-Based Multifunction Polymer. I Rheology-Structure Relationships", *J. Appl. Polym. Sci.*, **30**, 2431-2455 (1985).
11. C. D. Han and H. K. Chuang, "Criteria for the Rheological Compatibility of Polymer Blends", *J. Appl. Polym. Sci.*, **30**, 4431 (1985).
12. Z. Bartczak and A. Galeski, "Changes in Interface Shape During Crystallization in Two-Component Polymer Systems", *Polymer*, **27**, 544-548 (1986).
13. J. W. Teh, "Structure and Properties of Polyethylene-Polypropylene Blend", *J. Appl. Polym. Sci.*, **28**, 605-618 (1983).
14. S. Doroudiani, C. B Park, and M. T. Kortschot, "Processing and Characterization of Microcellular Foamed High-Density Polyethylene/Isotactic Polypropylene Blends", *Polym. Eng. Sci.*, **38** (7), 1205-1215 (1998).
15. H. P. Blom, J. W. Teh, T. Bremner, and A. Rudin, "Isothermal and Non-Isothermal Crystallization of PP: Effect of Annealing and of The Addition of HDPE", *Polymer*, **39** (17), 4011-4022 (1998).
16. B. L. Schürmann, U. Niebergall, N. Severin, Ch. Burger, W. Stocker, and H. P. Rabe, "Polyethylene (PEHD)/Polypropylene (iPP) Blends: Mechanical Properties, Structure and Morphology", *Polymer*, **39** (22), 5283-5291 (1998).
17. H. P. Blom, J. W. Teh, and A. Rudin, "iPP/HDPE Blends: Interactions at Lower HDPE Contents", *J. Appl. Polym. Sci.*, **58**, 995-1006 (1995).
18. A. J. Lovinger and M. L. Williams, "Tensile Properties and Morphology of Blends of Polyethylene and Polypropylene", *J. Appl. Polym. Sci.*, **25**, 1703-1713 (1980).

19. W. N. Kim, S. Hong, J. Choi, and K. Lee, "Morphology and Mechanical Properties of Biaxially Oriented Films of Polypropylene and HDPE Blends", *J. Appl. Polym. Sci.*, **54**, 1741-1750 (1994).
20. R. A. Shanks, J. Li, and L. Yu, "Polypropylene-Polyethylene Blend Morphology Controlled by Time-Temperature-Miscibility", *Polymer*, **41**, 2133-2139 (2000).
21. J. Li, R. A. Shanks, R. H. Olley, G. R. Greenway, "Miscibility and Isothermal Crystallization of Polypropylene in Polyethylene Melts", *Polymer*, **42**, 7685-7649 (2001).
22. K. Cho, F. Li, and J. Choi, "Crystallization and Melting Behavior of Polypropylene and Maleated Polypropylene Blends", *Polymer*, **40**, 1717-1729 (1999).
23. H. Sano, H. Yui, H. Li, and T. Inoue, "Regularly Phase-Separated Structure in An Injection-Molded Blend of Isotactic Polypropylene and High Density Polyethylene", *Polymer*, **39** (21), 5265-5267 (1998).
24. U. Niebergall, J. Bohse, S. Seidler, W. Grellmann, and B. L. Schürmnn, "Relationship of Fracture Behavior and Morphology in Polyolefin Blends", *Polym. Eng. Sci.*, **39**, 1405 (1999).
25. A. M. C. Souza and N. R. Demarquette, "Influence of Composition on The Linear Viscoelastic Behavior and Morphology of PP/HDPE Blends", *Polymer*, **43**, 1313-1321 (2002).
26. R. E. Robertson and D. R. Paul, "Stress-Strain Behavior of Polyolefin Blends", *J. Appl. Polym. Sci.*, **17**, 2579-2595 (1973).

27. J. Finlay S. Sheppard, S. Tookey, M. J. Hill, and P. J. Barham, "Unexpectedly High Young's Moduli Recorded for iPP/HDPE Blends", *J. Appl. Polym. Sci.*, **39**, 1404-1414 (2001).
28. R. Hettemam, J. Van Tol, and L. P. B. M. Janssen, "In-Situ Reactive Blending of Polyethylene and Polypropylene in Co-Rotating and Counter-Rotating Extruders", *Polym. Eng. Sci.*, **39** (9), 1628-1641 (1999).
29. H. P. Blom, J. W. Teh, and A. Rudin, , "iPP/HDPE Blends. II. Modification with EPDM and EVA", *J. Appl. Polym. Sci.*, **60**, 1405-1417 (1996).
30. H. P. Blom, J. W. Teh, and A. Rudin, "i-PP/HDPE Blends: III. Characterization and Compatibilization at Lower I-PP Contents", *J. Appl. Polym. Sci.*, **61**, 959-968 (1996).
31. C. Albano and G. Sanchez, "Study of The Mechanical, Thermal, and Thermodegradative Properties of Virgin PP with Recycled and Non-Recycled HDPE", *Polym. Eng. Sci.*, **39** (8), 1456-1462 (1999).
32. M. Gahleitner, "Melt Rheology of Polyolefins", *Prog. Polym. Sci.*, **26** (6), 895-944 (2001).
33. N. Kukaleva, F. Cser, M. Jollands, and E. Kosior, "Comparison of Structure and Properties of Conventional and "High-Crystallinity" Isotactic Polypropylenes and Their Blends with Metallocene-catalyzed Linear Low-Density Polyethylene .I. Relationships between Rheological Behavior and Thermal and Physical Properties", *J. Appl. Polym. Sci.*, **77**, 1591-1599 (2000).
34. J. Z. Liang, "Material Behavior: The Flow-Induced Crystallization Behavior in Capillary Extrusion of High Density Polyethylene Melts", *Polymer Testing*, **20**, 469-473 (2001).

35. B. Wunderlich, *Macromolecular physics*, Vol. 1, Crystal Structure, Morphology, Defects, Academic Press, New York (1973).
36. L. M. Matuana, C. B. Park, and J. J. Balatinecz, "Processing and Cell Morphology Relationships for Microcellular Foamed PVC/Cellulosic-Fiber Composites", *Polym. Eng. Sci.*, **37** (7), 1137-1147 (1997).
37. L. M. Matuana and F. Mengelöglu, "Microcellular Foaming of Impact-Modified Rigid PVC/Wood-Flour Composites", *J. Vinyl Addit. Technol.*, **7** (2), 67-75 (2001).
38. L. M. Matuana, C. B. Park, and J. J. Balatinecz, "Characterization of Microcellular PVC/Cellulosic-Fibre Composites", *J. Cellular Plast.*, **32** (5), 449-467 (1996).
39. J. S. Colton, "The Nucleation of Microcellular Foams in Semi-Crystalline Thermoplastics", *Materials & Manufacturing Processes*, **4**, 253-262 (1989).

CHAPTER 7

SUMMARY OF FINDINGS

In this dissertation, batch microcellular foaming technology was used to reduce the density and to improve impact strength of polymer blends of HDPE and PP as well as composites with wood fiber. In order to understand the foamability of the materials, the sorption behavior of the materials was determined by sorption experiments. The foaming phenomenon in the blends and composites was studied, and the critical processing parameters were determined. Differential Scanning Calorimetry (DSC), Optical Microscopy (OP) and Environmental Scanning Electron Microscopy (ESEM) were used to elucidate the effects of processing conditions (foaming time and temperature), blend composition, wood fiber content, and HDPE melt index on crystallinity, crystalline morphology, and void fraction as well as cellular morphology (average cell size and cell-population density) of foamed materials. The relationship between cellular morphology and the notched Izod impact strength of the materials was established. Based on the experimental results, the following conclusions can be drawn:

1. The study of the effects of processing conditions (foaming time and temperature), blend composition, and wood fiber content on the void fraction and cell morphology of the microcellular foams of polymer blends of HDPE and PP as well as composites with wood fiber indicates that blend composition, foaming time and temperature strongly influence the void fraction and cell morphology. To achieve a high void fraction, the foaming temperature had to be well above the melting temperature of the polymer, and the foaming time had to be long enough (30 sec).

Addition of wood fiber (30 phr) to the polymers inhibited the foaming ability, related to less total gas and fast gas loss.

2. Solubility of CO₂ in polymer blends decreased with increased HDPE content, due to an increase in total crystallinity. The solubility of gas was reduced by adding wood fiber in the composites because of the crystallinity of wood fiber. A trend of increasing solubility of CO₂ in composites with increasing HDPE content was observed; the reason for this is not well understood. In blends, the crystallinity of both HDPE and PP decreased.
3. A high void fraction was dependent more on the rate of gas loss (diffusivity) than on the solubility of gas in the polymers or composites. The amount of crystallinity affected the cell structure.
4. Optical micrographs of pure HDPE and PP showed a single phase and HDPE/PP blends exhibited phase separation. PP had a regular spherulite structure, whereas HDPE did not show the spherulite structure. HDPE particles hindered the regular growth of the spherulites of PP and the crystalline morphology showed an irregular pattern in blends.
5. Blending facilitated the formation of microcellular structures in polyolefins as the poorly bonded interfaces of immiscible HDPE/PP blends have a lower activation energy and allow the cell to start nucleating. However, to achieve a well-developed microcellular structure, foaming temperature and foaming time had to be relatively high. The foaming condition of 175°C for 30 sec was the best. Nevertheless, pure HDPE and PP did not foam well at any foaming conditions. They had large-celled structures near the surface. Despite the enhancement of the formation of

microcellular structures in polyolefins by blending, the 70:30 HDPE/PP blend had poor morphology because the higher HDPE content caused the matrix to be too soft and less viscous, causing cell coalescence. The 50:50 and 30:70 HDPE/PP blends were the best blending ratios, with the viscosity and stiffness appropriate for a well-developed microcellular structure. The cell morphology had a strong relationship with the impact strength. To improve impact strength, the cell morphology had to consist of a well-developed uniform microcellular structure with small cell size and high cell-population density.

6. The investigation of the effects of wood fiber content on the gas sorption behavior, cell morphology, and impact strength of microcellular foamed HDPE/PP blends demonstrated that the solubility of CO₂ in HDPE/PP blends decreased with increased wood fiber content due to the smaller volume of amorphous polymer in the composites, which meant less gas can be absorbed. The diffusion of CO₂ in HDPE/PP blends increased with increased wood fiber content, likely due to the poor interfacial adhesion between the polar wood fiber and non-polar polymer matrix providing channels through which gas can rapidly diffuse from the composites. The addition of wood fiber to HDPE/PP blends affected the void fraction and cell morphology of microcellular foamed HDPE/PP blends. The void fraction of foamed HDPE/PP blends dramatically decreased with the addition of wood fiber content, due to the decreased solubility of CO₂ gas, increased rate of CO₂ gas diffusion, increased matrix stiffness and acceleration of gas loss during foaming. Foaming of a 30:70 blend of HDPE/PP resulted in a uniform and well

developed microcellular morphology, but addition of wood fiber tended to reduce the average cell size and cell-population density.

7. The impact strength of HDPE/PP blends and their composites was related to wood fiber content and cell morphology. The impact strength of foamed HDPE/PP blends with a uniform and well-developed cell morphology improved significantly. The impact strengths of the foamed HDPE/PP blend composites with wood fiber were dependent on the cell morphology. There was little improvement if the microcellular structure was not well developed and uniform.
8. The influence of melt index of HDPE on microcellular foaming of HDPE/PP blends, crystallinity reduction of HDPE and PP, the melting temperature and total amount of crystallinity was examined as a function of HDPE melt index. The experimental results reveal that the neat HDPE with lower melt index had higher crystallinity. The crystallinity of HDPE and PP decreased in HDPE/PP blends regardless of blend composition and melt index. The total amount of crystallinity also decreased. Crystallinity reduction in HDPE was affected more by the melt index than crystallinity reduction in the PP fraction. The melting temperature also tended to decrease in blends regardless of melt index and blending.
9. The effects of blending, melt index, and processing conditions on void fraction and cell morphology were also investigated. The foamability was strongly dependent on blend composition. The 30:70 HDPE/PP blend always provided a higher void fraction than the 50:50 HDPE/PP blend regardless of blend composition, foaming condition and melt index. At a foaming temperature of 160°C, the void fraction increased with foaming time regardless of blend composition and melt index.

Foamability was facilitated by using a suitable HDPE/PP blend ratio at a high foaming temperature (175°C) and long enough foaming time (30 sec); however, the use of too high HDPE melt index in the blend had a negative effect on the void fraction and cell morphology because the polymer matrix lost strength during the foaming process. The void fraction and cell morphology of the blends were not only dependent on the foaming condition and blend composition, but also on the stiffness or strength of the polymer matrix at the foaming conditions.

RECOMMENDATIONS AND FUTURE WORK

A fundamental understanding of the criteria governing the foamability in HDPE/PP blends and the composites with wood fiber was investigated in this research. The critical processing parameters affecting the cellular morphology were identified. The relationship of cellular morphology and the Izod notched Impact strength was established. The impact strength of HDPE/PP blends can be significantly improved by foaming. However, there are many interesting things that should be further investigated. The following recommendations can be made:

1. The foamed composites with wood fiber did not succeed well in improving the impact strength, due to low CO₂ concentration, high diffusion and fast loss of gas during foaming. Therefore, the improvement of interphase adhesion through the addition of coupling agents or surface modification of either the continuous phase or the wood fiber should be investigated. Moreover, the addition of rheology-modifiers into the matrix to decrease the stiffness also should be studied.
2. The effect of melt flow index on melt strength of HDPE/PP blends, and the correlation of this behavior to foaming ability, cellular morphology and impact strength should be investigated.
3. Theoretical models and empirical models to predict the void fraction, cell size and cell density and impact strength in HDPE/PP blends should be studied.
4. Further development of the continuous foaming process is recommended because it is likely to be more cost effective.

APPENDIX

Measured solubility of CO₂ (%) in the polyolefin blends and composites with wood fiber (30 phr) as a function of blend composition.

%HDPE

| | | | | |
|-------|-------|-------|--------|--------|
| 100 | 70 | 50 | 30 | 0 |
| 2.137 | 2.558 | 3.43 | 3.8781 | 4.1973 |
| 2.168 | 2.571 | 3.733 | 3.8539 | 4.0938 |
| 2.103 | 2.613 | 3.6 | 3.835 | 4.3628 |

Composites (%HDPE)

| | | | | |
|--------|--------|--------|--------|--------|
| 100 | 70 | 50 | 30 | 0 |
| 2.4075 | 2.1197 | 1.545 | 1.5657 | 1.2573 |
| 2.5679 | 1.5943 | 1.2637 | 1.8898 | 1.6023 |
| 2.0871 | 2.549 | 1.6278 | 1.4059 | 1.4304 |

ANOVA: Single Factor Polymer blends

| %HDPE | Count | Sum | Average | Variance |
|-------|-------|---------|----------|----------|
| 100 | 3 | 6.408 | 2.136 | 0.001057 |
| 70 | 3 | 7.742 | 2.580667 | 0.000826 |
| 50 | 3 | 10.763 | 3.587667 | 0.023066 |
| 30 | 3 | 11.567 | 3.855667 | 0.000467 |
| 0 | 3 | 12.6539 | 4.217967 | 0.018411 |

ANOVA

Polymer blends

| Source of Variation | SS | df | MS | F | P-value | F crit |
|---------------------|----------|----|----------|----------|---------|---------|
| Between Groups | 9.310615 | 4 | 2.327654 | 265.5502 | 4.2E-10 | 3.47805 |
| Within Groups | 0.087654 | 10 | 0.008765 | | | |
| Total | 9.398269 | 14 | | | | |

ANOVA: Single Factor Composites

| %HDPE | Count | Sum | Average | Variance |
|-------|-------|--------|----------|----------|
| 100 | 3 | 7.0625 | 2.354167 | 0.059925 |
| 70 | 3 | 6.263 | 2.087667 | 0.228633 |
| 50 | 3 | 4.4365 | 1.478833 | 0.036426 |
| 30 | 3 | 4.8614 | 1.620467 | 0.060789 |
| 0 | 3 | 4.29 | 1.43 | 0.029756 |

ANOVA

Composites

| Source of Variation | SS | df | MS | F | P-value | F crit |
|---------------------|----------|----|----------|----------|----------|---------|
| Between Groups | 1.985899 | 4 | 0.496475 | 5.974001 | 0.010113 | 3.47805 |
| Within Groups | 0.831059 | 10 | 0.083106 | | | |
| Total | 2.816958 | 14 | | | | |

Percent Crystallinity in HDPE/PP Blends

%HDPE

| | | | |
|------|------|------|------|
| 100 | 70 | 50 | 30 |
| 70.5 | 67.0 | 61.9 | 52.3 |
| 80.4 | 72.2 | 60.4 | 62.4 |
| 68.9 | 66.7 | 68.1 | 58.3 |
| | | | 68.5 |
| | | | 67.9 |

%PP

| | | | |
|-------|--------|--------|--------|
| 100 | 70 | 50 | 30 |
| 44.56 | 44.675 | 38.947 | 40.064 |
| 49.81 | 40.068 | 38.153 | 48.022 |
| 53.06 | 47.758 | 43.263 | 41.994 |
| 49.23 | 43.404 | | |
| | 42.994 | | |

ANOVA: Single Factor Comparison percent crystallinity of PP (%)

SUMMARY

| Groups | Count | Sum | Average | Variance |
|--------|-------|----------|----------|----------|
| 100 | 4 | 196.6603 | 49.16507 | 12.28637 |
| 70 | 5 | 218.8995 | 43.7799 | 7.790526 |
| 50 | 3 | 120.3636 | 40.12121 | 7.561579 |
| 30 | 3 | 130.0797 | 43.35991 | 17.23463 |

ANOVA

| Source of Variation | SS | df | MS | F | P-value | F crit |
|---------------------|----------|----|----------|----------|----------|----------|
| Between Groups | 150.9156 | 3 | 50.30521 | 4.704874 | 0.023859 | 3.587431 |
| Within Groups | 117.6136 | 11 | 10.69215 | | | |
| Total | 268.5293 | 14 | | | | |

ANOVA: Single Factor Comparison of crystallinity of PP in blends

SUMMARY

| Groups | Count | Sum | Average | Variance |
|----------|-------|----------|----------|----------|
| Column 1 | 5 | 218.8995 | 43.7799 | 7.790526 |
| Column 2 | 3 | 120.3636 | 40.12121 | 7.561579 |
| Column 3 | 3 | 130.0797 | 43.35991 | 17.23463 |

ANOVA

| Source of Variation | SS | df | MS | F | P-value | F crit |
|---------------------|----------|----|----------|----------|----------|----------|
| Between Groups | 27.07628 | 2 | 13.53814 | 1.341165 | 0.314555 | 4.458968 |
| Within Groups | 80.75452 | 8 | 10.09432 | | | |
| Total | 107.8308 | 10 | | | | |

Ratio_HDPE*Temp*Time

Effect of Ratio on Void Fraction

| Effect | HDPE (%) | Temp | Time | Wood | HDPE (%) | Temp | Time | Wood | Adjp |
|----------------------|----------|------|------|------|----------|------|------|------|--------------|
| Ratio_HDPE*Temp*Time | 0 | 160 | 30 | | 30 | 160 | 30 | | 0.871 |
| Ratio_HDPE*Temp*Time | 0 | 160 | 30 | | 50 | 160 | 30 | | 0.999 |
| Ratio_HDPE*Temp*Time | 0 | 160 | 30 | | 70 | 160 | 30 | | 0.002 |
| Ratio_HDPE*Temp*Time | 0 | 160 | 30 | | 100 | 160 | 30 | | 0.000 |
| Ratio_HDPE*Temp*Time | 30 | 160 | 30 | | 50 | 160 | 30 | | 1.000 |
| Ratio_HDPE*Temp*Time | 30 | 160 | 30 | | 70 | 160 | 30 | | 0.399 |
| Ratio_HDPE*Temp*Time | 30 | 160 | 30 | | 100 | 160 | 30 | | 0.000 |
| Ratio_HDPE*Temp*Time | 50 | 160 | 30 | | 70 | 160 | 30 | | 0.096 |
| Ratio_HDPE*Temp*Time | 50 | 160 | 30 | | 100 | 160 | 30 | | 0.000 |
| Ratio_HDPE*Temp*Time | 70 | 160 | 30 | | 100 | 160 | 30 | | 0.132 |

| Effect | HDPE (%) | Temp | Time | Wood | HDPE (%) | Temp | Time | Wood | Adjp |
|----------------------|----------|------|------|------|----------|------|------|------|--------------|
| Ratio_HDPE*Temp*Time | 0 | 175 | 20 | | 30 | 175 | 20 | | 1.000 |
| Ratio_HDPE*Temp*Time | 0 | 175 | 20 | | 50 | 175 | 20 | | 1.000 |
| Ratio_HDPE*Temp*Time | 0 | 175 | 20 | | 70 | 175 | 20 | | 0.980 |
| Ratio_HDPE*Temp*Time | 0 | 175 | 20 | | 100 | 175 | 20 | | 0.000 |
| Ratio_HDPE*Temp*Time | 30 | 175 | 20 | | 50 | 175 | 20 | | 1.000 |
| Ratio_HDPE*Temp*Time | 30 | 175 | 20 | | 70 | 175 | 20 | | 1.000 |
| Ratio_HDPE*Temp*Time | 30 | 175 | 20 | | 100 | 175 | 20 | | 0.007 |
| Ratio_HDPE*Temp*Time | 50 | 175 | 20 | | 70 | 175 | 20 | | 0.903 |
| Ratio_HDPE*Temp*Time | 50 | 175 | 20 | | 100 | 175 | 20 | | 0.000 |
| Ratio_HDPE*Temp*Time | 70 | 175 | 20 | | 100 | 175 | 20 | | 0.062 |

*Adjp = Adjusted P-Value

Ratio_HDPE*Temp*Time

Effect of Temperature on Void Fraction

| Effect | HDPE (%) | Temp | Time | Wood | HDPE (%) | Temp | Time | Wood | Adjp |
|----------------------|----------|------|------|------|----------|------|------|------|--------------|
| Ratio_HDPE*Temp*Time | 70 | 135 | 20 | | 70 | 160 | 20 | | 0.529 |
| Ratio_HDPE*Temp*Time | 70 | 135 | 20 | | 70 | 175 | 20 | | 0.019 |
| Ratio_HDPE*Temp*Time | 70 | 160 | 20 | | 70 | 175 | 20 | | 0.999 |

| Effect | HDPE (%) | Temp | Time | Wood | HDPE (%) | Temp | Time | Wood | Adjp |
|----------------------|----------|------|------|------|----------|------|------|------|--------------|
| Ratio_HDPE*Temp*Time | 100 | 135 | 20 | | 100 | 160 | 20 | | 0.021 |
| Ratio_HDPE*Temp*Time | 100 | 135 | 20 | | 100 | 175 | 20 | | 0.000 |
| Ratio_HDPE*Temp*Time | 100 | 160 | 20 | | 100 | 175 | 20 | | 0.016 |

| Effect | HDPE (%) | Temp | Time | Wood | HDPE (%) | Temp | Time | Wood | Adjp |
|----------------------|----------|------|------|------|----------|------|------|------|--------------|
| Ratio_HDPE*Temp*Time | 0 | 135 | 30 | | 0 | 160 | 30 | | 1.000 |
| Ratio_HDPE*Temp*Time | 0 | 135 | 30 | | 0 | 175 | 30 | | 0.002 |
| Ratio_HDPE*Temp*Time | 0 | 160 | 30 | | 0 | 175 | 30 | | 0.005 |

| Effect | HDPE (%) | Temp | Time | Wood | HDPE (%) | Temp | Time | Wood | Adjp |
|----------------------|----------|------|------|------|----------|------|------|------|--------------|
| Ratio_HDPE*Temp*Time | 30 | 135 | 30 | | 30 | 160 | 30 | | 0.998 |
| Ratio_HDPE*Temp*Time | 30 | 135 | 30 | | 30 | 175 | 30 | | 0.016 |
| Ratio_HDPE*Temp*Time | 30 | 160 | 30 | | 30 | 175 | 30 | | 0.495 |

| Effect | HDPE (%) | Temp | Time | Wood | HDPE (%) | Temp | Time | Wood | Adjp |
|----------------------|----------|------|------|------|----------|------|------|------|--------------|
| Ratio_HDPE*Temp*Time | 70 | 135 | 30 | | 70 | 160 | 30 | | 0.004 |
| Ratio_HDPE*Temp*Time | 70 | 135 | 30 | | 70 | 175 | 30 | | 0.049 |
| Ratio_HDPE*Temp*Time | 70 | 160 | 30 | | 70 | 175 | 30 | | 1.000 |

| Effect | HDPE (%) | Temp | Time | Wood | HDPE (%) | Temp | Time | Wood | Adjp |
|----------------------|----------|------|------|------|----------|------|------|------|--------------|
| Ratio_HDPE*Temp*Time | 100 | 135 | 30 | | 100 | 160 | 30 | | 0.000 |
| Ratio_HDPE*Temp*Time | 100 | 135 | 30 | | 100 | 175 | 30 | | 0.000 |
| Ratio_HDPE*Temp*Time | 100 | 160 | 30 | | 100 | 175 | 30 | | 1.000 |

*Adjp = Adjusted P-Value

Ratio_HDPE*Temp*Time

Effect of Time on Void Fraction

| Effect | HDPE (%) | Temp | Time | Wood | HDPE (%) | Temp | Time | Wood | Adjp |
|----------------------|----------|------|------|------|----------|------|------|------|--------------|
| Ratio_HDPE*Temp*Time | 70 | 160 | 5 | | 70 | 160 | 10 | | 1.000 |
| Ratio_HDPE*Temp*Time | 70 | 160 | 5 | | 70 | 160 | 20 | | 0.310 |
| Ratio_HDPE*Temp*Time | 70 | 160 | 5 | | 70 | 160 | 30 | | 0.001 |
| Ratio_HDPE*Temp*Time | 70 | 160 | 10 | | 70 | 160 | 20 | | 0.623 |
| Ratio_HDPE*Temp*Time | 70 | 160 | 10 | | 70 | 160 | 30 | | 0.003 |
| Ratio_HDPE*Temp*Time | 70 | 160 | 20 | | 70 | 160 | 30 | | 0.803 |

| Effect | HDPE (%) | Temp | Time | Wood | HDPE (%) | Temp | Time | Wood | Adjp |
|----------------------|----------|------|------|------|----------|------|------|------|--------------|
| Ratio_HDPE*Temp*Time | 100 | 160 | 5 | | 100 | 160 | 10 | | 1.000 |
| Ratio_HDPE*Temp*Time | 100 | 160 | 5 | | 100 | 160 | 20 | | 0.006 |
| Ratio_HDPE*Temp*Time | 100 | 160 | 5 | | 100 | 160 | 30 | | 0.000 |
| Ratio_HDPE*Temp*Time | 100 | 160 | 10 | | 100 | 160 | 20 | | 0.135 |
| Ratio_HDPE*Temp*Time | 100 | 160 | 10 | | 100 | 160 | 30 | | 0.000 |
| Ratio_HDPE*Temp*Time | 100 | 160 | 20 | | 100 | 160 | 30 | | 0.005 |

| Effect | HDPE (%) | Temp | Time | Wood | HDPE (%) | Temp | Time | Wood | Adjp |
|----------------------|----------|------|------|------|----------|------|------|------|--------------|
| Ratio_HDPE*Temp*Time | 0 | 175 | 5 | | 0 | 175 | 10 | | 1.000 |
| Ratio_HDPE*Temp*Time | 0 | 175 | 5 | | 0 | 175 | 20 | | 0.189 |
| Ratio_HDPE*Temp*Time | 0 | 175 | 5 | | 0 | 175 | 30 | | 0.001 |
| Ratio_HDPE*Temp*Time | 0 | 175 | 10 | | 0 | 175 | 20 | | 0.971 |
| Ratio_HDPE*Temp*Time | 0 | 175 | 10 | | 0 | 175 | 30 | | 0.023 |
| Ratio_HDPE*Temp*Time | 0 | 175 | 20 | | 0 | 175 | 30 | | 0.838 |

| Effect | HDPE (%) | Temp | Time | Wood | HDPE (%) | Temp | Time | Wood | Adjp |
|----------------------|----------|------|------|------|----------|------|------|------|--------------|
| Ratio_HDPE*Temp*Time | 30 | 175 | 5 | | 30 | 175 | 10 | | 1.000 |
| Ratio_HDPE*Temp*Time | 30 | 175 | 5 | | 30 | 175 | 20 | | 0.330 |
| Ratio_HDPE*Temp*Time | 30 | 175 | 5 | | 30 | 175 | 30 | | 0.010 |
| Ratio_HDPE*Temp*Time | 30 | 175 | 10 | | 30 | 175 | 20 | | 0.998 |
| Ratio_HDPE*Temp*Time | 30 | 175 | 10 | | 30 | 175 | 30 | | 0.290 |
| Ratio_HDPE*Temp*Time | 30 | 175 | 20 | | 30 | 175 | 30 | | 0.999 |

| Effect | HDPE (%) | Temp | Time | Wood | HDPE (%) | Temp | Time | Wood | Adjp |
|----------------------|----------|------|------|------|----------|------|------|------|--------------|
| Ratio_HDPE*Temp*Time | 70 | 175 | 5 | | 70 | 175 | 10 | | 0.997 |
| Ratio_HDPE*Temp*Time | 70 | 175 | 5 | | 70 | 175 | 20 | | 0.008 |
| Ratio_HDPE*Temp*Time | 70 | 175 | 5 | | 70 | 175 | 30 | | 0.014 |
| Ratio_HDPE*Temp*Time | 70 | 175 | 10 | | 70 | 175 | 20 | | 0.376 |
| Ratio_HDPE*Temp*Time | 70 | 175 | 10 | | 70 | 175 | 30 | | 0.507 |
| Ratio_HDPE*Temp*Time | 70 | 175 | 20 | | 70 | 175 | 30 | | 1.000 |

| Effect | HDPE (%) | Temp | Time | Wood | HDPE (%) | Temp | Time | Wood | Adjp |
|----------------------|----------|------|------|------|----------|------|------|------|--------------|
| Ratio_HDPE*Temp*Time | 100 | 175 | 5 | | 100 | 175 | 10 | | 0.724 |
| Ratio_HDPE*Temp*Time | 100 | 175 | 5 | | 100 | 175 | 20 | | 0.000 |
| Ratio_HDPE*Temp*Time | 100 | 175 | 5 | | 100 | 175 | 30 | | 0.000 |
| Ratio_HDPE*Temp*Time | 100 | 175 | 10 | | 100 | 175 | 20 | | 0.000 |
| Ratio_HDPE*Temp*Time | 100 | 175 | 10 | | 100 | 175 | 30 | | 0.000 |
| Ratio_HDPE*Temp*Time | 100 | 175 | 20 | | 100 | 175 | 30 | | 1.000 |

*Adjp = Adjusted P-Value

Ratio_HDPE_*Wood

Effect of Wood on Void Fraction

| Effect | HDPE (%) | Temp | Time | Wood | HDPE (%) | Temp | Time | Wood | Adjp |
|------------------|----------|------|------|------|----------|------|------|------|-----------------|
| Ratio_HDPE_*Wood | 30 | | | 0 | 30 | | | 30 | 1.12E-07 |

| Effect | HDPE (%) | Temp | Time | Wood | HDPE (%) | Temp | Time | Wood | Adjp |
|------------------|----------|------|------|------|----------|------|------|------|-----------------|
| Ratio_HDPE_*Wood | 70 | | | 0 | 70 | | | 30 | 4.43E-06 |

| Effect | HDPE (%) | Temp | Time | Wood | HDPE (%) | Temp | Time | Wood | Adjp |
|------------------|----------|------|------|------|----------|------|------|------|-----------------|
| Ratio_HDPE_*Wood | 100 | | | 0 | 100 | | | 30 | 2.84E-04 |

Ratio_HDPE_*Wood

Effect of Ratio on Void Fraction

| Effect | HDPE (%) | Temp | Time | Wood | HDPE (%) | Temp | Time | Wood | Adjp |
|------------------|----------|------|------|------|----------|------|------|------|-----------------|
| Ratio_HDPE_*Wood | 0 | | | 0 | 30 | | | 0 | 4.70E-05 |
| Ratio_HDPE_*Wood | 0 | | | 0 | 50 | | | 0 | 1.00E+00 |
| Ratio_HDPE_*Wood | 0 | | | 0 | 70 | | | 0 | 2.08E-04 |
| Ratio_HDPE_*Wood | 0 | | | 0 | 100 | | | 0 | 1.57E-06 |
| Ratio_HDPE_*Wood | 30 | | | 0 | 50 | | | 0 | 2.52E-05 |
| Ratio_HDPE_*Wood | 30 | | | 0 | 70 | | | 0 | 1.00E+00 |
| Ratio_HDPE_*Wood | 30 | | | 0 | 100 | | | 0 | 8.83E-01 |
| Ratio_HDPE_*Wood | 50 | | | 0 | 70 | | | 0 | 1.10E-04 |
| Ratio_HDPE_*Wood | 50 | | | 0 | 100 | | | 0 | 8.89E-07 |
| Ratio_HDPE_*Wood | 70 | | | 0 | 100 | | | 0 | 5.36E-01 |

| Effect | HDPE (%) | Temp | Time | Wood | HDPE (%) | Temp | Time | Wood | Adjp |
|------------------|----------|------|------|------|----------|------|------|------|-----------------|
| Ratio_HDPE_*Wood | 0 | | | 30 | 30 | | | 30 | 1.00E+00 |
| Ratio_HDPE_*Wood | 0 | | | 30 | 50 | | | 30 | 1.00E+00 |
| Ratio_HDPE_*Wood | 0 | | | 30 | 70 | | | 30 | 9.99E-01 |
| Ratio_HDPE_*Wood | 0 | | | 30 | 100 | | | 30 | 3.50E-03 |
| Ratio_HDPE_*Wood | 30 | | | 30 | 50 | | | 30 | 9.82E-01 |
| Ratio_HDPE_*Wood | 30 | | | 30 | 70 | | | 30 | 9.66E-01 |
| Ratio_HDPE_*Wood | 30 | | | 30 | 100 | | | 30 | 1.17E-03 |
| Ratio_HDPE_*Wood | 50 | | | 30 | 70 | | | 30 | 1.00E+00 |
| Ratio_HDPE_*Wood | 50 | | | 30 | 100 | | | 30 | 1.57E-02 |
| Ratio_HDPE_*Wood | 70 | | | 30 | 100 | | | 30 | 2.01E-02 |

*Adjp = Adjusted P-Value

Ratio*Temp*Time

Effect of Time on Void fraction

| Ratio | Temp(°C) | Significant Difference |
|-------|----------|------------------------|
| 0 | 135 | No |
| | 160 | No |
| | 175 | No |
| 30 | 135 | No |
| | 160 | No |
| | 175 | Yes |
| 50 | 135 | No |
| | 160 | No |
| | 175 | No |
| 70 | 135 | No |
| | 160 | Yes |
| | 175 | Yes |
| 100 | 135 | No |
| | 160 | Yes |
| | 175 | Yes |

Effect of Ratio on Void Fraction

| Temp(°C) | Time(s) | Significant Difference |
|----------|---------|------------------------|
| 135 | 5 | No |
| | 10 | No |
| | 20 | No |
| | 30 | No |
| 160 | 5 | No |
| | 10 | No |
| | 20 | No |
| | 30 | Yes |
| 175 | 5 | No |
| | 10 | No |
| | 20 | Yes |
| | 30 | Yes |

Effect of Temperature on Void Fraction

| Ratio | Time(s) | Significant Difference |
|-------|---------|------------------------|
| 0 | 5 | No |
| | 10 | No |
| | 20 | No |
| | 30 | Yes |
| 30 | 5 | No |
| | 10 | No |
| | 20 | No |
| | 30 | Yes |
| 50 | 5 | No |
| | 10 | No |
| | 20 | No |
| | 30 | No |
| 70 | 5 | No |
| | 10 | No |
| | 20 | Yes |
| | 30 | Yes |
| 100 | 5 | No |
| | 10 | No |
| | 20 | Yes |
| | 30 | Yes |

Temp*Time*Wood

Effect of time on Void Fraction

| Effect | HDPE (%) | Temp | Time | Wood | HDPE (%) | Temp | Time | Wood | Adjp |
|----------------|----------|------|------|------|----------|------|------|------|--------------|
| Temp*Time*Wood | | 160 | 5 | 0 | | 160 | 10 | 0 | 0.419 |
| Temp*Time*Wood | | 160 | 5 | 0 | | 160 | 20 | 0 | 0.002 |
| Temp*Time*Wood | | 160 | 5 | 0 | | 160 | 30 | 0 | 0.000 |
| Temp*Time*Wood | | 160 | 10 | 0 | | 160 | 20 | 0 | 0.617 |
| Temp*Time*Wood | | 160 | 10 | 0 | | 160 | 30 | 0 | 0.000 |
| Temp*Time*Wood | | 160 | 20 | 0 | | 160 | 30 | 0 | 0.017 |

| Effect | HDPE (%) | Temp | Time | Wood | HDPE (%) | Temp | Time | Wood | Adjp |
|----------------|----------|------|------|------|----------|------|------|------|--------------|
| Temp*Time*Wood | | 160 | 5 | 30 | | 160 | 10 | 30 | 1.000 |
| Temp*Time*Wood | | 160 | 5 | 30 | | 160 | 20 | 30 | 0.835 |
| Temp*Time*Wood | | 160 | 5 | 30 | | 160 | 30 | 30 | 0.003 |
| Temp*Time*Wood | | 160 | 10 | 30 | | 160 | 20 | 30 | 0.998 |
| Temp*Time*Wood | | 160 | 10 | 30 | | 160 | 30 | 30 | 0.015 |
| Temp*Time*Wood | | 160 | 20 | 30 | | 160 | 30 | 30 | 0.270 |

| Effect | HDPE (%) | Temp | Time | Wood | HDPE (%) | Temp | Time | Wood | Adjp |
|----------------|----------|------|------|------|----------|------|------|------|--------------|
| Temp*Time*Wood | | 175 | 5 | 0 | | 175 | 10 | 0 | 0.007 |
| Temp*Time*Wood | | 175 | 5 | 0 | | 175 | 20 | 0 | 0.000 |
| Temp*Time*Wood | | 175 | 5 | 0 | | 175 | 30 | 0 | 0.000 |
| Temp*Time*Wood | | 175 | 10 | 0 | | 175 | 20 | 0 | 0.000 |
| Temp*Time*Wood | | 175 | 10 | 0 | | 175 | 30 | 0 | 0.000 |
| Temp*Time*Wood | | 175 | 20 | 0 | | 175 | 30 | 0 | 0.106 |

| Effect | HDPE (%) | Temp | Time | Wood | HDPE (%) | Temp | Time | Wood | Adjp |
|----------------|----------|------|------|------|----------|------|------|------|--------------|
| Temp*Time*Wood | | 175 | 5 | 30 | | 175 | 10 | 30 | 1.000 |
| Temp*Time*Wood | | 175 | 5 | 30 | | 175 | 20 | 30 | 0.092 |
| Temp*Time*Wood | | 175 | 5 | 30 | | 175 | 30 | 30 | 0.047 |
| Temp*Time*Wood | | 175 | 10 | 30 | | 175 | 20 | 30 | 0.249 |
| Temp*Time*Wood | | 175 | 10 | 30 | | 175 | 30 | 30 | 0.139 |
| Temp*Time*Wood | | 175 | 20 | 30 | | 175 | 30 | 30 | 1.000 |

*Adjp = Adjusted P-Value

Temp*Time*Wood

Effect of Temperature on Void Fraction

| Effect | HDPE (%) | Temp | Time | Wood | HDPE (%) | Temp | Time | Wood | Adjp |
|----------------|----------|------|------|------|----------|------|------|------|-----------------|
| Temp*Time*Wood | | 135 | 10 | 0 | | 160 | 10 | 0 | 0.615148 |
| Temp*Time*Wood | | 135 | 10 | 0 | | 175 | 10 | 0 | 0.003685 |
| Temp*Time*Wood | | 160 | 10 | 0 | | 175 | 10 | 0 | 0.573784 |

| Effect | HDPE (%) | Temp | Time | Wood | HDPE (%) | Temp | Time | Wood | Adjp |
|----------------|----------|------|------|------|----------|------|------|------|-----------------|
| Temp*Time*Wood | | 135 | 20 | 0 | | 160 | 20 | 0 | 0.027765 |
| Temp*Time*Wood | | 135 | 20 | 0 | | 175 | 20 | 0 | 3.29E-08 |
| Temp*Time*Wood | | 160 | 20 | 0 | | 175 | 20 | 0 | 2.17E-05 |

| Effect | HDPE (%) | Temp | Time | Wood | HDPE (%) | Temp | Time | Wood | Adjp |
|----------------|----------|------|------|------|----------|------|------|------|-----------------|
| Temp*Time*Wood | | 135 | 20 | 30 | | 160 | 20 | 30 | 0.975772 |
| Temp*Time*Wood | | 135 | 20 | 30 | | 175 | 20 | 30 | 0.021815 |
| Temp*Time*Wood | | 160 | 20 | 30 | | 175 | 20 | 30 | 0.529907 |

| Effect | HDPE (%) | Temp | Time | Wood | HDPE (%) | Temp | Time | Wood | Adjp |
|----------------|----------|------|------|------|----------|------|------|------|-----------------|
| Temp*Time*Wood | | 135 | 30 | 0 | | 160 | 30 | 0 | 2.69E-06 |
| Temp*Time*Wood | | 135 | 30 | 0 | | 175 | 30 | 0 | 2.9E-08 |
| Temp*Time*Wood | | 160 | 30 | 0 | | 175 | 30 | 0 | 0.000153 |

| Effect | HDPE (%) | Temp | Time | Wood | HDPE (%) | Temp | Time | Wood | Adjp |
|----------------|----------|------|------|------|----------|------|------|------|-----------------|
| Temp*Time*Wood | | 135 | 30 | 30 | | 160 | 30 | 30 | 0.026533 |
| Temp*Time*Wood | | 135 | 30 | 30 | | 175 | 30 | 30 | 0.036718 |
| Temp*Time*Wood | | 160 | 30 | 30 | | 175 | 30 | 30 | 1 |

*Adjp = Adjusted P-Value

Temp*Time*Wood

Effect of Wood on Void Fraction

| Effect | HDPE (%) | Temp | Time | Wood | HDPE (%) | Temp | Time | Wood | Adjp |
|----------------|----------|------|------|------|----------|------|------|------|---------------|
| Temp*Time*Wood | | 160 | 30 | 0 | | 160 | 30 | 30 | 0.0035 |

| Effect | HDPE (%) | Temp | Time | Wood | HDPE (%) | Temp | Time | Wood | Adjp |
|----------------|----------|------|------|------|----------|------|------|------|---------------|
| Temp*Time*Wood | | 175 | 10 | 0 | | 175 | 10 | 30 | 0.0213 |

| Effect | HDPE (%) | Temp | Time | Wood | HDPE (%) | Temp | Time | Wood | Adjp |
|----------------|----------|------|------|------|----------|------|------|------|--------------|
| Temp*Time*Wood | | 175 | 20 | 0 | | 175 | 20 | 30 | 2E-06 |

| Effect | HDPE (%) | Temp | Time | Wood | HDPE (%) | Temp | Time | Wood | Adjp |
|----------------|----------|------|------|------|----------|------|------|------|--------------|
| Temp*Time*Wood | | 175 | 30 | 0 | | 175 | 30 | 30 | 3E-08 |

*Adjp = Adjusted P-Value

Temp*Time*Wood

Effect of Wood on Void Fraction

| Temp (°C) | Time (s) | Significant Difference |
|-----------|----------|------------------------|
| 135 | 5 | No |
| | 10 | No |
| | 20 | No |
| | 30 | No |
| 160 | 5 | No |
| | 10 | No |
| | 20 | No |
| | 30 | Yes |
| 175 | 5 | No |
| | 10 | Yes |
| | 20 | Yes |
| | 30 | Yes |

Effect of Time on Void Fraction

| Temp(°C) | Wood (phr) | Significant Difference |
|----------|------------|------------------------|
| 135 | 0 | No |
| | 30 | No |
| 160 | 0 | Yes |
| | 30 | Yes |
| 175 | 0 | Yes |
| | 30 | Yes |

Effect of Temperature on Void Fraction

| Time (S) | Wood (phr) | Significant Difference |
|----------|------------|------------------------|
| 5 | 0 | No |
| | 30 | No |
| 10 | 0 | Yes |
| | 30 | No |
| 20 | 0 | Yes |
| | 30 | Yes |
| 30 | 0 | Yes |
| | 30 | Yes |

Impact Strength of Unfoamed HDPE/PP Blends

| Effect | trt | HDPE (%) | trt | HDPE (%) | Adj p |
|----------|-----|----------|------|----------|--------------|
| trt*hdpe | 0_0 | | 00_0 | 30 | 1.000 |
| trt*hdpe | 0_0 | | 00_0 | 50 | 1.000 |
| trt*hdpe | 0_0 | | 00_0 | 70 | 1.000 |
| trt*hdpe | 0_0 | | 00_0 | 100 | 0.000 |
| trt*hdpe | 0_0 | 300_0 | | 50 | 1.000 |
| trt*hdpe | 0_0 | 300_0 | | 70 | 1.000 |
| trt*hdpe | 0_0 | 300_0 | | 100 | 0.000 |
| trt*hdpe | 0_0 | 500_0 | | 70 | 1.000 |
| trt*hdpe | 0_0 | 500_0 | | 100 | 0.000 |
| trt*hdpe | 0_0 | 700_0 | | 100 | 0.000 |

*Adj p = Adjusted P-Value

Impact Strength of Foamed HDPE/PP Blends

Effect of Blending Ratio

175°C20s

| Effect | trt | hdpe | trt | hdpe | Adj p |
|----------|--------|----------|---------|------|--------------|
| trt*hdpe | 175_20 | | 0175_20 | 30 | 0.879 |
| trt*hdpe | 175_20 | | 0175_20 | 50 | 0.999 |
| trt*hdpe | 175_20 | | 0175_20 | 70 | 1.000 |
| trt*hdpe | 175_20 | | 0175_20 | 100 | 0.000 |
| trt*hdpe | 175_20 | 30175_20 | | 50 | 1.000 |
| trt*hdpe | 175_20 | 30175_20 | | 70 | 0.994 |
| trt*hdpe | 175_20 | 30175_20 | | 100 | 0.000 |
| trt*hdpe | 175_20 | 50175_20 | | 70 | 1.000 |
| trt*hdpe | 175_20 | 50175_20 | | 100 | 0.000 |
| trt*hdpe | 175_20 | 70175_20 | | 100 | 0.000 |

175°C30s

| Effect | trt | hdpe | trt | hdpe | Adj p |
|----------|--------|----------|---------|------|--------------|
| trt*hdpe | 175_30 | | 0175_30 | 30 | 0.698 |
| trt*hdpe | 175_30 | | 0175_30 | 50 | 0.753 |
| trt*hdpe | 175_30 | | 0175_30 | 70 | 1.000 |
| trt*hdpe | 175_30 | | 0175_30 | 100 | 0.000 |
| trt*hdpe | 175_30 | 30175_30 | | 50 | 1.000 |
| trt*hdpe | 175_30 | 30175_30 | | 70 | 1.000 |
| trt*hdpe | 175_30 | 30175_30 | | 100 | 0.038 |
| trt*hdpe | 175_30 | 50175_30 | | 70 | 1.000 |
| trt*hdpe | 175_30 | 50175_30 | | 100 | 0.029 |
| trt*hdpe | 175_30 | 70175_30 | | 100 | 0.003 |

*Adj p = Adjusted P-Value

Impact Strength of Foamed HDPE/PP Blends

Effect of Foaming Temperature

HDPE 100%

| Effect | trt | hdpe | trt | hdpe | Adj p |
|----------|----------|------|--------|------|-----------------|
| trt*hdpe | unfoamed | 100 | 135_30 | 100 | 1 |
| trt*hdpe | unfoamed | 100 | 160_30 | 100 | 0.32586 |
| trt*hdpe | unfoamed | 100 | 175_30 | 100 | 0 |
| trt*hdpe | 135_30 | 100 | 160_30 | 100 | 1 |
| trt*hdpe | 135_30 | 100 | 175_30 | 100 | 0.021519 |
| trt*hdpe | 160_30 | 100 | 175_30 | 100 | 0.024165 |

HDPE/PP 70:30

| Effect | trt | hdpe | trt | hdpe | Adj p |
|----------|----------|------|--------|------|----------|
| trt*hdpe | unfoamed | 70 | 135_30 | 70 | 0.999999 |
| trt*hdpe | unfoamed | 70 | 160_30 | 70 | 0.999926 |
| trt*hdpe | unfoamed | 70 | 175_30 | 70 | 0.375691 |
| trt*hdpe | 135_30 | 70 | 160_30 | 70 | 1 |
| trt*hdpe | 135_30 | 70 | 175_30 | 70 | 0.999965 |
| trt*hdpe | 160_30 | 70 | 175_30 | 70 | 0.998393 |

HDPE/PP 50:50

| Effect | trt | hdpe | trt | hdpe | Adj p |
|----------|----------|------|--------|------|-----------------|
| trt*hdpe | unfoamed | 50 | 135_30 | 50 | 0.510111 |
| trt*hdpe | unfoamed | 50 | 160_30 | 50 | 0.001765 |
| trt*hdpe | unfoamed | 50 | 175_30 | 50 | 0.000229 |
| trt*hdpe | 135_30 | 50 | 160_30 | 50 | 0.999922 |
| trt*hdpe | 135_30 | 50 | 175_30 | 50 | 0.994842 |
| trt*hdpe | 160_30 | 50 | 175_30 | 50 | 1 |

HDPE/PP 30:70

| Effect | trt | hdpe | trt | hdpe | Adj p |
|----------|----------|------|--------|------|-----------------|
| trt*hdpe | unfoamed | 30 | 135_30 | 30 | 1 |
| trt*hdpe | unfoamed | 30 | 160_30 | 30 | 0.030006 |
| trt*hdpe | unfoamed | 30 | 175_30 | 30 | 2.57E-06 |
| trt*hdpe | 135_30 | 30 | 160_30 | 30 | 0.869542 |
| trt*hdpe | 135_30 | 30 | 175_30 | 30 | 0.047354 |
| trt*hdpe | 160_30 | 30 | 175_30 | 30 | 0.998718 |

PP 100%

| Effect | trt | hdpe | trt | hdpe | Adj p |
|----------|----------|------|--------|------|----------|
| trt*hdpe | unfoamed | 0 | 135_30 | 0 | 0.829149 |
| trt*hdpe | unfoamed | 0 | 160_30 | 0 | 0.976719 |
| trt*hdpe | unfoamed | 0 | 175_30 | 0 | 0.949113 |
| trt*hdpe | 135_30 | 0 | 160_30 | 0 | 1 |
| trt*hdpe | 135_30 | 0 | 175_30 | 0 | 1 |
| trt*hdpe | 160_30 | 0 | 175_30 | 0 | 1 |

*Adj p = Adjusted P-Value

SAS Program 1

```
PROC IMPORT OUT= WORK.foaming
      DATAFILE= "D:\SSC Information\326 - foaming.xls"
      DBMS=EXCEL2000 REPLACE;
      GETNAMES=YES;
RUN;
proc contents data=foaming;
run;
data foaming;
  set foaming;
  drop f6-f11;
  if void_fraction____^=.;
run;
proc freq data=foaming;
  tables Ratio_HDPE_ Temp Time Wood Ratio_HDPE_*Temp*Time*Wood
  /nocol nocum norow nopercnt;
run;
proc mixed data=foaming;
  class Ratio_HDPE_ Temp Time Wood;
  model void_fraction____ = Ratio_HDPE_|Temp|Time Ratio_HDPE_|Temp|Wood
    Ratio_HDPE_|Time|Wood Temp|Time|Wood/solution ddfm=satterth
  outp=yhat;
  random Ratio_HDPE_*Temp*Time*Wood;
  lsmeans Ratio_HDPE_|Temp|Time Ratio_HDPE_|Temp|Wood
    Ratio_HDPE_|Time|Wood Temp|Time|Wood/diff adjust=tukey;
  ods listing exclude lsmeans; ods output lsmeans=lsmeans;
  ods listing exclude diffs; ods output diffs=diffs;
run;
proc gplot data=yhat;
  title 'Residuals - Void Fraction Analysis';
  plot resid*pred/ legend frame
  vref=0;
run;
proc gplot data=yhat;
  title 'Residuals - Void Fraction Analysis';
  plot resid*pred/ legend frame
  vref=0
  vref=-8.649
  vref=8.649;
run;
proc univariate data = yhat normal;
  var resid;
  histogram resid / normal;
  qqplot resid / normal;
run;
quit;
```

SAS Program 2

```
data strength;
  input sample temp time hdpe strength;
  trt=COMPRESS(temp||'_'||time,' ');
  lstrength=log(strength);
  cards;
run;
proc freq;
  tables trt/
  nocol norow nocum nopercnt;
run;
proc mixed data=strength;
  class sample trt hdpe;
  model lstrength= trt|hdpe/ ddfm=satterth outp=yhat;
  lsmeans trt*hdpe/diff cl adjust=tukey;
  ods listing exclude lsmeans; ods output lsmeans=lsmeans;
  ods listing exclude diffs; ods output diffs=diffs;
run;
proc gplot data=yhat;
  title 'Residuals - Strength Analysis';
  plot resid*pred resid*trt resid*hdpe/ legend frame
  vref=0;
run;
proc univariate data = yhat normal plot;
  var resid;
  histogram resid / normal;
  qqplot resid / normal;
run;
quit;
```

SAS Program 3

```
PROC IMPORT OUT= WORK.foaming
      DATAFILE= "D:SCC Information\326 - foaming.xls"
      DBMS=EXCEL2000 REPLACE;
      GETNAMES=YES;
RUN;
proc contents data=foaming;
run;
data foaming;
  set foaming;
  drop f6-f11;
  if void_fraction____ ^=.;
  sqrt3_void=void_fraction____**(1/3);
run;
proc freq data=foaming;
  tables Ratio_HDPE_ Temp Time Wood Ratio_HDPE_*Temp*Time*Wood
  /nocol nocum norow nopercnt;
run;
proc mixed data=foaming;
  class Ratio_HDPE_ Temp Time Wood;
  model void_fraction____ = Ratio_HDPE_|Temp|Time|Wood /ddfm=satterth
  outp=yhat;
  lsmeans Ratio_HDPE_*Temp*Time*Wood/diff adjust=tukey;
  ods listing exclude lsmeans; ods output lsmeans=lsmeans;
  ods listing exclude diffs;  ods output diffs=diffs;
run;
proc gplot data=yhat;
  title 'Residuals - Void Fraction Analysis';
  plot resid*pred/ legend frame
  vref=0
  vref=-8.649
  vref=8.649;
run;
proc univariate data = yhat normal;
  var resid;
  histogram resid / normal;
  qqplot resid / normal;
run;
proc mixed data=foaming;
  class Ratio_HDPE_ Temp Time Wood;

  model sqrt3_void= Ratio_HDPE_|Temp|Time|Wood /solution ddfm=satterth
  outp=yhat;
run;
proc gplot data=yhat;
  title 'Residuals - Void Fraction Analysis';
  plot resid*pred/ legend frame
  vref=0
run;
quit;
```